EVALUATION OF PARTIAL MELTING MODELS OF THE ORIGIN

OF SOME AUSTRALIAN BASALTS: TRACE ELEMENT EVIDENCE

by

STEPHEN DONALD ROY

S.B., Massachusetts Institute of Technology
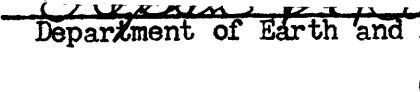
1973

SUBMITTED IN PARTIAL FULFILLMENT OF THE

REQUIREMENTS FOR THE DEGREE OF

MASTER OF SCIENCE

at the

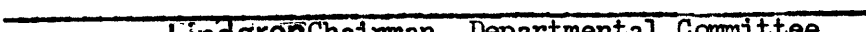MASSACHUSETTS INSTITUTE OF TECHNOLOGY

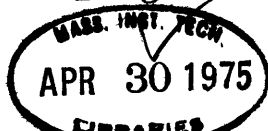January, 1975

Signature of Author _____
Department of Earth and Planetary Sciences
January 22, 1975

Certified by _____
Thesis Supervisor

Accepted by _____
Lindgren Chairman, Departmental Committee
on Graduate Students

EVALUATION OF PARTIAL MELTING MODELS OF THE ORIGIN

OF SOME AUSTRALIAN BASALTS: TRACE ELEMENT EVIDENCE

by

STEPHEN DONALD ROY

SUBMITTED IN PARTIAL FULFILLMENT OF THE

REQUIREMENTS FOR THE DEGREE OF

MASTER OF SCIENCE

ABSTRACT

Ten samples of Australian basalts, ranging from olivine melilite nephelinite to quartz tholeiite have been analyzed for their content of rare-earths (REE) Sc, Cr, Co, Hf, Ta and Th.

The results of experimental studies in high-temperature, high-pressure petrology have led to the hypothesis that basaltic magma is the result of partial melting of upper mantle peridotite and that different degrees of silica-saturation are due to different degrees of partial melting. This study was an attempt to test the theories of Dr. D.H. Green concerning specific degrees of partial melting from a specific source (pyrolite), by using trace element geochemistry, particularly the REE, and certain models of trace-element partitioning between minerals and liquid.

It was found that the nepheline-normative rocks could be generated by this method, with the assumption of 1) partition coefficients, 2) chondritic RE distribution in the source and 3) a total equilibrium model. Limits can then be placed on the degree of partial melting and the RE content of the source: exact specification depends on which model one chooses.

It was also determined that the tholeiitic rocks could not be generated in this manner and that the assumption of a chondritic distribution of REE in the source of the tholeiites was untenable.

Thesis Supervisor: F.A. Frey
Title: Associate Professor of Geochemistry

TABLE OF CONTENTS

LIST OF TABLES

LIST OF FIGURES

Evaluation of Partial Melting Models of the Origin

of Some Australian Basalts: Trace Element Evidence

I. INTRODUCTION

The results of experimental studies in high-temperature, high-pressure

petrology (e.g., Green 1973a,b, Irving 1971, Ito and Kennedy 1967) have lead

to the hypothesis that basaltic magma is the result of partial melting of

upper mantle peridotite and that different degrees of silica-(under)sat-

uration are due to different degrees of partial melting. Both the crys-

tallization behavior of basaltic magmas at high pressure (e.g., Green

1973a,b, Green and Ringwood 1967) and the melting behavior of peridotites

(e.g., Kushiro et al., 1972, Kushiro et al. 1968, Green 1973a,b, and O'Hara

and Yoder 1967) have been extensively studied; attempts have been made to

synthesize this data, notably by Green and Ringwood (1967) with the pyro-

lite model. Green (1970b, 1971) has published a "petrogenetic grid",

summarizing the petrogenetic implications of melting studies. This is

shown in Figure 1, which indicates pressure (depth) of origin versus per-

cent melting of a pyrolite composition source. Figure 2 shows a more recent

version from Green (1973b), but for our purposes, the more detailed presen-

tation shown in Figure 3 from Green (1970b) will be more useful, since it

illustrates possible relationships between basalt magma types, indicates

possible P-T conditions, and therefore source mineralogy, and also indi-

cates paths of fractional crystallization and partial melting.

Trace-element geochemistry, particularly studies of the rare-earth

elements (REE) has been utilized as a tool to decipher igneous petrogene-

Figure 1: Petrogenetic Grid from Green 1970a (Green's Caption):"A petro-
genetic grid for mantle-derived basaltic magmas. Various basalt
magma types are assigned to a % Melt, Pressure grid (implying
also specific % H_2O and temperature of melting ...) in which
they are regarded as partial melting products of a pyrolite com-
position containing 0.1% H_2O. The numbers placed with each basalt
type refer to the normative olivine content of this liouid at its
depth of origin- because of the expansion of the olivine crystal-
lization field at low pressure most basalts will precipitate
olivine before other phases if fractionation occurs at <u>lower</u>
pressures. The dashed boundaries marked with a mineral name show
that this mineral will occur among the residual phases remaining
after extraction of magma types to the left of the boundary.
Olivine is present in equilibrium, i.e. is a residual phase in
the pyrolite composition for all the magma types ...."

% MELTING

Pressure Kb / Depth Km

% H_2O in melt for simple melting of pyrolite containing 0·1% H_2O

Qz. Tholeiite

Tholeiite
0-5

Olivine Tholeiite
5 - 15

High-Al_2O_3
Olivine Tholeiite
5 - 10

Orthopyroxene

Olivine
Trachybasalt
10-15

Hawaiite
15-20

High Al_2O_3
Alkaline Olivine
Basalt
15-20

High Al_2O_3
Olivine Tholeiite
10-15

Olivine
Tholeiite
15-20

Olivine-rich
Basanite
15-25

Plagioclase

Amphibole

Alkaline Olivine Basalt
20-30

Olivine
Basalt
20-25

Olivine Tholeiite
20-25

Olivine
Nephelinite
20-25

Olivine-rich
Basanite
20-30

Alkaline Picrite
30-35

Tholeiitic Picrite
~30

Spinel

Clinopyroxene

Olivine
Melilite
Nephelinite
25-35

Garnet

Olivine Nephelinite
30-35

Picritic
Basanite
30-35

Alkaline
Picrite
30-35

Tholeiitic
Picrite
~35

Phlogopite

Olivine
Melilitite
~35-40

Olivine Melilite
Nephelinite
~35-40

-10-

Figure 2: Petrogenetic Grid from Green 1973b (Green's Caption): "Diagram
summarizing the petrogenetic applications of the melting studies
on pyrolite composition. The column to the left illustrates the
mineralogical character of the lithosphere and depth to the onset
of partial melting in the island arc situation and the normal
oceanic crust-mantle situation. In the right side of the diagrams,
the character of magma derived by partial melting of pyrolite is
plotted as a function of depth of magma segregation and degree of
partial melting. Numbers in parentheses adjacent to basalt names
refer to the normative olivine content of the partial melt. The
hatched areas illustrate the range of conditions over which quartz-
normative magmas may be derived by direct partial melting and
magma segregation from pyrolite. (A) is compiled for melting
under water-undersaturated conditions, with a water content in
the source pyrolite of about 0.2%. (B) is compiled for melting
under water-saturated conditions. The asterists denote the spe-
cific liquid compositions calculated at 10 kb and 20 kb in this
paper."

DEPTH Km

| 120 | 100 | 80 | 60 | 40 | 20 |

LOW VEL. ZONE . LITHOSPHERE Crust OCEAN BASIN

Ol+Opx+Ga+Cpx±Ilm : Ol+Opx+Cpx+Amph :? (Pl
±Phlog+Melt +Ga +Sp

Ol melilite neph   Ol Nephelinite   ?Trachy
Ol neph   basalt
Ol-rich basanite   Basanite

                                             Hi-Al
                          Alk.Ol.Basalt   Alk Ol
                                             Bas

Alkali-picrite

                                             Hi-Al Ol
                                             Basalt
                          Ol Basalt   Hi-Al ol
                                             Tholeiite
                                             (10-15)
                                             Ol Tholeiite
Tholeiitic Picrite   (15-20)
(30-35)
                          Ol Tholeiite
                          (20-25)

% MELTING

— 10
— 20
— 30

A

DEPTH Km

| 120 | 100 | 80 | 60 | 40 | 20 |

LOW VELOCITY ZONE OR : LITHOSPHERE . . . . ISLAND ARC
ANOMALOUS MANTLE
OL+Opx+Cpx+Melt   Ol+Opx+Amph±Cpx Crust
±Ga   ±Sp

?Shoshonite ?

?Alk Ol Basalt

?Alkali-rich
Qz Tholeiite? Basaltic

Olivine   Mg-rich Andesite
▼ (6)   Basaltic to
              Andesite
✷ (11)   Quartz Quartz
Tholeiite   Tholeiite Tholeiite
Olivine
Tholeiite
(0-5)

% MELTING

— 10
— 20
— 30
— 40

B

Figure 3: Petrogenetic Grid from Green 1970b (Green's Caption): "Diagram-
matic synthesis of relationships between basalt magma types. The
rectangular boxes denote magmas related by crystal fractionation
processes operating at various depth or pressure regimes. They
are also derived by possible partial melting processes from a
pyrolite source. The approximate mineralogy of the pyrolite source
at 1150°C, 9 kb; 1250°C, 15 kb and 1250°C, 27 kb is shown. This
is not necessarily the immediate subsolidus mineralogy involved
in the melting processes- both the mineralogy and the tempera-
ture of the solidus will be dependent on P_{H2O}, P_{Load} rela-
tionships."

PARTIAL MELTING OF PYROLITE AND
FRACTIONATION OF BASALTIC MAGMA AT VARIOUS PRESSURES

Pyrolite Anhydrous Mineralogy

Accessories
Al–Opx ~3% Al_2O_3 ~18% CaO
Olivine
~5% Al_2O_3 ~20% CaO
Al–Cpx
Plagioclase
Spinel
1150 °C

Acc.
Al–Opx ~6% Al_2O_3 ~2% CaO
Ol
Al–Cpx ~8% Al_2O_3 15% CaO
Sp
1250 °C

Acc
Al–Opx ~4% Al_2O_3 ~2% CaO
Ol
Al–Cpx ~15% CaO
Garnet
1250 °C

ALKALI OLIVINE BASALT
High Al_2O_3 & 10-20% normative olivine

ALKALI OLIVINE BASALT
High Al_2O_3

OLIVINE THOLEIITE
High Al_2O_3 5-15% normative olivine & 5-15% hypersthene

~20-25% Melting of Pyrolite at 9Kb (30Km)

Olivine + Clinopyroxene

Olivine + Enstatite + Clinopyroxene

Olivine + Low Al_2O_3 Enstatite

OLIVINE BASANITE
~6% normative nepheline

Aluminous Clinopyroxene
± Aluminous Enstatite

ALKALI OLIVINE BASALT
Low Al_2O_3 ; 25% normative olivine, 1-2% normative nepheline

Aluminous Enstatite + Aluminous & sub-calcic clinopyroxene ± olivine

OLIVINE BASALT
Low Al_2O_3, 25-30% normative olivine, (5% orthopyroxene)

Aluminous Enstatite (minor olivine)

OLIVINE THOLEIITE
Low Al_2O_3 20-28% normative olivine, 5-15% normative hypersthene

~25-30% Melting of Pyrolite at 13-18Kb (35-70Km)

Depression of liquidus by increasing water

~20-25% anhydrous melting
< 20%   "   "
or ~15-20% hydrous melting
~5-15%   "   "
< 10%   "   "

OLIVINE NEPHELINITE
(5% normative albite, 20-25% normative olivine)

Aluminous Enstatite Increas.water +Aluminous Clinopyroxene

OLIVINE BASANITE
5-15% norm. nepheline 20-25% norm olivine

Aluminous Enstatite + minor olivine

Olivine + Aluminous Enstatite

OLIVINE MELILITE NEPHELINITE
Norm leucite and/or larnite 25-35% norm olivine

Garnet ?-increas H_2O+CO_2 +Clinopyroxene

OLIVINE MELILITITE

Aluminous Enstatite Increas water +Garnet ± Aluminous Clinopyroxene

OLIVINE-RICH NEPHELINITE
(5% normative albite 30-35% normative olivine

Aluminous Enstatite Increas water ± Olivine

OLIVINE BASANITE
>5% norm. nepheline 30-35% norm olivine

Aluminous Enstatite (Increas water) ± Olivine

ALKALI PICRITE
30-35% norm olivine, 0-5% normative nepheline

Aluminous Enstatite + minor Olivine

THOLEIITIC PICRITE
30-35% norm olivine 10-20% normative hypersthene

~35-40% Melting of Pyrolite at 18-27Kb (70-100Km)

~20-30% hydrous melting
~10-20%   "   "
~5-15%   "   "
< 10%   "   "

sis for different sequences of rocks: for the Hawaiian Islands (Schilling and Winchester 1969, Reid and Frey 1971), for Gough Island (Zielinski and Frey 1970), for Steens Mountain in Oregon (Helmke and Haskin 1973), etc. This study is an attempt to determine what can be learned by combining the results of experimental petrology and its implications regarding major elements in igneous processes and trace-element studies of natural basalts. Based upon the work of Green (1970a,b, 1973a,b) on the melting of pyrolite as a source for basaltic magmas, limits can be placed on the degrees of partial melting required to generate specific lavas. Using an equilibrium partial melting model, trace-element contents can be calculated from the data on trace-element partitioning between solid phases and a liquid phase. The analyses of natural basalts can then be compared with these calculations to determine the fit of the model.

II. PREVIOUS WORK

The samples used in this study are ten basaltic rocks: six from the Newer Volcanics in Victoria, Australia (Irving 1971, Singleton and Joyce 1969) and four from the Cenozoic volcanic province in Tasmania (Sutherland 1969). The nomenclature used in this paper follows that of Green (1970a,b) and is based on the normative mineralogy. Briefly:

> Tholeiite: basalt with normative hypersthene
> Quartz tholeiite: basalt with normative hypersthene and quartz
> Olivine tholeiite: basalt with normative hypersthene and
>   olivine, hypersthene greater than 3%
> Olivine basalt: basalt with normative olivine and with
>   0-3% normative hypersthene; no normative nepheline
> Alkali olivine basalt: basalt with normative olivine and
>   nepheline; nepheline less than 5%
> Basanite: basalt with normative olivine, nepheline and
>   albite, with nepheline greater than 5% and albite
>   greater than 2%
> Olivine nephelinite: basalt-like composition with major

normative olivine and nepheline; albite less than 2%,
normative orthoclase and/or leucite but no normative
larnite;
Olivine melilite nephelinite: basalt-like composition with
normative olivine, nepheline, leucite and larn^ a
(Green 1970b, p. 221).

On this basis, the samples studied range from quartz tholeiite to olivine

melilite nephelinite and thus cover the Hawaiian spectrum, but from a con-

tinental environment. Sample locations are shown in Figure 4. The sam-

ples were obtained from Dr. D.H. Green.

A. Sample Descriptions

Since all samples were obtained as powders, all petrographic data are

from Irving (1971) or Irving and Green (1974).

1. Quartz tholeiite 2177, Mt. Eckersley: this is the only quartz
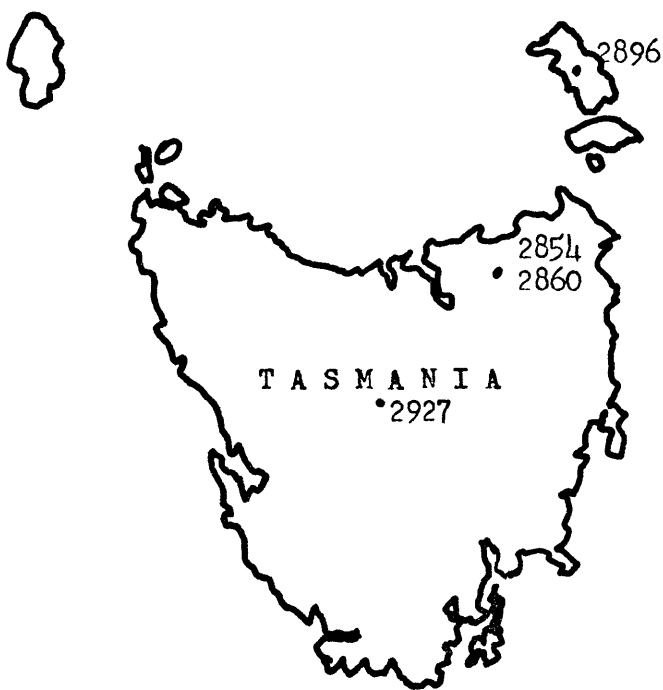
tholeiite found in the province.

"The minor (1%) normative quartz is possibly a primary
feature, but may alternatively be a consequence of the
secondary alteration particularly evident in this sam-
ple. The rock is relatively rich in plagioclase which,
with uncommon olivine (partly iddingsitized), form phe-
nocrysts in a medium-grained intersertal groundmass of
plagioclase, pale brownish clinopyroxene, opaque laths,
and interstitial turbid material (possible altered glass)
(Irving 1971)."

2. Olivine tholeiites: 69-1018 Mt. Gellibrand, 2152 Marida Yallock,

and 69-1026 Mt. Widderin:

"The tholeiites of ... Mt. Gellibrand are distinctly
richer in normative hypersthene and poorer in olivine
than the tholeiitic flows near Mt. Widderin, ..., /and/
Marida Yallock .... The rocks of this second group are
transitional to olivine basalts. .... All these rocks
consist of plagioclase with pale greenish-brown clino-
pyroxene, granular or rod-like opaques and rare turbid
altered glass (?) .... Most of these rocks have a do-
leritic aspect .... (Irving 1971)."

Figure 4: Map showing Victoria and Tasmania, Australia and the locations
          of the ten samples used in this study.
                    2177 Mt. Eckersley
                 69-1018 Mt. Gellibrand
                    2152 Marida Yallock
                 69-1026 Mt. Widderin
                 69-1036 Mt. Frazer
                    2128 Mt. Porndon
                    2854 Scottsdale
                    2860 Scottsdale
                    2896 Flinders Island
                    2927 Happy Jack Marsh

VICTORIA

• 69-1036

Melbourne

• 69-1026

2177   2152   • 69-10??

2128

2896

2854
2860

TASMANIA
• 2927

3. Alkali olivine basalt 69-1036, Mt. Frazer:

> "The alkali olivine basalts from Mt. Frazer ... all con-
> tain /olivine-rich/ lherzolite xenoliths /with Cr-diop-
> side/. The lavas consist of olivine phenocrysts in a
> groundmass of olivine, plagioclase, titanaugite, titano-
> magnetite and minor apatite (Irving 1971)."

4. Nepheline basanite 2128, Mt. Porndon:

> "The rocks forming the conspicuous scoria and lava cones
> of Mt. Porndon ... are nepheline basanites .... /The/
> eruptive centre /is/ characterized by the presence of
> /olivine-rich/ lherzolite xenoliths /with Cr-diopside/;
> the majority also have wehrlite xenoliths and pyroxene
> and anorthoclase megacrysts. ... Microscopically, the
> basanites are characterized by plagioclase of andesine-
> labradorite composition and by groundmass containing a-
> patite with interstitial brown glass and/or nepheline
> (Irving 1971)."

No detailed petrography is available for the Tasmanian rocks. For
a general review of the Tasmanian volcanics, including chemistry and
petrology, see Sutherland (1969). The olivine nephelinites 2854 (Scotts-
dale) and 2896 (Flinders Id.) and the olivine melilite nephelinite 2927
(Happy Jack Marsh) all have lherzolite inclusions at the sample localities.

B. Chemical Analyses

Irving (1971) did extensive geochemical and high-pressure experimental
studies on the xenoliths, megacrysts and basalts from southeastern Austra-
lia; his major element analyses on the six Victorian rocks, along with the
major element analyses of the Tasmanian rocks supplied by Green (personal
communication) are shown in Table I, with the CIPW norms (calculated with
the USGS rock norm program M0015). Fe_2O_3/FeO weight percent ratios have
in each case been recalculated to 0.2 to counter the effects of oxidation
during or after eruption. Irving (1971) chose 0.2 because some of the
least oxidized rocks (samples that may be primary magmas, see below) have

TABLE I

Major element analyses
NEWER VOLCANICS OF VICTORIA

Rock Type	Qtz Thol	Ol Thol	Ol Thol	Ol Basalt	Alk Ol Bas	Basanite
Sample No	2177	69-1018	2152	69-1026	69-1036	2128
Locality	Mt. Eckersley	Mt. Gellibrand	Marida Yallock	Mt. Widderin	Mt. Frazer	Mt. Porndon
SiO_2	53.53	50.70	50.11	49.83	48.00	46.21
TiO_2	1.80	2.07	1.89	1.73	2.14	2.51
Al_2O_3	15.32	14.30	14.56	14.88	13.91	12.38
Fe_2O_3	1.59	1.92	1.85	1.90	1.85	2.00
FeO	7.94	9.60	9.26	9.51	9.27	9.98
MnO	0.11	0.16	0.17	0.17	0.16	0.18
MgO	6.52	7.95	8.48	8.49	11.39	11.71
CaO	8.38	8.90	8.75	8.60	8.35	8.56
Na_2O	3.65	3.24	3.37	3.45	3.23	3.54
K_2O	0.85	0.81	1.15	1.09	1.18	2.01
P_2O_5	0.31	.0.35	0.40	0.34	0.51	0.90
$\frac{100\ Mg}{Mg+FeII}$	59.4	59.6	62.0	61.4	68.6	67.6
H_2O	1.79	0.67	0.95	1.16	0.46	0.42
Fe_2O_3 *	4.32	2.23	6.52	6.20	4.55	3.50
$\frac{100\ Mg}{Mg+FeII}$*	68.0	60.3	74.7	72.5	74.8	70.8

CIPW Norms

qz	1.06	-	-	-	-	-
or	5.02	4.79	6.80	6.44	6.97	11.88
ab	30.89	27.42	28.52	29.20	24.98	14.96
an	22.91	22.08	21.21	21.90	19.97	11.96
lc	-	-	-	-	-	-
ne	-	-	-	-	1.28	8.13
di	13.58	16.14	15.95	15.12	14.62	19.88
wo	6.95	8.26	8.18	7.75	7.57	10.29
en	16.24	13.57	8.06	6.23	4.92	6.66
fs	10.50	8.86	4.84	3.94	2.13	2.94
hy	20.11	14.54	5.13	2.79	-	-
ol	-	7.51	15.21	17.73	24.26	23.45
fo	-	4.37	9.16	10.45	16.43	15.78
fa	-	3.14	6.05	7.27	7.83	7.67
mt	2.31	2.78	2.68	2.75	2.68	2.90
il	3.42	3.93	3.59	3.29	4.07	4.77
ap	0.74	0.83	0.95	0.81	1.21	2.13

All major element chemical analyses from Irving 1971. Fe_2O_3/FeO ratios have been recalculated to 0.2 to counter the effects of oxidation. * indicates Fe_2O_3 as actually determined (Mg-value as determined).

TABLE I Continued

Major element analyses
TASMANIA

Rock Type Sample No Locality	Ol Neph 2854 Scottsdale	Neph 2860 Scottsdale	Ol Neph 2896 Flinders Island	Ol Melil 2927 Happy Jack Marsh
SiO_2	39.31	39.14	42.17	38.05
TiO_2	3.37	3.56	2.68	2.71
Al_2O_3	9.45	13.40	11.10	9.54
Fe_2O_3	2.59	2.16	2.26	2.20
FeO	12.93	10.77	11.25	11.04
MnO	0.20	0.18	0.18	0.24
MgO	13.90	5.25	11.97	16.34
CaO	11.20	13.72	8.64	13.14
Na_2O	2.98	3.96	4.61	3.75
K_2O	1.53	3.10	2.12	1.42
P_2O_5	2.30	4.45	2.77	1.34
$\frac{100\ Mg}{Mg+FeII}$	65.7	46.5	65.5	72.5
H_2O	-.	-.	-.	-
Fe_2O_3*	5.07	5.30	4.94	4.25
$\frac{100\ Mg}{Mg+FeII}*$	69.9	54.1	70.8	76.0

CIPW Norms

qz	-	-	-	-
or	7.19	14.56	12.56	-
ab	-	-	9.77	-
an	7.91	9.66	3.34	5.02
lc	1.47	2.99	-	6.60
ne	13.69	18.21	15.89	17.23
di	26.46	24.33	17.39	14.82
wo	13.66	12.30	8.97	7.71
en	8.68	6.16	5.64	5.25
fs	4.12	5.87	2.78	1.86
ol	27.76	9.99	26.23	34.64
fo	18.24	4.87	16.99	24.91
fa	9.53	5.11	9.23	9.73
mt	3.76	3.14	3.28	3.20
il	6.42	6.78	5.10	5.16
ap	5.46	10.57	6.58	3.18
cs	-	-	-	10.24

All major element analyses from Green (personal communication). See other notes on page 20.

Fe$_2$O$_3$/FeO ratios approaching or approximately equal to 0.2; it is believed that this value is appropriate for the Tasmanian rocks also. All samples are considered as one suite since similar parent magmas are hypothesized to be involved (Sutherland 1969). As an aid to visualizing the nomenclature and the major element abundances, a normative plot, of the type used by Coombs (1963) is shown in Figure 5. Irving (personal communication) also did some trace element analyses, and these are shown in Table II.
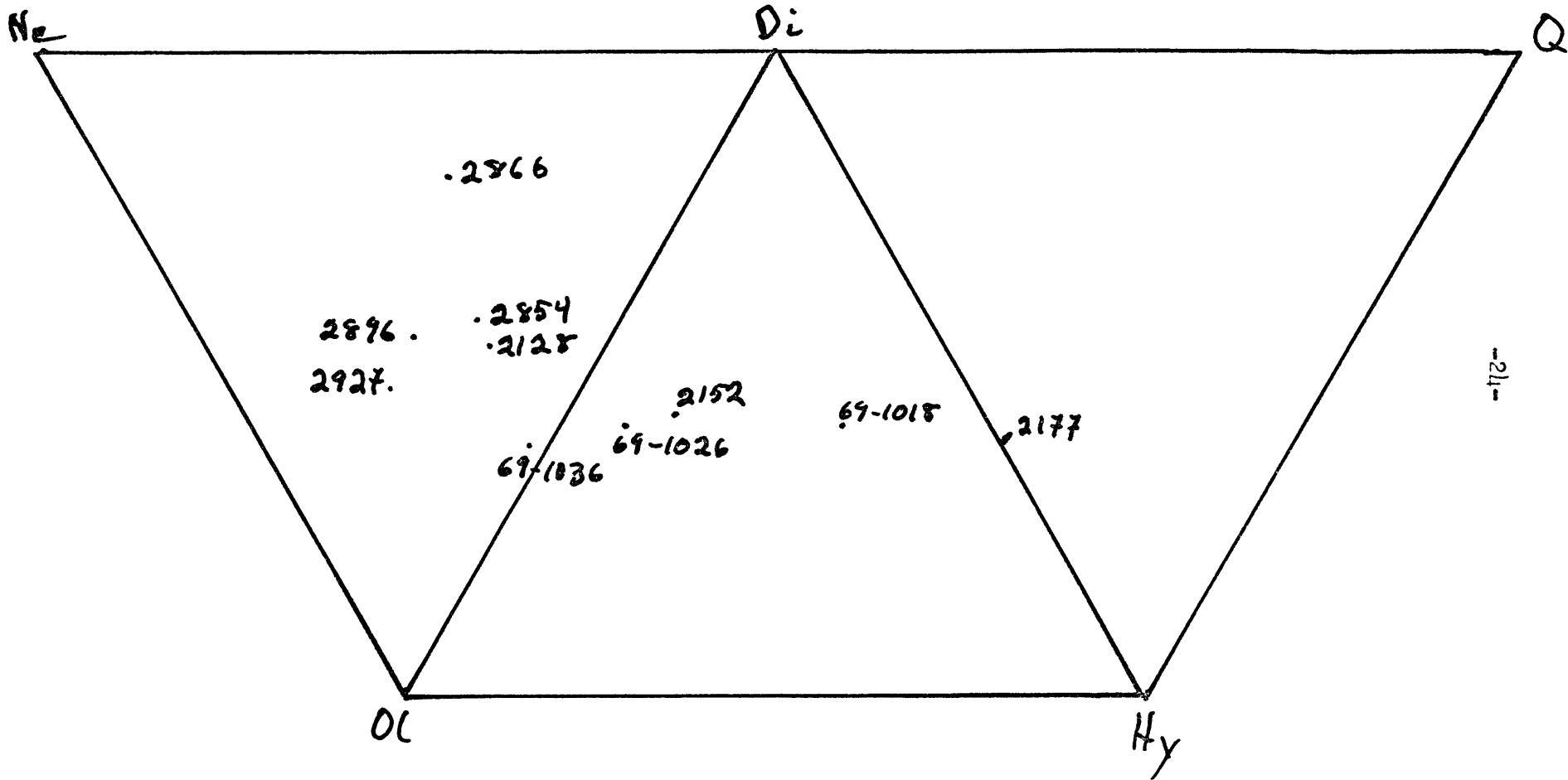
TABLE II

Trace element analyses of A.J. Irving (unpublished)

Element	Ol Thol 69-1016 Mt. Gellibrand	Ol Basalt 69-1026 Mt. Widderin	Basanite 2131 Mt. Porndon	Basanite 2136 Mt. Porndon
Sc	24	29	20	19
V	28	188	235	211
Cr	400	397	570	444
Co	60		76	69
Ni	196	247	318	261
Cu	48	53	53	52
Rb (XRF)	22	21	43	52
Sr "	427	471	847	897
Y "	26	55	29	31
Zr "	143	151	309	336
Zr	157	181	265	262
Ba	710	1670	505	542
La	23	67	68	65
Th (XRF)	2.7	3.8	5.2	6.2

All analyses are emission spectrography unless otherwise indicated.
All numbers are ppm.

Figure 5: Coombs plot

Ne   Di   Q

.2866

2896.   .2854
         .2128
2927.
              .2152
       69-1036 69-1026   69-1018   .2177

                                              -24-

Ol   Hy

C. Basalt Petrogenesis

For the Newer Volcanics, Irving (1971) concluded the following: only the basanites and the olivine nephelinites could have been primary melts of upper mantle peridotite. This conclusion is based upon the high $Mg/(Mg+Fe^{+2})$ atomic ratios (the Mg-value) and the presence of lherzolite nodules in these samples. Using data of Roeder and Emslie (1970) on the partitioning of Fe and Mg between olivine and liquid, Irving derived the following expression for the distribution of Fe and Mg between olivine and liquid:

$$X_{ol} = X_L / (X_L + K(100 - X_L)),$$

where X is the Mg-value, and $K = (Mg/Fe)_L / (Mg/Fe)_{ol}$. Roeder and Emslie (1970) determined K to be 0.3. Estimates of the chemical composition of the undepleted upper mantle (e.g., Ringwood 1966, Nicholls 1967, Carter 1970) have Mg-values between 87.5 and 89.3. Olivines of these peridotitic assemblages would have similar ratios; if the range Fo_{86} to Fo_{91} is considered, Irving's expression implies equilibrium with basaltic liquids with Mg-values between 65 and 76. See either Kesson (1973) or Irving (1971) for more details.

Basanite 2128 (and olivine nephelinites 2854 and 2896 and olivine melilite nephelinite 2927) meet these criteria. Alkali olivine basalt 69-1036 does also, but Irving (personal communication) feels that some xenocrystal olivine from the lherzolite xenoliths common in the hand specimens (Irving 1971) may have been included in the analysis.

Recent experimental studies (e.g., Ito and Kennedy 1967, Green 1973a, etc.) indicate that basanites with about 25% normative olivine and about 10% normative nepheline may be derived by small degrees (5-6%) of partial

melting of hydrous mantle peridotite at pressures of about 25 to 30 kb.

Experimental evidence also suggests that olivine nephelinite magmas may

be derived by extremely small degrees (less than 5%) of partial melting of

hydrous peridotite at pressures of 20 to 30 kb (Bultitude and Green 1968).

The tholeiites and olivine basalts of the Newer Volcanics are too Fe-

rich to be primary melts of a peridotite mantle produced by high degrees

(greater than 20%) of partial melting. The tholeiites have Mg-values of

59.4 to 59.6 and are poor or lacking in normative olivine and are most

likely low pressure (less than 5 kb) fractionates of more olivine-rich

tholeiitic magmas. The olivine basalts and the olivine tholeiites trans-

itional to them have slightly higher Mg-values (61.4 to 62.0) and very much

higher normative olivine contents (15.2 to 17.7%). Such differences are

explicable in terms of different degrees of partial melting of source peri-

dotite and thus different olivine/hypersthene proportions for parental mag-

mas, with the further complication of variable olivine or olivine plus

pyroxene fractionation at low pressures. The quartz tholeiite is seen as

a low pressure fractionate also.

The major objective of this research was to utilize trace-element

data to evaluate melting models based on major-element data.

III. ANALYTICAL DATA

Table III shows the trace-element analyses along with the chondrite-

normalized values for the REE for all samples. The analytical determin-

ations were all done by instrumental neutron activation analysis, as de-

scribed by Gordon et al. (1968). The photopeaks used for analysis, counting

times and similar information can be found in Appendix I. The values shown

TABLE III

Trace element analyses

Rock Type	Qtz Thol	Ol Thol	Ol Thol	Ol Basalt	Alk Ol Bas
Sample No	2177	69-1018	2152	69-1026	69-1036
Locality	Mt. Eckersley	Mt. Gellibrand	Marida Yallock	Mt. Widderin	Mt. Frazer
Sc	19.55±0.07	21.82±0.07	20.97±0.07	22.42±0.06	24.21±0.06
Cr	245±3	229±3	293±3	249±2	392±3
Co	52.7±0.4	65.4±0.4	102.9±0.6*	106.4±0.7	71.2±0.4
La**	48.2±(0.5)	16.0±(0.5)	50.1±(0.1)	52.7±(0.3)	23.9±(0.5)
Ce	81.7±3.0	29.8±1.6	100.8±3.5	156±6	44.7±2.6
Nd	50.1±3.5	17.4±1.9	45.7±3.2	50.6±4.1	25.5±2.7
Sm	12.1±0.1	4.63±0.05	10.0±0.1	12.2±0.07	5.51±0.04
Eu**	3.86±(0.10)	1.57±(0.02)	3.03±(0.03)	3.52±(0.09)	2.05±(0.05)
Tb	1.83±0.09	0.72±0.07	1.57±0.08	1.64±0.06	0.91±0.05
Ho	2.51±0.40	0.74±0.27	1.92±0.37	2.14±0.23	1.04±0.18
Yb**	5.0±(0.2)	1.9±(0.2)	3.3±(0.3)	3.7±(0.7)	2.4±0.9
Lu	0.78±0.13	0.24±0.11	0.41±0.12	0.44±0.22	0.49±0.22
Hf	3.60±0.21	3.48±0.22	3.68±0.22	3.57±0.18	4.15±0.18
Ta**	4.26±(0.44)	3.30±(0.21)	3.87±(0.23)	4.38±(0.07)	5.75±(0.18)
Th	2.51±0.18	1.91±0.17	2.81±0.19	2.62±0.13	2.78±0.13

Chondrite-normalized REE analyses

	Qtz Thol	Ol Thol	Ol Thol	Ol Basalt	Alk Ol Bas
La	146±(1.5)	48.5±(1.5)	152±(0.3)	160±(0.9)	72.5±(1.5)
Ce	92.8±3.4	33.9±1.9	115±4	178±9	51±3.3
Nd	83.4±5.8	29.0±3.1	76.2±5.4	84.3±6.8	42.4±4.5
Sm	66.7±0.5	25.5±0.3	55.5±0.5	67.9±0.4	30.6±0.2
Eu	55.9±(1.5)	22.7±(0.3)	44±(0.4)	51.0±(1.3)	29.8±(0.7)
Tb	39.0±1.8	15.3±1.5	33.4±1.8	34.8±1.2	19.4±1.1
Ho	35.9±5.7	10.6±3.8	27.4±5.2	30.5±3.3	14.9±2.6
Yb	25.0±(1.0)	9.6±(1.0)	16.6±(1.5)	16.7±(3.5)	12.0±4.5
Lu	22.8±3.9	7.0±3.2	11.9±3.7	13±6.5	14.3±6.2

* WC contamination in sample produces anomalous Co abundance.
** La, Eu, Yb (sometimes) and Ta are the averages of two determinations from different gamma-ray peak; errors in parentheses indicate the net differences. Chondrite values are from Haskin et al. (1968): La 0.330, Ce 0.880, Nd 0.600, Sm 0.181, Eu 0.069, Tb 0.047, Ho 0.070, Yb 0.200, Lu 0.034.

TABLE III Continued

Trace element analyses

Rock Type Sample No Locality	Basanite 2128 Mt. Porndon	Ol Neph 2854 Scotts- dale	Neph 2860 Scotts- dale	Ol Neph 2896 Flinders Island	Ol Melil 2927 Happy Jack Marsh
Sc	19.61 ± 0.05	19.20 ± 0.06	10.46 ± 0.04	14.61 ± 0.05	23.32 ± 0.07
Cr	385 ± 3	428 ± 3	11.0 ± 1.7	545 ± 4	494 ± 4
Co**	71.3 ± 0.4	77.2 ± 0.5	44.2 ± 0.3	83.2 ± 0.5	83.3 ± 0.5
La**	$48.4\pm(0.5)$	$61.8\pm(2.1)$	$100.9\pm(1.1)$	$64.8\pm(0.1)$	$72.1\pm(1.3)$
Ce	82.5 ± 3.8	116.7 ± 3.3	133.1 ± 6.6	114.3 ± 3.2	127.8 ± 3.5
Nd	44.1 ± 3.8	57.3 ± 2.8	66.1 ± 6.1	59.8 ± 2.9	59.5 ± 2.9
Sm**	9.59 ± 0.06	12.06 ± 0.20	16.98 ± 0.11	12.60 ± 0.17	12.14 ± 0.17
Eu**	$2.96\pm(0.14)$	$4.02\pm(0.36)$	$6.34\pm(0.17)$	$4.20\pm(0.42)$	$3.68\pm(0.06)$
Tb	1.26 ± 0.05	1.60 ± 0.08	2.55 ± 0.08	1.63 ± 0.07	1.77 ± 0.08
Ho	1.11 ± 0.21	***	1.50 ± 0.22	***	***
Yb**	1.07 ± 0.11	1.87 ± 0.78	$1.75\pm(0.21)$	1.87 ± 0.90	1.28 ± 0.85
Lu	0.35 ± 0.22	0.10 ± 0.10	0.18 ± 0.06	0.26 ± 0.16	0.29 ± 0.15
Hf	7.48 ± 0.19	8.78 ± 0.23	10.70 ± 0.22	9.31 ± 0.22	5.82 ± 0.24
Ta**	$11.3\pm(0.1)$	$15.7\pm(0.6)$	$14.9\pm(0.5)$	$14.8\pm(0.9)$	$13.0\pm(0.9)$
Th	5.73 ± 0.15	6.91 ± 0.20	12.6 ± 0.3	3.83 ± 0.16	13.6 ± 0.3

Chondrite-normalized REE analyses

La	$147\pm(1.5)$	$187\pm(6.3)$	$306\pm(3.3)$	$197\pm(0.3)$	$219\pm(3.9)$
Ce	93.8 ± 4.7	133 ± 4	151 ± 8	130 ± 4	145 ± 4
Nd	73.6 ± 6.3	95.5 ± 4.7	110 ± 10	99.6 ± 4.8	99.2 ± 4.9
Sm	53.0 ± 0.3	66.6 ± 1.1	93.8 ± 0.6	69.6 ± 1.0	66.6 ± 0.9
Eu	$42.9\pm(2.0)$	$58.2\pm(5.2)$	$91.9\pm(2.5)$	$60.9\pm(6.1)$	$53.4\pm(0.87)$
Tb	26.7 ± 1.1	34.0 ± 1.6	54.3 ± 1.8	34.7 ± 1.6	37.7 ± 1.8
Ho	15.9 ± 3.0	***	21.4 ± 3.1	***	***
Yb	5.3 ± 0.6	9.3 ± 3.9	$8.7\pm(1.0)$	9.3 ± 4.5	6.4 ± 4.2
Lu	10.4 ± 6.3	3.0 ± 2.9	5.3 ± 1.8	7.6 ± 4.7	8.5 ± 4.4

*** Due to scheduling difficulties with the counting equipment, analysis
for Ho in these three samples was not possible.
See other notes on page 27.

in Table III are derived from counting statistics after the method of Wasson (quoted in Baedecker 1971). The chondrite normalized patterns are shown in Figure 6 for the nephelinitic rocks and in Figure 7 for the tholeiitic group.

In order to test the accuracy and precision of the analyses, three separate analyses of BCR-1 were done. The data, corrected for flux variations, are presented in Table IV, with the average of the three, the standard deviation of the three analyses, the error from counting statistics and a survey of analyses of BCR-1 in the current literature.

Accuracy: For the following elements, the average of the three analyses is within 5% of Flanagan's (1973) recommended values: Co, Nd, Sm, Eu, Yb and Lu; for Ba, La, Ce, Tb, Hf, Ta, and Th, the average is within 10%, for Sc within 15% and for Ho, within 20%. The Cr analysis is out of line with the literature values, being 39% too low. No obvious explanation presents itself, but the low amount of Cr in the sample, along with the uncertainty of the Cr content in the standard is probably responsible.

Precision: The standard deviation $\left(\sqrt{\sum_i^n \dfrac{(x_i - m)^2}{n-1}}\right.$, m=mean) is shown in column 5 of Table IV. Column 6 shows the error from counting statistics (see Appendix II). It is of interest to compare the two: in 17 out of 22 cases, the error from counting statistics is greater than or approximately equal to the standard deviation of the three analyses, indicating that there can be high confidence in the analysis within the limits of the counting statistics.

There seems to be a systematic error in Ce, in that the chondrite-normalized Ce value is in every case but one (69-1026) lower than expected by interpolation between the La and Nd values, for no known reason.

Figure 6: Chondrite-normalized REE patterns for the nephelinitic rocks:

△——△   Basantie 2128
◻······◻   Olivine nephelinite 2854
●·····●   Olivine nephelinite 2896
○‑‑‑○   Nephelinite 2860
✗‑·—✗   Olivine melilite nephelinite 2927
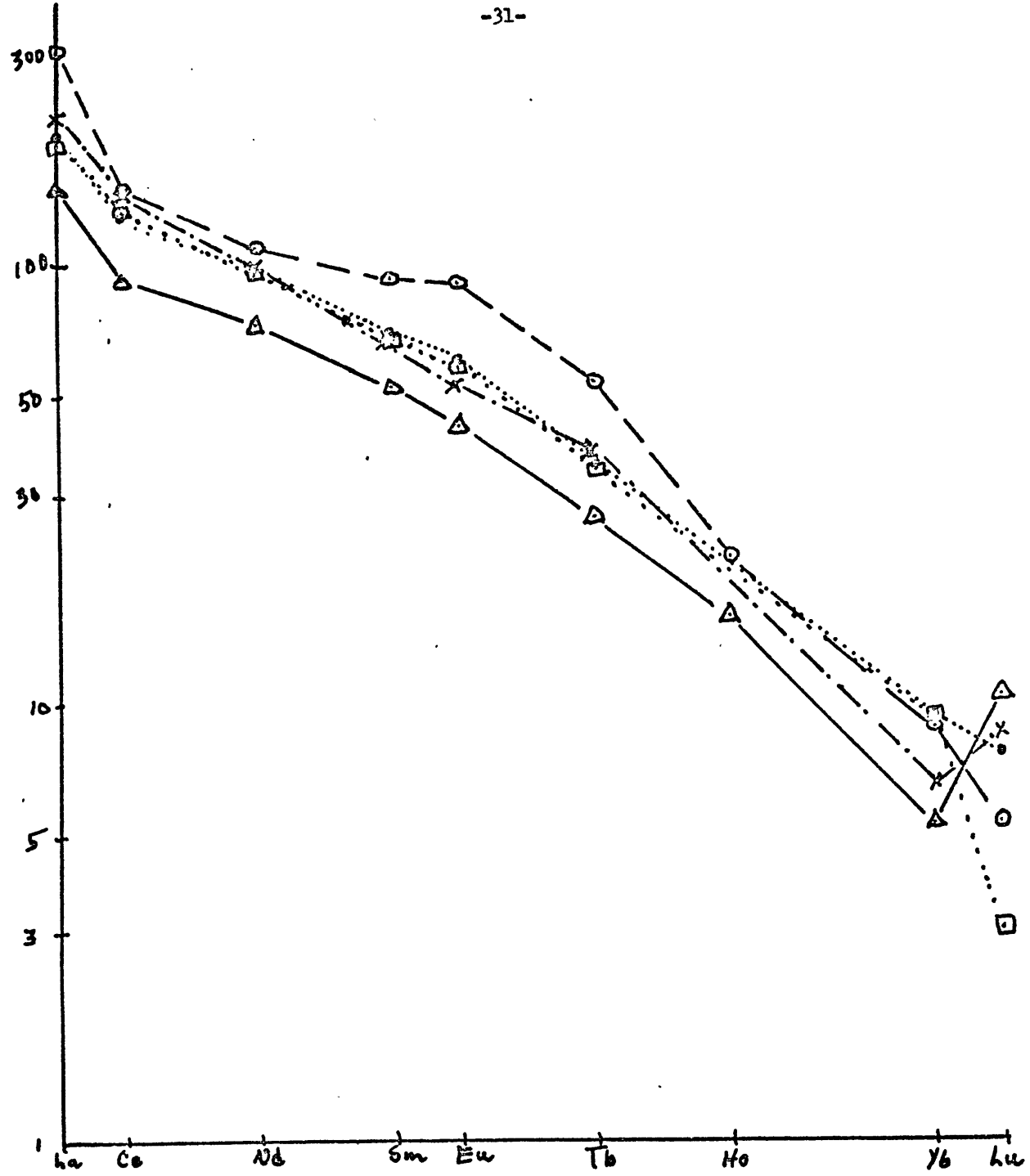
All data taken from Table III.

Figure 7: Chondrite-normalized REE pattern for the tholeiitic rocks:
  ● ─·─ ● Alkali olivine basalt 69-1036
  + ····· + Olivine basalt 69-1026
  ○ ─ ─ ○ Olivine tholeiite 2152
  □ ···· □ Olivine tholeiite 69-1018
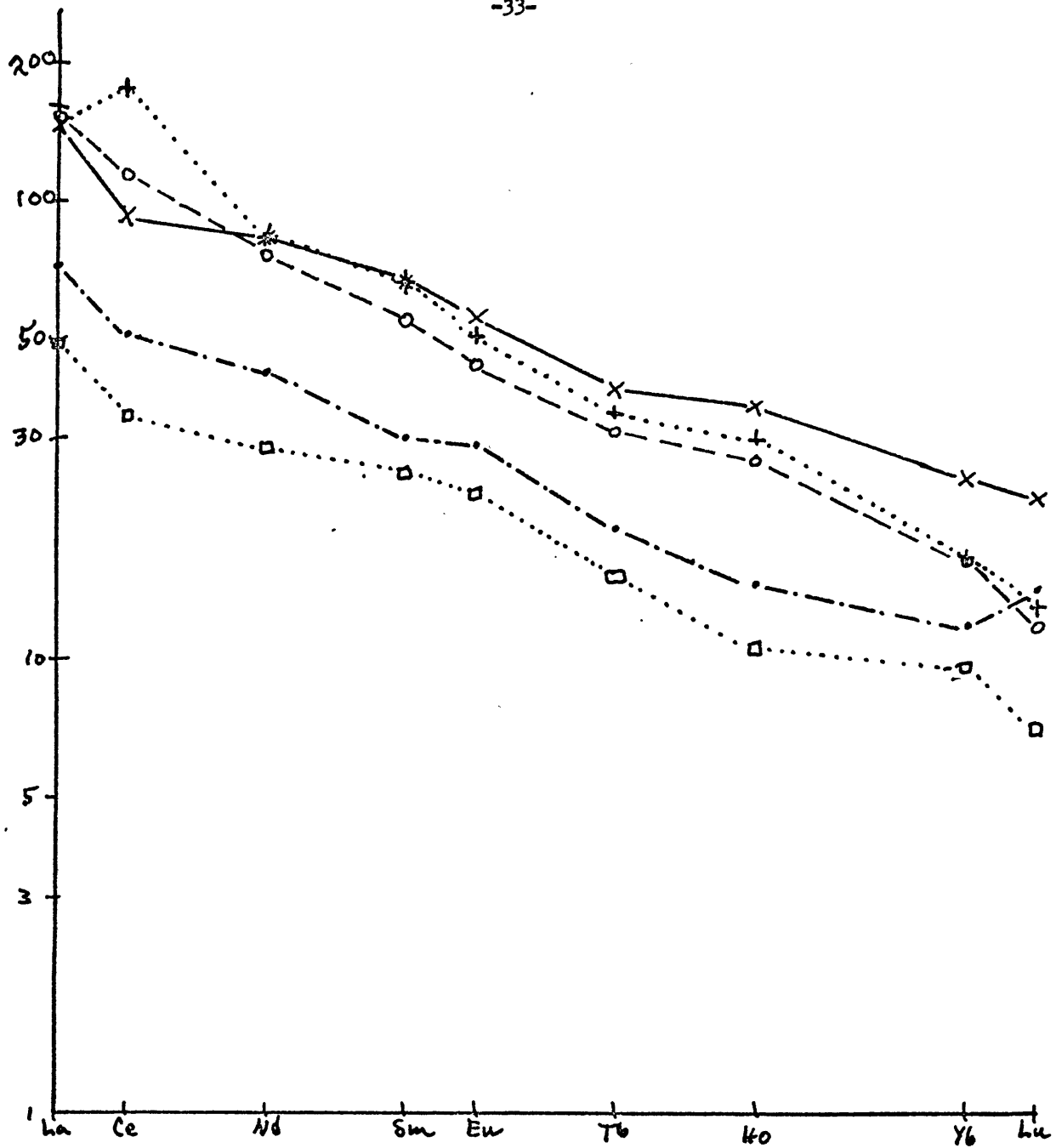 X ── X Quartz tholeiite 2177
All data taken from Table III.

TABLE IV

Analyses of BCR-1

	Photopeak (kev)	1	2	3	average
Sc	889	37.21±0.15	37.29	35.39	36.63±1.07
Cr	320	9.5± 4.3	11.8	9.1	10.1 ±1.5
Co	1332	39.6± 0.5	39.1	38.1	38.9 ±0.8
Ba	216	778 ±137	930	777	828 ±88
Ba	496	677 ±134	558	644	626 ±61
La	487	24.5±0.5	23.8	22.6	23.6 ±1.0 ⎫ 24.1±1.6
La	1595	25.7±0.4	24.2	24.1	24.7 ±0.9 ⎭
Ce	145	50.3±2.8	48.9	53.3	50.8 ±2.2
Nd	92	26.0±2.4	29.3	29.6	28.3 ±2.0
Sm	103	6.49±0.04	6.44	6.68	6.54±0.13
Eu	122	2.05±0.07	2.01	1.83	1.96±0.12 ⎫ 1.90±0.18
Eu	1408	1.96±0.10	1.76	1.84	1.85±0.10 ⎭
Tb	298	1.02±0.14	1.17	1.16	1.12±0.08
Ho	81	1.42±0.19	1.39	1.54	1.45±0.08
Yb	283	3.57±0.56	3.12	3.50	3.40±0.24 ⎫ 3.44±0.24
Yb	396	3.76±0.28	3.21	3.46	3.48±0.28 ⎭
Lu	208	0.537±0.04	0.567	0.559	0.554±0.016
Hf	133	5.03±0.31	4.71	5.16	4.97±0.23 ⎫ 5.21±0.59
Hf	482	5.36±0.52	5.84	5.15	5.45±0.35 ⎭
Ta	1189	1.3 ±0.5	0.5	0.4	0.7 ±0.5
Ta	1222	0.73±0.25	0.88	0.88	0.83±0.09
Th	313	5.81±0.39	5.50	5.63	5.65±0.16

All figures have been corrected for flux variations by means of an Fe

wire flux monitor. All such corrections were less than 3%.

The plus/minus value in column one is the statistical error associated

with the analysis; it is identical for the three samples. The plus/

minus value with the average is the standard deviation of the three

analyses:

$$\text{sigma} = \sqrt{\sum_{1}^{3} (m - x_i)^2 \ / \ 2}$$

TABLE IV Continued

Analyses of BCR-1 in the literature

	1	2	3	4	5	6	7	8
Sc	32		31.9±0.6					33*
Cr			19±5					17.6*
Co	36		35.8±0.7					38*
Ba	700	700	656±4	646		697		675
La	26	26.1	25.2±1.0			24.4		26*
Ce	53	54.9	54.2±1.2	53.9	54.3	54.3	53.7	53.9
Nd		28.8	30.5±4.3	28.6	27.7	28.9	29.0	29
Sm	7.0	6.74	7.23±0.37	6.62	6.38	6.72	6.74	6.6*
Eu	2.0	1.96	1.97±0.04	1.942	1.91	1.98	2.02	1.94
Tb	0.96		1.15±0.05					1.0
Ho			1.34±0.12					1.2**
Yb	3.6	3.68	3.48±0.12	3.38	3.35	3.39	3.49	3.36*
Lu	0.55	0.590	0.526±0.15	0.536	0.546	0.501		0.55
Hf	4.7		5.23±0.24					4.7*
Ta	0.74		0.90±0.09					0.91
Th								6.0

References: 1. Laul et al. 1972
2. Gast et al. 1970 (average of 2)
3. Haskin et al. 1970 (average of 2)
4. Philpotts et al. 1970b
5. Arth 1973
6. Nakamura and Masuda 1973
7. Shimizu 1974
8. Flanagan 1973: * indicates an average value, ** a magnitude; all others are recommended values.

The uncertainty in the Ce content of the standard may be responsible; alternatively an unidentified interference may be present in the gamma-ray spectrum.

Additional analyses of five samples from the Hawaiian Islands (supplied by D. Clague) were done, but the results are not interpreted in this thesis. They are shown as Appendix III, together with a literature survey of similar data.

IV. PARAMETERS INVOLVED IN MODELS FOR TRACE ELEMENT BEHAVIOR

A. ANATEXIS

ANATEXIS is a computer program for calculating trace-element concentrations in a melt phase and up to ten coexisting solid phases initially present in specified weight fractions which are allowed to form the liquid according to specified liquid weight fractions (i.e., melting proportions). Both Doerner-Hoskins (Rayleigh fractionation) and Berthelot-Nernst equilibria are calculated, using equations of Shaw (1970). The program was written by R. Kay in 1970 and modified by F.A. Frey, R.A. Zielinski and D.N. Skibo in July 1972. All computer runs were made on the MIT IBM 370/165. To run ANATEXIS, three basic quantites must be specified: the initial weight fractions, the melting proportions and the partition coefficients for the specified phases. Other control variables which must be specified are the initial melt percent, the final melt percent and the increment to be used. When any phase is exhausted, the program automatically goes on to the next element.

B. Initial Upper Mantle Mineralogy

Initial upper mantle mineralogy is dependent upon composition, pressure

and temperature. Green and Ringwood (1963) presented calculated mineralogies for several different anhydrous pressure-temperature regimes based on pyrolite I. Later papers (e.g., Green and Ringwood 1970) have not presented any quantitative mineralogy: Green (1970b) gave approximat₃ mineralogies for plagioclase pyrolite, pyroxene pyrolite and garnet pyrolite, but stated that they were not necessarily the immediate subsolidus mineralogies involved in the melting of pyrolite, since both the mineralogy and the temperature of the solidus are P_{H_2O} and P_{Load} dependent. Therefore the starting compositions used with ANATEXIS were derived in the following ways: 1) directly from Green and Ringwood (1963); 2) directly from Green (1970b); and 3) by using Doherty and Wright's (1971) Mineral Distribution program with mineral compositions from Green (1973a and b).

Mineral Distribution is a program designed to calculate rock modes and to model schemes of magmatic differentiation by the least-squares solution of an overdetermined system of linear equations. The program fits the chemical composition of a rock by calculating proportions of two or more minerals that make up the rock. Mineral Distribution was used to determine what combination of high-temperature, high-pressure olivine, orthopyroxene, garnet and amphibole could best match pyrolite III (Green 1973a). Clinopyroxene was omitted and amphibole included since Irving's (1971) model calls for a hydrous source, and Green's (1973b) phase diagram for pyrolite with 0.2% H_2O (Figure 8) has this mineralogy at pressures above 20 kb. This approach is made difficult by the lack of appropriate analyses. The mineral compositions used with the computer program are shown in Table V and are from Green (1973a) for a 30 kb, 1250°C, 0.3±0.1%

Figure 8: Phase Diagram for pyrolite plus 0.2% H_2O (Green 1973b) (Green's
Caption): "Experimental determination of solidus for water-
undersaturated (at P$<$30 kb) melting of pyrolite minus 40%
olivine and of sub-solidus and above-solidus mineralogy for
a water content in pyrolite equivalent to approximately 0.2%.
The "dotted" curve shows the position of the solidus deduced
from preliminary data on amphibole stability in pyrolite and
in the melting interval of undersaturated basaltic compositions.
The data points are shown by heavy dots and the minerals present
in the subsolidus disappear during melting along the dashed
curves marked with the mineral names. Amphibole disappears at
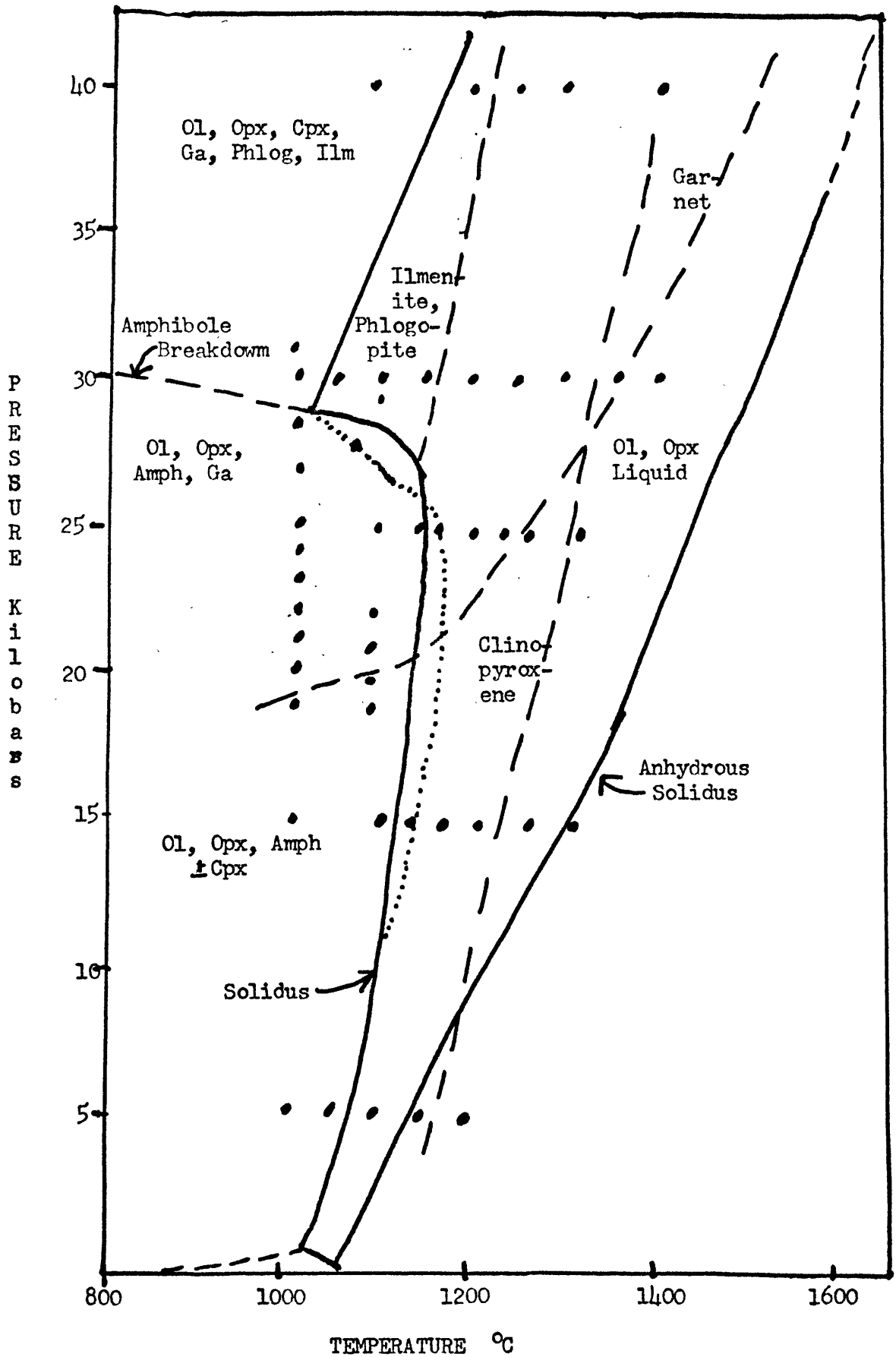the solidus (within the limints of the experimental points)
for P$<$30 kb."

PRESSURE Kilobars

40 —

Ol, Opx, Cpx,
Ga, Phlog, Ilm

Gar-
net

35 —

Ilmen-
ite,
Phlogo-
pite

Amphibole
Breakdown

30 —

Ol, Opx
Liquid

Ol, Opx,
Amph, Ga

25 —

Clino-
pyrox-
ene

Anhydrous
Solidus

15 —

Ol, Opx, Amph
± Cpx

10 —

Solidus

5 —

800   1000   1200   1400   1600

TEMPERATURE °C

TABLE V

Pyrolite ≈ olivine + orthopyroxene + amphibole: I

	OL	OPX	GA	AMPH	Pyrolite	Calculation	Difference
SiO_2	41.20	55.85	41.60	42.89	45.43	45.36	0.08
Al_2O_3	0.00	3.40	21.10	11.35	3.48	3.16	0.33
FeO	12.40	7.10	9.20	5.68	8.75	9.48	-0.72
MgO	46.40	31.27	20.70	22.48	37.68	37.28	0.40
CaO	0.00	1.70	5.80	11.24	3.09	3.05	0.04
Na_2O	0.00	0.20	0.00	1.96	0.60	0.53	0.07
H_2O	0.00	0.00	0.00	1.76	0.20	0.43	-0.22
TiO_2	0.00	0.50	1.40	2.58	0.70	0.73	-0.02
MnO	0.00	0.00	0.20	0.11	0.10	0.03	0.08

Solution: 52.28 25.63 -2.29 24.40

Olivine composition taken from Green 1973a, Table 5.

Orthopyroxene and garnet compositions taken from Green 1973a, Table 3.

Amphibole composition taken from Green 1973b, Table 6.

Adjustments have been made to the MgO and FeO values to reflect more realistic equilibrium Mg-values.

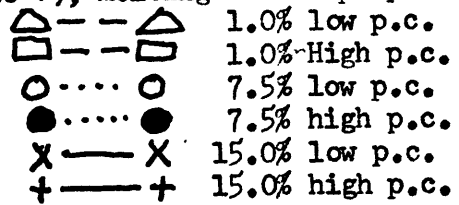The sum of the residuals squared is 0.8554.

H_2O experimental run for the olivine, orthopyroxene and garnet, and from Green (1973b) for an amphibole coexisting with olivine, orthopyroxene and clinopyroxene. Adjustments have been made to the MgO and FeO values to reflect more realistic equilibrium Mg-values.

The program yielded the results shown in the line labeled "solution" in Table V. The column labeled "Difference" is the difference between the composition to be matched (pyrolite) is the best fit the program came up with. with ("Calculation"). The fit is good, with the sum of the residuals squared being 0.85. This solution indicates that garnet is not involved, and includes a very high percentage of amphibole (24.4%). This state of affairs is not entirely satisfactory. To determine the effects of this mineralogy on REE patterns, this composition was run with ANATEXIS, and the results are shown in Figure 9.

For purposes of comparison, Green's mineral compositions (with unadjusted Fe/Mg ratios) were also run with Mineral Distribution; the results are shown in Table VI: the fit is not good; the olivine/orthopyroxene ratio is quite different, and the amount of amphibole is one-third lower. Garnet is still not involved. Mineral Distribution was rerun with an additional constraint: if the water is all in the amphibole (1.6% H_2O in the amphibole), 12% amphibole is expected in pyrolite with 0.2% H_2O. This changes the solution slightly (Table VII), this time including 1.7% garnet.

All three of these starting compositions (1, 2, and 3 of Table VIII) were run with ANATEXIS and the REE patterns which result are shown in Figures 9, 10 and 11. The melting proportions were chosen to reflect the belief that essentially amphibole alone is melting, since the phase dia-

Figure 9: Chondrite-normalized REE pattern produced by a source with
composition 50% olivine, 25.6% orthopyroxene and 24.4% amphi-
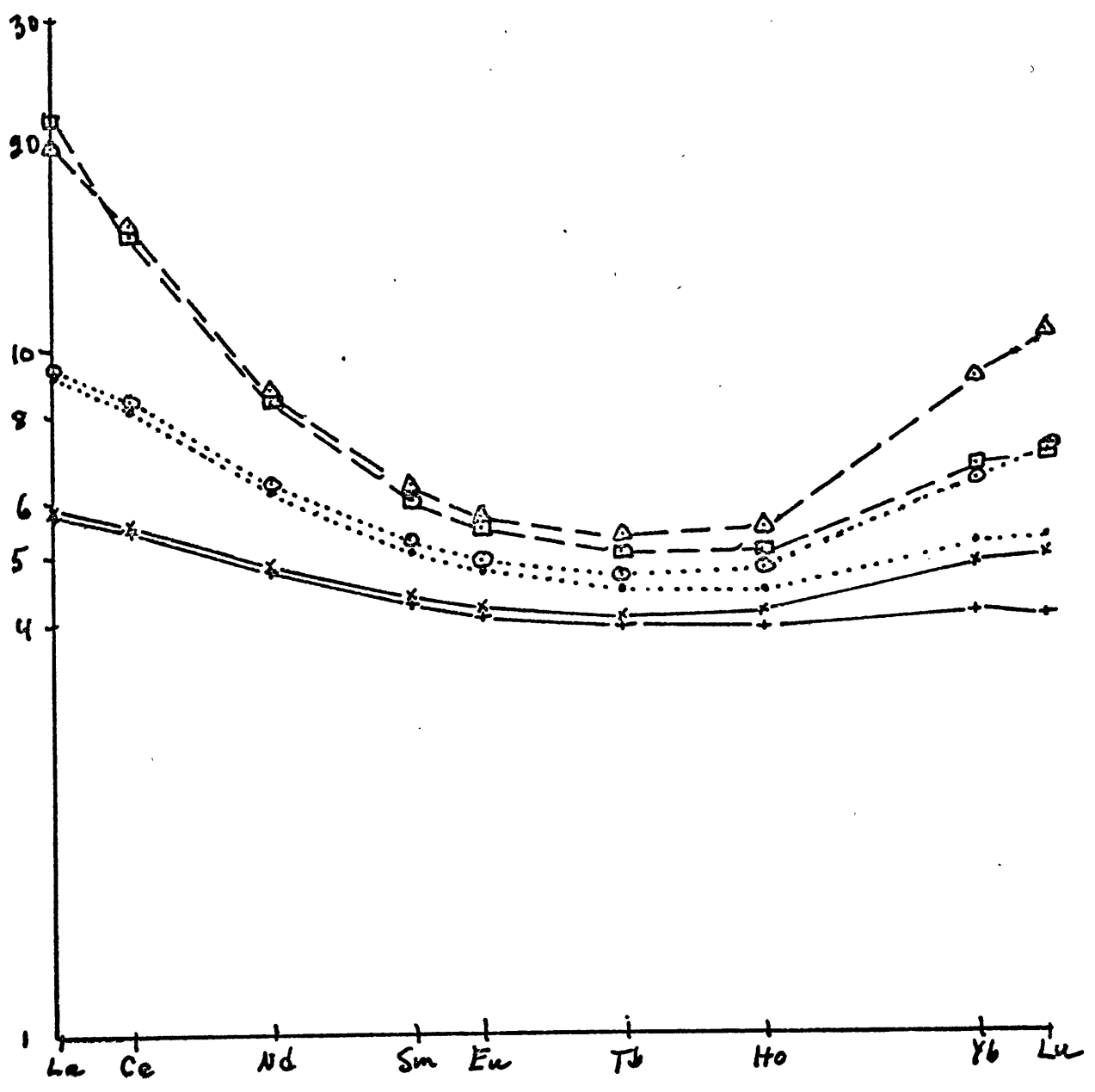bole (Table V), melting in the proportions 1:1:8.

△ — — △   1.0% low p.c.
□ — — □   1.0%-High p.c.
○ ···· ○   7.5% low p.c.
● ····· ●   7.5% high p.c.
X —— X   15.0% low p.c.
+ —— +   15.0% high p.c.

TABLE VI

Pyrolite = olivine + orthopyroxene + amphibole: II

	OL	OPX	GA	AMPH	Pyrolite	Calculation	Difference
SiO_2	44.37	55.50	40.89	43.96	45.30	45.46	-0.15
Al_2O_3	1.60	3.40	20.85	15.23	3.51	3.98	-0.46
FeO	10.67	7.10	9.02	6.56	8.52	9.64	-1.12
MgO	42.78	31.00	20.25	16.64	37.58	37.36	0.22
CaO	0.50	1.70	5.82	11.90	3.11	2.46	0.66
Na_2O	0.00	0.20	0.00	2.83	0.61	0.48	0.13
H_2O	0.00	0.00	0.00	1.72	0.21	0.28	-0.07
TiO_2	0.10	0.50	1.41	1.11	0.71	0.31	0.40
MnO	0.00	0.00	0.00	0.11	0.11	0.02	0.09
Cr_2O_3	0.00	0.60	1.81	0.00	0.41	0.07	0.34

Solution: 73.60   10.34   0.00   16.07

Olivine, orthopyroxene and garnet compositions taken from Green 1973a, Table 3, with unchanged MgO and FeO values.

Amphibole composition taken from Deer, Howie and Zussman, analysis of a Tinaquillo amphibole, v. 2, Table 43, column 5, p. 286, pargasite.

The sum of the residuals squared is 2.3065.

TABLE VII

Pyrolite = olivine + orthopyroxene + amphibole + garnet

	OL	OPX	GA	AMPH	Pyrolite	Calculation	Difference
SiO_2	44.37	55.50	40.89	43.96	45.30	45.92	-0.62
Al_2O_3	1.60	3.40	20.85	15.23	3.51	3.82	-0.31
FeO	10.67	7.10	9.02	6.56	8.52	9.63	-1.11
MgO	42.78	31.00	20.25	16.64	37.58	37.53	0.05
CaO	0.50	1.70	5.82	11.90	3.11	2.14	0.97
Na_2O	0.00	0.20	0.00	2.83	0.61	0.38	0.23
H_2O	0.00	0.00	0.00	1.72	0.21	0.21	0.00
TiO_2	0.10	0.50	1.41	1.11	0.71	0.31	0.40
MnO	0.00	0.00	0.00	0.11	0.11	0.01	0.10
Cr_2O_3	0.00	0.60	1.81	0.00	0.41	0.12	0.29

Solution: 71.56 14.79 1.65 12.00

Compositions used in this calculation are the same as those in Table VI.
This solution was determined by having the computer fit olivine, orthopyr-
oxene and garnet to an adjusted pyrolite. The adjusted pyrolite assumed
that 12.0% amphibole was an unvariable component of the mineralogy. The
computer fit was then recalculated to the form shown here.

The sum of the residuals squared is 2.9630.

TABLE VIII

Starting compositions used with ANATEXIS

	OL	OPX	CPX	GA	AMPH	SP	Source
1	50	25.6			24.4		Min. Dist.: Table V
2	73.6	10.3			16.1		Min. Dist.: Table VI
3	71.4	14.8		1.7	12.0		Min. Dist.: Table VII
4	57	17.5	15.5	10			Min. Dist.: Table IX
5	68	8	11	13			Green & Ringwood 1963
6	58	22	15	5			Green 1970b
7	62	17	15			6	Green & Ringwood 1963
8	51.1	21.4	22.5			5.0	Carter 1970
9	72.5	20.0	7.5				Derived from no. 4: see discussion of tholeiitic rocks
10	66.6	16.1	17.3				Green & Ringwood 1963
11	67	33					See discussion of tholeiitic rocks
	50	27	12	11			Chen (1971) for comparison only

gram for pyrolite plus 0.2% H_2O (Figure 8) indicates that the solidus is

essentially defined by the amphibole breakdown curve. None of the patterns

produced resemble the patterns actually shown by any of the rocks. If Fig-

ures 9 and 10 are compared with Figure 6, it is fairly clear that those

patterns produced by starting compositions 1 and 2 are either too flat or

have a rise between Ho and Yb. Using starting composition 3 (the one with

1.7% garnet) the patterns produced (Figure 11) by the low set of partition

coefficients are too flat, and the patterns produced by the high set of

partition coefficients are too flat for the LREE and too steep for the

HREE. This last point is worthy of note: even the inclusion of small

Figure 10: REE pattern produced by a source with composition 73.6%
olivine, 10.3% orthopyroxene and 16.1% amphibole (see
Table VI).

△ ─ ─ △ 1.0% low p.c.
□ ─ ─ ─ □ 1.0% high p.c.
○ ·····○ 7.5% low p.c.
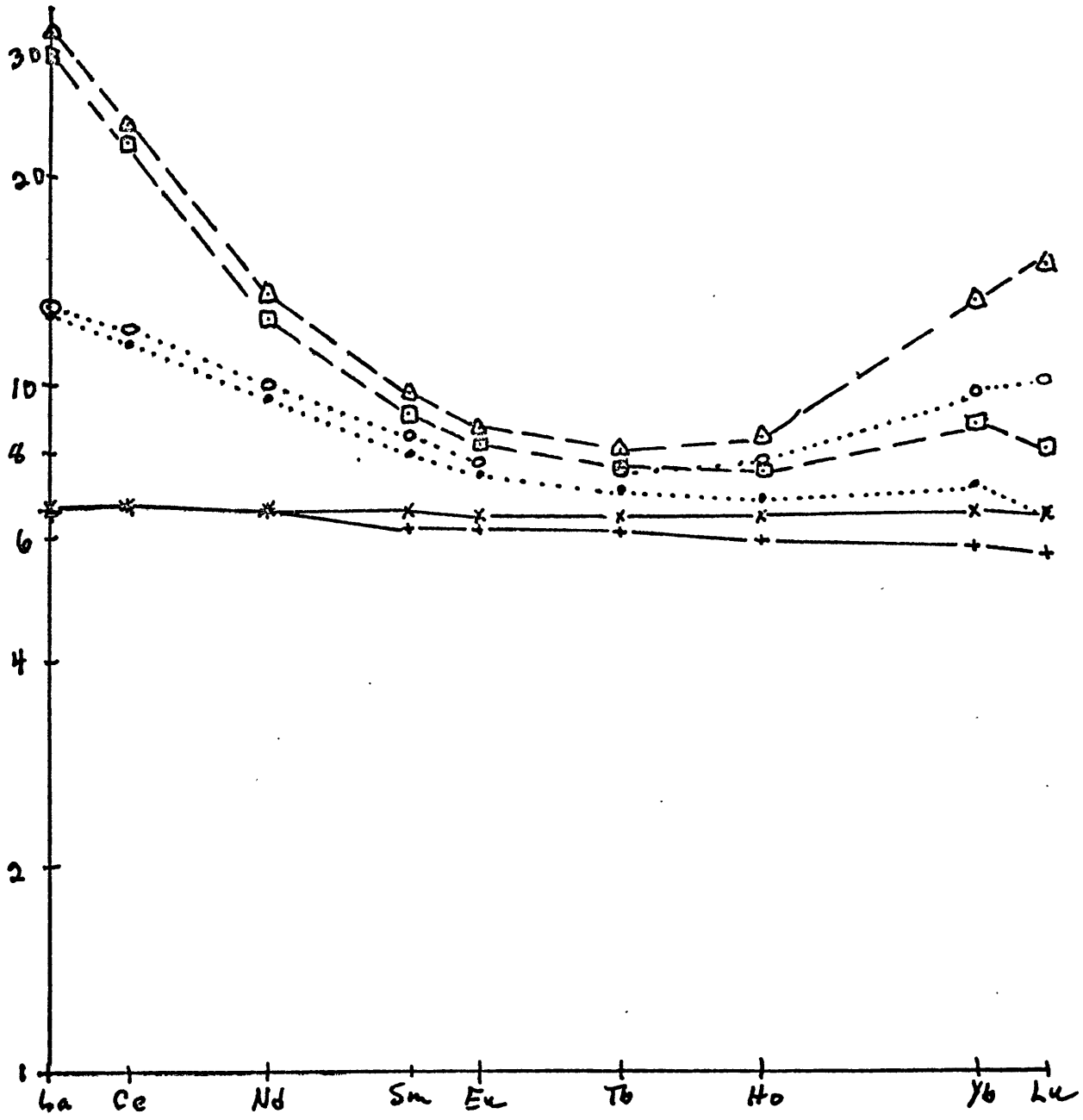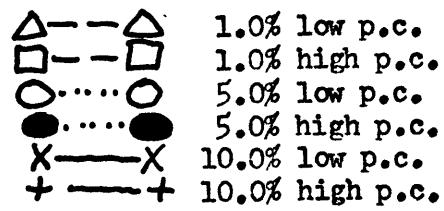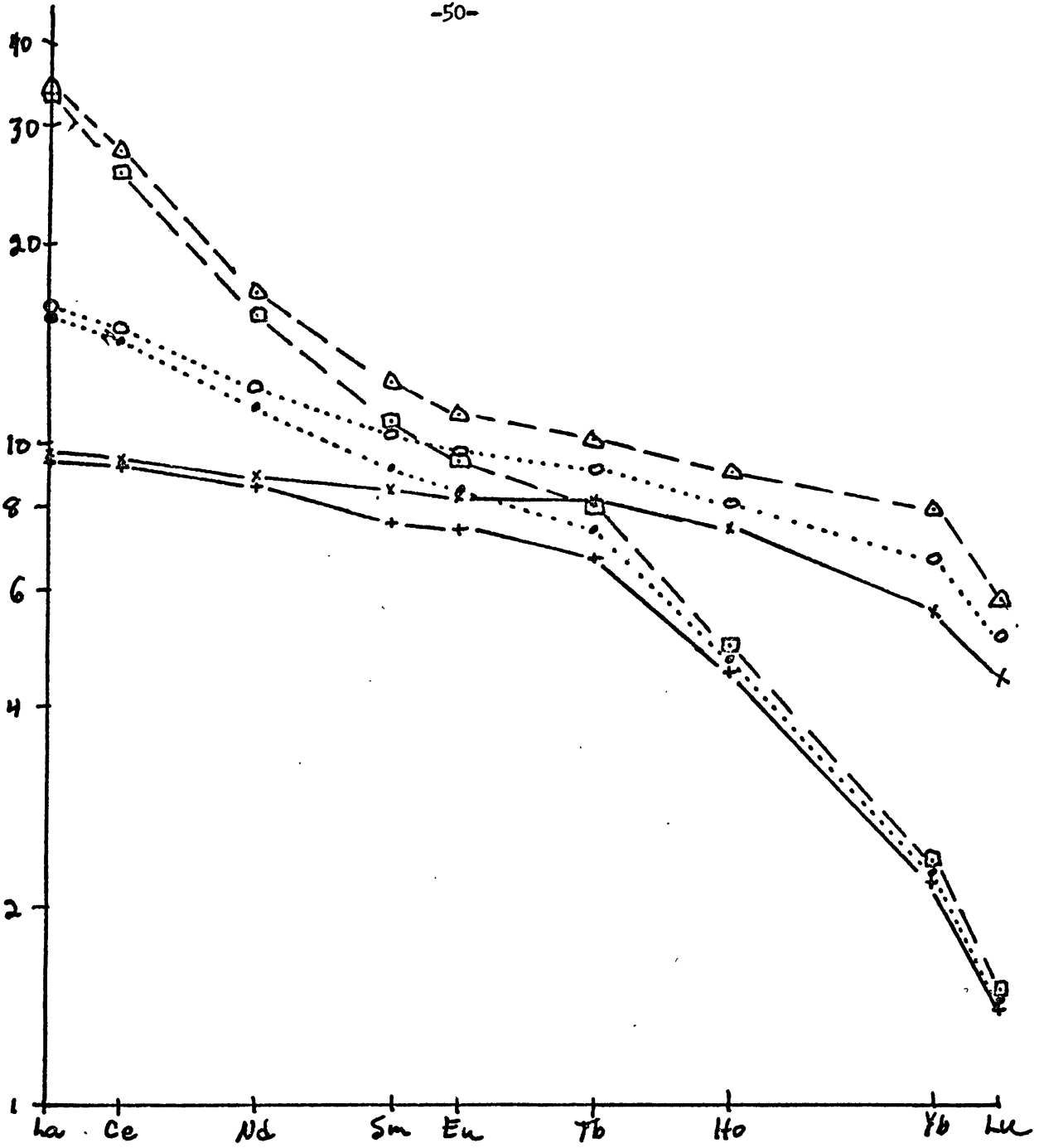●·····● 7.5% high p.c.
X────X 15.0% low p.c.
+────+ 15.0% high p.c.

Figure 11: REE pattern produced by a starting composition of 71.5%
olivine, 14.8% orthopyroxene, 12% amphibole and 1.7%
garnet (see Table VII).

△——△   1.0% low p.c.
□——□   1.0% high p.c.
○·····○   5.0% low p.c.
●·····●   5.0% high p.c.
X———X 10.0% low p.c.
+———+ 10.0% high p.c.

amounts of garnet completely negates the rise in the HREE produced by the amphibole. Thus it would seem unlikely that any combination of olivine, orthopyroxene, amphibole and garnet would yield a REE pattern similar to that shown by the rocks.

On the strength of this evidence, it is concluded that amphibole is not in equilibrium with any of these magmas. Amphibole may not be an important phase at the solidus because of its immediate breakdown, as mentioned above. In any case, once the amphibole has melted, its previous presence would be undetectable under conditions of total equilibrium (Harris et al. 1972).

The three olivine-orthopyroxene-clinopyroxene-garnet assemblages used with ANATEXIS are derived from a) a Mineral Distribution type of fit of Green's (1973a) mineral composition to pyrolite (see Table IX) (starting composition 4 of Table VIII); b) from Table 3 in Green and Ringwood (1963) (starting composition 5); and c) from the approximate mineralogy of Figure 2 in Green (1970b) (starting composition 6).

It is to be noted that the procedure followed here is distinctly different from that of Kay and Gast (1973), in that I am attempting to follow the conclusions of Irving and Green as closely as possible in order to test the applicability of their models (based on major element data) to trace element data. Kay and Gast (1973) determined the best fit of upper mantle models to their REE data by varying initial modal composition and the degree of melting. It should be pointed out that Kay and Gast (1973) base their results on Shaw's (1970) equation 14 (for fractional melting), whereas I am using Shaw's equation 15, for batch melting, which I believe to be closer to Green's theories and experimental research.

TABLE IX

Pyrolite = olivine + orthopyroxene + clinopyroxene + garnet

	OL	OPX	CPX	GA	Pyrolite	Calculation	Difference
SiO_2	40.0	55.5	53.5	40.9	45.2	44.9	0.3
Al_2O_3	0.0	4.0	5.2	21.0	3.5	3.5	0.0
FeO	9.4	6.9	4.5	9.0	8.5	8.2	0.3
MgO	48.4	30.8	18.1	20.0	37.5	37.8	-0.3
CaO	0.0	1.7	14.8	6.0	3.1	3.2	-0.1
Na_2O	0.0	0.0	1.9	0.0	0.6	0.3	0.3
TiO_2	0.2	0.6	0.9	1.4	0.7	0.5	0.2
MnO	0.2	0.0	0.0	0.0	0.1	0.1	0.0
Cr_2O_3	1.7	0.6	1.3	2.0	0.4	0.5	-0.1

Solution: 57.0   17.5   15.5   10.0

Compositions used in this calculation are taken from Green 1973a, Table 3 and Table 5. This is a hand-calculated fit.

The sum of the residuals squared is 0.42.

Models for the source region of the tholeiitic rocks are discussed in section V-B.

As a summary, Table VIII lists the major initial compositions used in the computer runs with ANATEXIS.

C. Partition Coefficients

1. REE: A survey of the available literature (e.g., Philpotts and Schnetzlar 1968a,b, 1972; Schnetzlar and Philpotts 1968; Grutzek et al. 1973; Nagasawa et al. 1969; Jensen 1973; Masuda and Kushiro 1970) quickly reveals that the relative values of the partition coefficients are known with much more certainty than the absolute values; therefore, two sets of partition coefficients were used in the computer runs: a high set and a low set (see Table X), more or less covering the range of observed values.

Clinopyroxene: the two sets of partition coefficients were chosen to cover the range found in natural systems. The low set is a bit lower than that chosen by Kay and Gast (1973) but agrees with data of Frey (unpublished) and some data of Schnetzlar and Philpotts (1970). The high set is clinopyroxene megacryst/host alkalie olivine basalt (Takashima, Japan) data from Onuma et al. (1968), except for the Ho value, which is interpolated.

Orthopyroxene: the two sets of orthopyroxene/liquid partition coefficients were determined by choosing a set of orthopyroxene/clinopyroxene partition coefficients (Table XI) and then calculating

$$D^{opx/l} = D^{cpx/l}/D^{cpx/opx}$$

The low set so determined agrees somewhat with that of Kay and Gast (1973); the high set agrees with Onuma et al. (1968) and Frey's unpublished New Zealand megacryst/matrix data.

TABLE X

REE Solid/liquid partition coefficients

	CPX	OPX	GA	OL	SP	AMPH	AP
Low Partition Coefficients							
La	0.02	0.0005	0.001	0.0005	0.526	0.167	52
Ce	0.04	0.0009	0.0033	0.0008	0.136	0.232	52
Nd	0.09	0.0019	0.0184	0.0013	0.167	0.436	81
Sm	0.14	0.0028	0.0823	0.0019	0.029	0.617	90
Eu	0.16	0.0036	0.1333	0.0019	0.016	0.692	50
Tb	0.19	0.0059	0.2568	0.0019	0.0148	0.740	69
Ho	0.195	0.0089	1.083	0.0020	0.0157	0.720	60
Yb	0.20	0.0286	4.0	0.0040	0.0204	0.390	37
Lu	0.19	0.038	7.0	0.0048	0.0200	0.310	30
High Partition Coefficients							
La	0.084	0.0021	0.004	0.0021	2.2	*	*
Ce	0.166	0.0040	0.0138	0.0033	0.255		
Nd	0.382	0.0083	0.0780	0.0055	0.707		
Sm	0.736	0.0147	0.4329	0.0098	0.153		
Eu	0.753	0.0171	0.6275	0.0088	0.075		
Tb	0.97	0.0303	1.311	0.0097	0.0758		
Ho	1.03	0.0468	5.7	0.0103	0.083		
Yb	1.01	0.1443	20.20	0.0202	0.1031		
Lu	0.95	0.1900	35.2	0.0238	0.1000		

* only one set of partition coefficients was used for amphibole and apatite.

TABLE XI

REE Solid/solid partition coefficients

	CPX/OPX	CPX/GA	CPX/OL	CPX/SP
La	40	20	40	0.038
Ce	42	12	50	0.66
Nd	46	4.9	70	0.54
Sm	50	1.7	75	4.8
Eu	44	1.2	85	10.0
Tb	32	0.74	100	12.8
Ho	22	0.18	100	12.4
Yb	7	0.05	50	9.8
Lu	5	0.027	40	9.5

Garnet: the garnet/liquid partition coefficients were determined by the same method as the orthopyroxene/liquid coefficients. The garnet/clinopyroxene partition coefficients were taken from mineral separate data of Haskin et al. (1966), Philpotts et al. (1972) and Early (1973). The $D^{gar/l}$ so calculated are consistent with an experimental study by Wildeman et al. (1973)[1] and Kakanui garnet xenocryst/lava partition coefficients (Philpotts et al. (1972).

Olivine: olivine/clinopyroxene partition coefficients were taken from available pairs in the literature and the olivine/liquid partition coefficients calculated. The low set is similar to Kay and Gast (1973) and the high set to Higuchi and Nagasawa (1969) and Corliss (1970). Since the olivine/liquid (and orthopyroxene/liquid) partition coefficients are so much less than 1, the exact value used in the calculations is not critical.

Amphibole: amphibole/liquid partition coefficients are based on phenocryst/matrix data of Philpotts et al. (1972) and Higuchi and Nagasawa (1969) and are consistent with data of Lopez (unpublished).

Spinel: clinopyroxene/spinel partition coefficients were taken from Frey (1969) and spinel/liquid coefficients were calculated. Spinel partitioning of the REE is less well understood than that of the previous minerals, and seems to vary widely. Until more work is done with spinel, little confidence can be placed in any particular set of partition coefficients. Spinel was not considered by Kay and Gast (1973).

Apatite: apatite/liquid data is from Nagasawa (1970) and is from an acidic matrix, but it is the only data available.

2. Other trace elements: In order to evaluate the models using the

---

1. Wildeman's data was a personal communication.

other trace elements determined in this study (Hf, Ta, Sc, Co and Th) and in some unpublished work of Irving (personal communication)(V, Ni, Cu, Rb, Sr, Y, Zr and Ba) for some of the rocks, a brief literature search was conducted in an attempt to determine partition coefficients for these elements. Table XII shows those partition coefficients chosen. A complete presentation of the data found is made in Table XIII.

TABLE XII

Trace-element (non-REE) solid/liquid partition coefficients

	CPX	OPX	GA	OL
Sc	3.1	1.1	6.5	0.25
V	1.5	0.3	0.27	0
Cr	33			
Co	1.5	3.3	2.6	3.3
Ni	3.3	6.3	0.6	10.8
Cu	0.023	0.1	0.2	0.06
Rb	0.05	0.02	0.02	0.01
Sr	0.017	0.016	0.014	0.016
Y	1.0	0.05	5.7	0.01
Zr	0.3	0	0.33	0.1
Ba	0.06	0.01	0.04	0.01
Hf	0	0	10	0
Ta	0	0	0	0
Th	0	0	0	0

See Table XIII for sources.

TABLE XIII

Non-REE trace element partitioning data

	CPX	OPX	GA	OL
Sc	3.3 (1) 2.9 (2) 3 (3) 2.8 (6) 3.3 (10) 3.1	1.23 (2) 1 -2 (3) 0.15 (11) 1.1	8.3 (10) 10.3 (11) 1.0 (12) 6.5	0.33 (1) 0.17 (6) 0.25
V	1 (3) 1.0 (10) 1.9 (14) 1.5	0.5 (3) 0.08 (11) 0.3	0.2 (10) 0.26 (11) 0.34 (12) 0.27	0 (14)
Cr	33 (10) 12.5 (14)			0.1 (14)
Co	1.2 (1) 1.1 (2) 2 (3) 1 (6) 2.0 (11) 1.1-2.5 (14) 1.5	2.1 (2) 3.5 (3) 4.2 (11) 3.3	4.0 (10) 2.16 (11) 1.5 (12) 2.6	3.1 (1) 3.0 (4) 1.9-4.5 (5) 3.9 (6) 3.0-5.5 (14) 3.3
Ni	6 (3) 1.8 (6) 3.3 (7) 2.2 (9) 1.2-5.0 (14) 3.3	8 (3) 6.7 (7) 2.96 (9) 7.5 (11) 5.6 (13) 6.2	0.5 (7) 0.85 (9) 0.7 (10) 0.5 (11) 0.6 (12) 0.6	10 (4) 4.9-18.6 (5) 11.8 (6) 16.7 (7) 2.96 (9) 9.5-12 (14) 10.8
Cu	0.071 (1) 0.2 (3) 0.1-0.7 (14) 0.1	0.2 (3)	0.06 (12)	0.023 (1) 0 (4) 0.08-0.9 (14) 0
Rb	0.05 (7) 0.045 (8) 0.05 (9) 0.06 (10) 0.05	0.025 (7) 0.022 (8) 0.01 (9) 0.02	0.008 (7) 0.008 (8) 0.04 (9) 0.03 (10) 0.02	0 (4) 0.01 (7) 0.01 (8) 0.008 (9) 0.01

TABLE XIII Continued

Non-REE trace element partitioning data

	CPX	OPX	GA	OL
Sr	0.11 (2) 0.2 (7) 0.166 (8) 0.2 (9) 0.15 (10) 0.02 (14) __0.165__	0.02 (7) 0.017 (8) 0.01 (9) __0.016__	0.015 (7) 0.015 (8) 0.015 (9) 0.009 (12) __0.014__	0 (4) 0.014 (7) 0.014 (8) 0.02 (9) __0.016__
Y*	0.59 (10) 2.0 (14) __1.0__		5.9 (10) 5.2 (12) __5.7__	0 (4) __0.01__
Zr	0.02-0.6 (14) __0.3__		0.33** 10	0 (4) __0.1__
Hf$				
Ba	0.05 (1) 0.0035 (2) 0.067 (8) 0.08 (9) 0.08 (10) 0.02-0.1 (14) __0.06__	0.013 (8) 0.01 (9) __0.01__	0.017 (8) 0.04 (9) 0.04 (10) 0.06 (12) __0.04__	0.05 (1) 0 (4) 0.01 (8) 0.01 (9) __0.01__
Ta#				
Th¢	0.013 (9) __0__			0.013 (2) 0.01 (9) __0__

General notes: horizontal line indicates generally an average was used. Absence of numbers means that no data was found in the literature.

* Y: geochemically Y behaves very similarly to Ho; since very little data concerning Y was found, the high set of Ho partition coefficients was used.

** Zr: one value for ga/cpx was found: 1.1 (12); ga/l was calculated with this value. In recognition of the similarity with Hf, 10 was also used.

$ Hf: My original assumption that all Hf partition coefficients were zero lead to answers an order of magnitude off; therefore it was assumed that Hf would behave similarly to Lu; this is plausible since the ionic radius of Hf^{+4} (0.91, Whittaker and Muntus (1970)) is not too different from that of Lu^{+3} (1.05) and Sc^{+3} (0.95) and we know that both Sc and Lu are enriched in garnet. Therefore, the Hf partition coefficient for garnet was taken as 10. For the other minerals, the partition coefficients were taken to be zero. Hf may also enter the pyroxenes (Vlasov 1966), but as a first order calculation, this was not taken into account.

TABLE XIII Continued

Non-REE trace element partitioning data

Ta: no data was found concerning Ta: all partition coefficients were assumed to be zero.
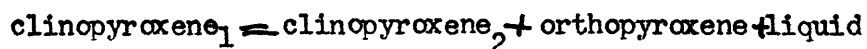
¢ Th: very little data was found for Th: all partition coefficients were assumed to be zero due to the large size of the Th^{+4} ion (1.08- 1.17A).

References:

(1) Paster et al. 1974
(2) Onuma et al. 1968
(3) Ewart et al. 1973
(4) Gunn 1971
(5) Henderson and Dale 1970
(6) Dale and Henderson 1971
(7) DeLong 1974
(8) Philpotts and Schnetzlar 1970a
(9) Shaw 1973
(10) Gill 1974
(11) Taylor et al. 1969
(12) Coleman et al. 1965
(13) Turekian and Carr 1960
(14) Wager and Mitchell 1951

D. Melting Proportions

Melting proportions are difficult numbers to come by, since much of the melting actually takes place by means of complex incongruent melting reactions. For example,

orthopyroxene ⇌ olivine + liquid

garnet ⇌ orthopyroxene + liquid

$clinopyroxene_1$ ⇌ $clinopyroxene_2$ + orthopyroxene + liquid

Experimental research (e.g., Ito, Green, Kushiro) indicates that phases such as clinopyroxene, garnet and amphibole all disappear before orthopyroxene and olivine. Thus for the computer model, simple assumptions can be made. The importance of these assumptions can be tested by varying the melting proportions and comparing the resulting models. This was done using three sets of melting proportions:

	OL	OPX	CPX	GA
1	.1	.1	.3	.5
2	.1	.1	.4	.4
3	.1	.1	.5	.3

The results for all such tests are essentially identical until one of the phases is exhausted, after which the pattern is determined by the three remaining phases, as required by the equilibrium assumptions. Since it is definite that olivine and orthopyroxene will be the last remaining phases they were given the least weight in all computer runs. The figures reported in the next section are based on Set No. 2, which is in agreement with the hypothetical mineralogy in Green's (1973a) Table 5.

V. DISCUSSION

The results of this study will be considered in two sections: first, the rocks with greater than 5% normative nepheline (the basanites, the olivine nephelinintes and the melilite nephelinite) and second, the rocks with less than 5% normative nepheline (the tholeiites, the olivine basalt and the alkali olivine basalt).

A. Rocks with greater than 5% normative nepheline (2128, 2854, 2860, 2896 and 2927)

Green's (1970b, 1973a) experimental work has shown that 5 - 15% partial melting of pyrolite with 0.2% H_2O at 25 - 30 kb and 1200 - 1300°C will generate strongly undersaturated nephelinitic or basanitic magma. These liquids (such as 2128, 2854, 2896 and 2927) are in equilibrium with olivine, orthopyroxene, clinopyroxene and garnet as residual phases. With the exception of nephelinite 2860, all of these rocks have Mg-values between 65 and 75 (see Table I) and have lherzolite inclusions; on the basis of this evidence, they are thought to be primary melts of upper mantle peridotite.

1. Basanite 2128: under pressures of 25 - 30 kb, the subsolidus mineralogy of pyrolite with 0.2% H_2O (see figure 8) is olivine, orthopyroxene, garnet and amphibole (Green 1973b). As pointed out in section IV, no pattern produced by this starting composition resembled any of the patterns actually exhibited by the rocks. Therefore, it is assumed that amphibole is not in equilibrium with any of the magmas investigated, that is, that the percent melt involved is always higher than that required for all the amphibole to disappear. Thus our assumption of equilibrium batch melting allows us to ignore the initial presence of amphibole since

the REE will redistribute themselves among the remaining phases (or phases now present, since clinopyroxene is added when the amphibole melts incongruently).

Thus the solid phases which are in equilibrium with the basanite magma are olivine, orthopyroxene, clinopyroxene and garnet (Green 1973a). Using ANATEXIS with starting compositions 4, 5, and 6 from Table VIII (these are the relevant ones, see above discussion and section IV-B), with the high and low sets of partition coefficients, the best fits of the calculated REE pattern with the rock (2128) pattern are shown in figures 12 and 13.

In determining the fit the following method was used. The chondrite-normalized REE pattern is usually characterized by a negative slope (La/Yb ratio greater than 1); however examination of the 2128 REE pattern shows that there is a definite change in slope at Tb, and therefore the pattern was characterized by two numbers, the La/Tb ratio and the Tb/Yb[1] ratio. These ratios were calculated for the computer-generated "melts" and the ones with the closest match were chosen.

Table XIV gives a numerical comparison between the different models and the basanite, and also illustrates the method used. Although all of

---

L. Yb was used in these ratios, since using Lu presents problems: the statistical error of the Lu-177 208.4 kev peak is fairly large, and often the determined value would cause a distinct change in slope between Yb and Lu. Yb-175 has two peaks (282.6 and 396.1 kev) which almost always give results well within the statistical errors of the two peaks. An average of the values determined from the two peaks was used in the calculations, with the minor exceptions of those rocks whose Yb content was so low that the two Yb-175 peaks were not detectable; in these cases an adjusted value of the Yb-169 63.3 kev peak was used. (The adjustment was made by comparing the Yb-169 peaks with the Yb-175 peaks in those samples (by far the greater majority) for which both isotopes yielded integratable peaks).

Figure 12: Graphical comparison of the REE pattern of basanite 2128 and
the pattern produced by starting composition 6 (Model A).

●——● 2128
X·······X Model A low p.c.
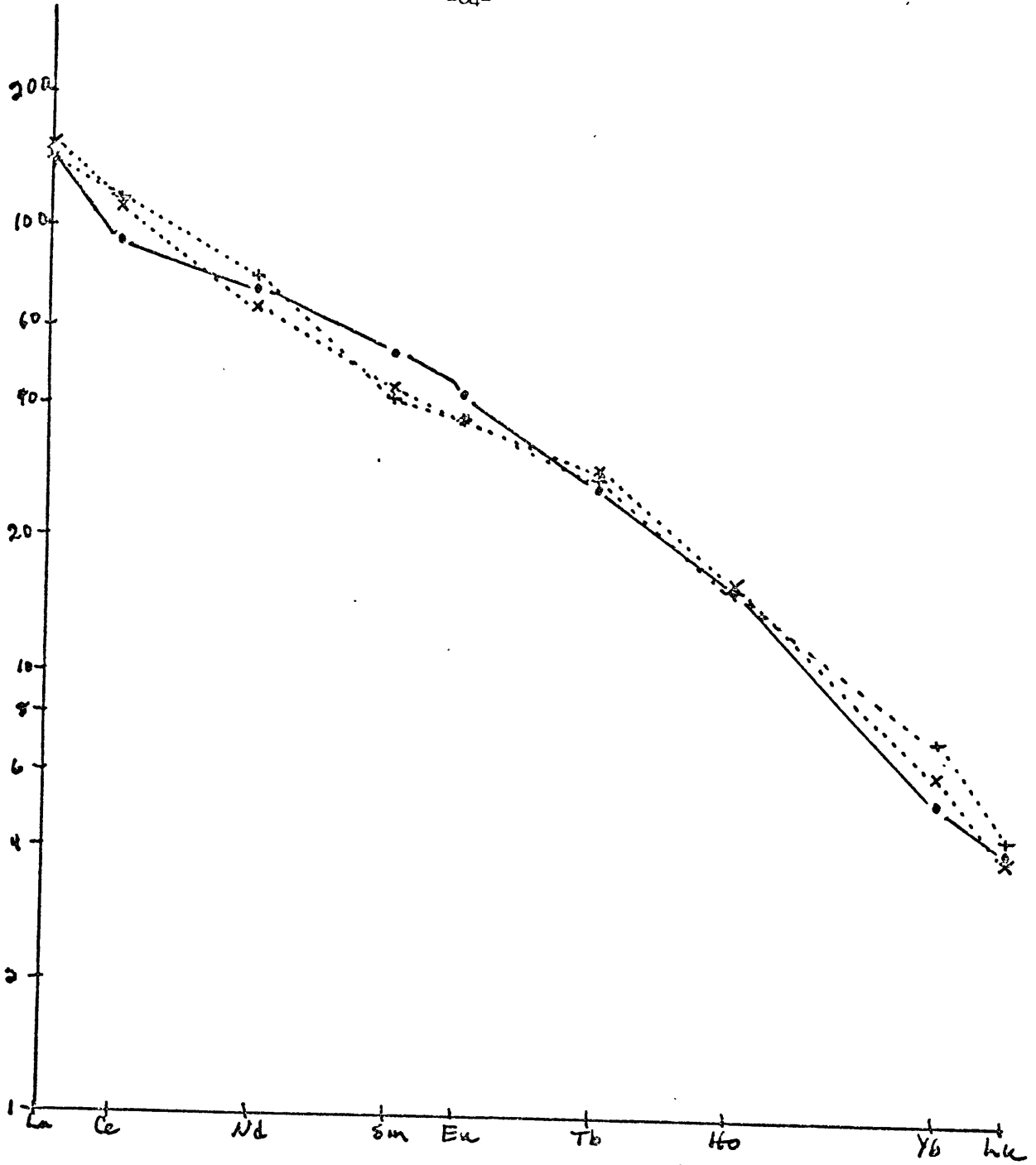+·····+ Model A high p.c.

Figure 13: Graphical comparison of the REE pattern of basanite 2128 and
the pattern produced by starting composition 4 (Model B).
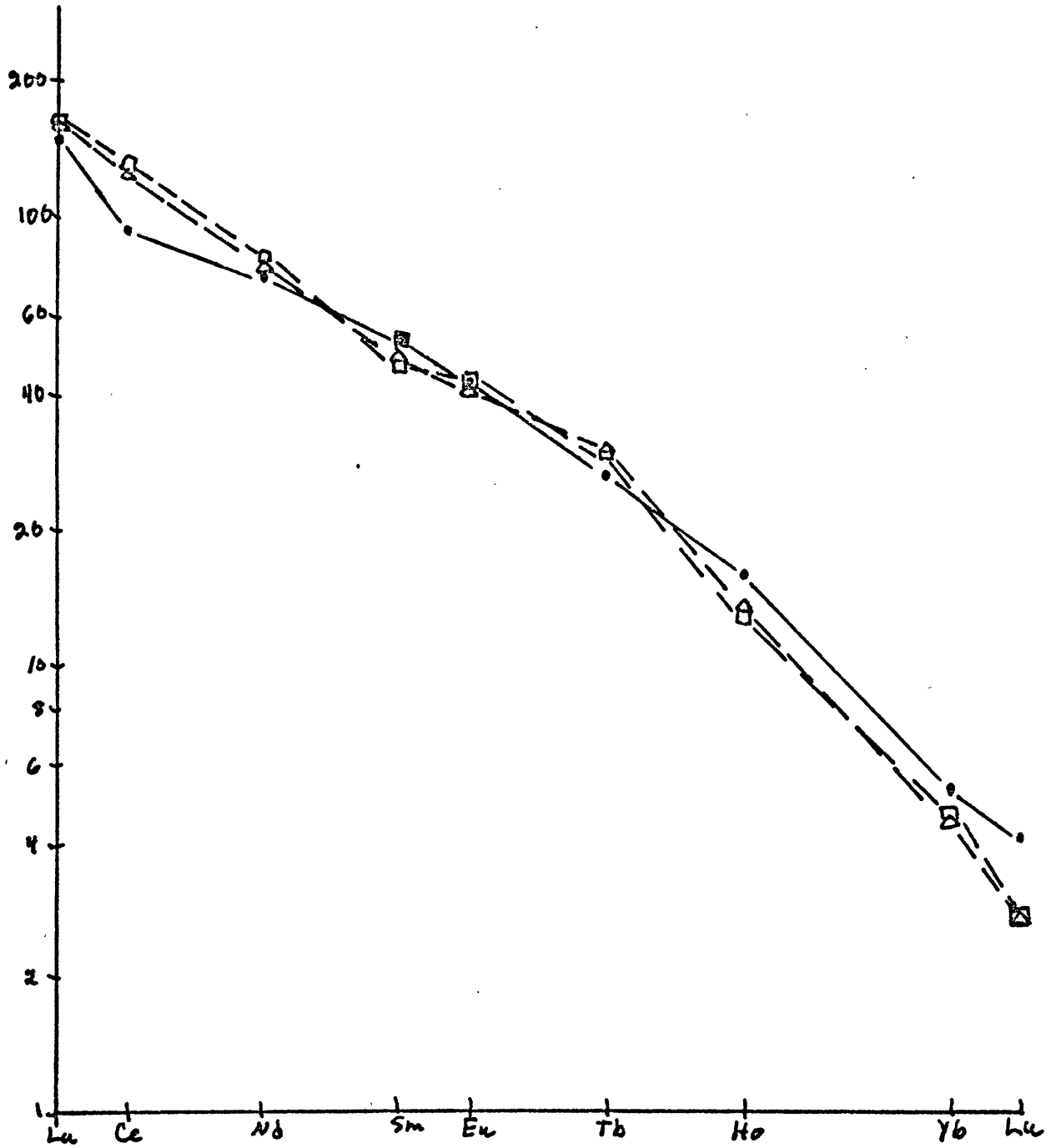
●——● 2128
△---△ Model B low p.c.
□--□ Model B high p.c.

TABLE XIV

Total equilibrium models for basanite 2128

Model B	La	Ce	Nd	Sm	Eu
2128	147	93.8	73.6	53.0	42.7
SC4 0.9% low	80.0	62.6	39.3	25.2	20.9
R1	1.837	1.500	1.873	2.103	2.053
M	157	123	77	49.4	41.0
R2	0.936	0.764	0.956	1.073	1.046

Model B	Tb	Ho	Yb	Lu	ave.
2128	26.7	15.9	5.3	4.1	
SC4 0.9% low	15.5	6.9	2.3	1.4	
R1	1.723	2.314	2.294	(2.929)	1.962
M	30.4	13.5	4.5	2.7	
R2	0.878	1.178	1.170	(3.8)	1.0001±0.144

Model B	La	Ce	Nd	Sm	Eu
SC4 4.1% high	18.3	14.8	9.52	5.34	4.86
R1	8.033	6.338	7.731	9.925	8.827
M	159	128	82.7	46.4	42.2
R2	0.925	0.730	0.890	1.142	1.017

Model B	Tb	Ho	Yb	Lu	ave.
SC4 4.1% high	3.38	1.48	0.53	0.3	
R1	7.899	10.61	10.095	(13.667)	8.682
M	29.3	12.8	4.6	2.7	
R2	0.911	1.227	1.152	(3.8)	0.9992±0.166

Notes for Table XIV are on page 70.

TABLE XIV Continued

Total equilibrium models for basanite 2128

Model C	La	Ce	Nd	Sm	Eu
2128	147	93.8	73.6	53.0	42.7
SC5 0.9% low	85.8	69.8	45.5	27.9	22.5
R1	1.702	1.347	1.626	1.900	1.911
M	167	136	88.5	54.3	43.8
R2	0.874	0.692	0.836	0.976	0.982

Model C	Tb	Ho	Yb	Lu	ave.
2128	26.7	15.9	5.3	4.1	
SC5 0.9% low	15.8	5.96	1.86	1.09	
R1	1.709	2.684	2.688	(3.761)	1.946
M	30.7	11.6	3.6	2.1	
R2	0.879	1.379	1.381	(4.7)	1.098 ± 0.378

Model C	La	Ce	Nd	Sm	Eu
SC5 4.3% high	18.8	15.8	10.8	5.91	5.22
R1	7.77	5.95	6.85	8.97	8.24
M	164	138	94.2	51.5	45.5
R2	0.890	0.609	0.787	1.029	0.945

Model C	Tb	Ho	Yb	Lu	ave.
SC5 4.3% high	3.47	1.30	0.42	0.25	
R1	7.78	12.3	11.9	(16.4)	8.72
M	30.3	11.3	3.7	2.2	
R2	0.891	1.455	1.351	(4.5)	0.995 ± 0.282

Notes for Table XIV are on page 70.

TABLE XIV Continued

Total equilibrium models for basanite 2128

Model A	La	Ce	Nd	Sm	Eu
2128	147	93.8	73.6	53.0	42.9
SC 6 0.6% low	106	78.5	46.8	30.9	26.4
R1	1.387	1.195	1.573	1.715	1.625
M	151	112	66.9	44.1	37.7
R2	0.974	0.838	1.100	1.202	1.138

Model A	Tb	Ho	Yb	Lu	ave.
2128	26.7	15.9	5.3	4.1	
SC 6 0.6% low	20.6	11.3	4.3	2.7	
R1	1.296	1.407	1.23	(1.519)	1.377
M	29.4	16.1	6.1	3.9	
R2	0.908	0.988	0.869	(1.051)	0.99988 ± 0.143

Model A	La	Ce	Nd	Sm	Eu
SC 6 2.8% high	23.4	18.3	11.1	6.38	6.02
R1	6.24	5.14	6.67	8.31	7.14
M	147	115	69.8	40.1	37.8
R2	0.993	0.817	1.060	1.322	1.138

Model A	Tb	Ho	Yb	Lu	ave.
SC6 2.8% high	4.45	2.53	1.06	0.67	
R1	6.07	6.32	4.72	(6.119)	6.29
M	28.0	15.9	6.66	4.2	
R2	0.964	1.006	0.751	(0.976)	1.000 ± 0.167

Notes for Table XIV are on page 70.

TABLE XIV Continued

Total equilibrium models for basanite 2128

Notes for Table XIV: This table shows the best fits for basanite 2128 using all relevant starting compositions (see Table VIII). The first line in each section (labeled "2128") gives the REE chondrite-normalized abundances in the basanite; each page of the table tabulates a different starting composition, both high and low sets of partition coefficients.

SC is starting composition.

R1 is the ratio of the rock to the calculated pattern

M is the computer-generated value multiplied by the average value of R1 (the Model).

R2 is the ratio of the rock to the model.

Percent figures are the percent of partial melting required by the model.

The plus/minus values are one standard deviation.

Parentheses indicate values not included in computing the average.

Although Lu is fit well by model A, it was not included in the averages for consistency with the other starting compositions.

the models fit well on the average of all the elements, the standard deviation indicates the actual closeness of the fit.

The model with the best fit (smallest standard deviation), which I will call "Model A", uses starting composition 6 (Table VIII) with low partition coefficients, and calls for a 0.6% melt. Assuming that the mantle REE pattern is not fractionated with respect to chondrites, this indicates an upper mantle RE content of 1.4 x chondrites. If high partition coefficients are used, 2.8% melt is needed, and the RE content of the upper mantle is 6.3 x chondrites. The fit is still acceptable.

Using starting composition 4, "Model B", with low partition coefficients, the data can be matched almost as closely as with Model A: the standard deviation is 0.144 versus 0.143. This model produces 0.9% melt, and calls for an upper mantle REE content of 2.0 x chondrites. If we shift to the high partition coefficients, percent melt rises to 4.1 and the REE content of the upper mantle changes to 8.7 x chondrites. The fit is still acceptable, and very comparable to the previous model.

It should be noted here that these are limits that the models place on the percent melt and RE content of the upper mantle: since the partition coefficients could be anywhere between the high and low values I have chosen, the percent melt and RE content of the upper mantle will fall within the limits indicated in each model.

Starting composition 5[*](the one closest to Chen's (1971) mantle mineralogy) does not yield satisfactory results: the average fit is acceptable, but the standard deviation is too high. It is interesting to note that the parameters generated by this model (percent melt and upper mantle REE content) are very similar to those required by the two models which do fit the

---

*Model C

data well.

Although I feel that total equilibrium follows Green's experiments more closely than surface equilibrium, it is worthwhile to consider surface equilibrium, if only to look at the complete picture. Reality may well be somewhere in between these two models.

Both Models A and B were examined. Model A gave good results: low partition coefficients required 1% melting and 1.5 x chondrites. The standard deviation is 0.118, quite good a fit. With high partition coefficients, 4% melting and an upper mante RE content of 6.3 x chondrites are required. The fit isn't quite as good, with a standard deviation of 0.148. This data is presented in Table XV and Figure 14. Note that Lu is fit with this model.

Interestingly, Model B did not yield an acceptable fit: with low partition coefficients the standard deviation was 0.254 and with high partition coefficients, 0.264 if Lu is included, and 0.182 and 0.206 respectively if we leave out Lu.

Other trace elements: Several other trace elements were determined in this study: Sc, Cr, Co, Hf, Ta and Th. The following is an attempt to fit these data to the two models.

Using estimates of Lopez-Escobar et al. (1974) for upper mantle abundances of Sc and Co, and of Shaw (1973) for Th, and using chondritic averages of Ehmann and Rebegay (1971) for Hf, and of Ehmann (1971) for Ta, (in each case times the appropriate facter determined above from the REE models), we can calculate the expected abundances of these trace elements and compare the results with the analytical determinations. For these calculations, the partition coefficients discussed in section IV-C-2

TABLE XV

Surface equilibrium model for basanite 2128

Model A	La	Ce	Nd	Sm	Eu
2128	147	93.8	73.6	53.0	42.7
1.0% low	94.6	77.2	47.7	31.5	26.8
R1	1.555	1.216	1.545	1.682	1.600
M	137	112	68.3	45.7	38.9
R2	1.065	0.838	1.079	1.159	1.102

Model A	Tb	Ho	Yb	Lu	ave.
2128	26.7	15.9	5.3	4.1	
1.0% low	20.8	11.3	4.3	2.7	
R1	1.283	1.406	1.236	1.538	1.453
M	30.2	16.4	6.2	3.9	
R2	0.883	0.969	0.855	1.051	1.0001 ± 0.118

Model A	La	Ce	Nd	Sm	Eu
4.0% high	23.6	19.3	11.7	6.54	6.14
R1	6.239	4.860	6.291	8.104	6.987
M	149	122	73.8	41.3	38.8
R2	0.986	0.768	0.998	1.283	1.103

Model A	Tb	Ho	Yb	Lu	ave.
4.0% high	4.46	2.44	0.998	0.628	
R1	5.987	6.516	5.311	6.529	6.313
M	28.2	15.4	6.3	4.0	
R2	0.946	1.032	0.841	1.024	0.9979 ± 0.148

Figure 14: Graphical comparison of the REE pattern of basanite 2128 and
the pattern produced by a surface equilibrium model using
starting composition 6. (Model A)

●———● 2128
X·····X low p.c.
△——△ high p.c.
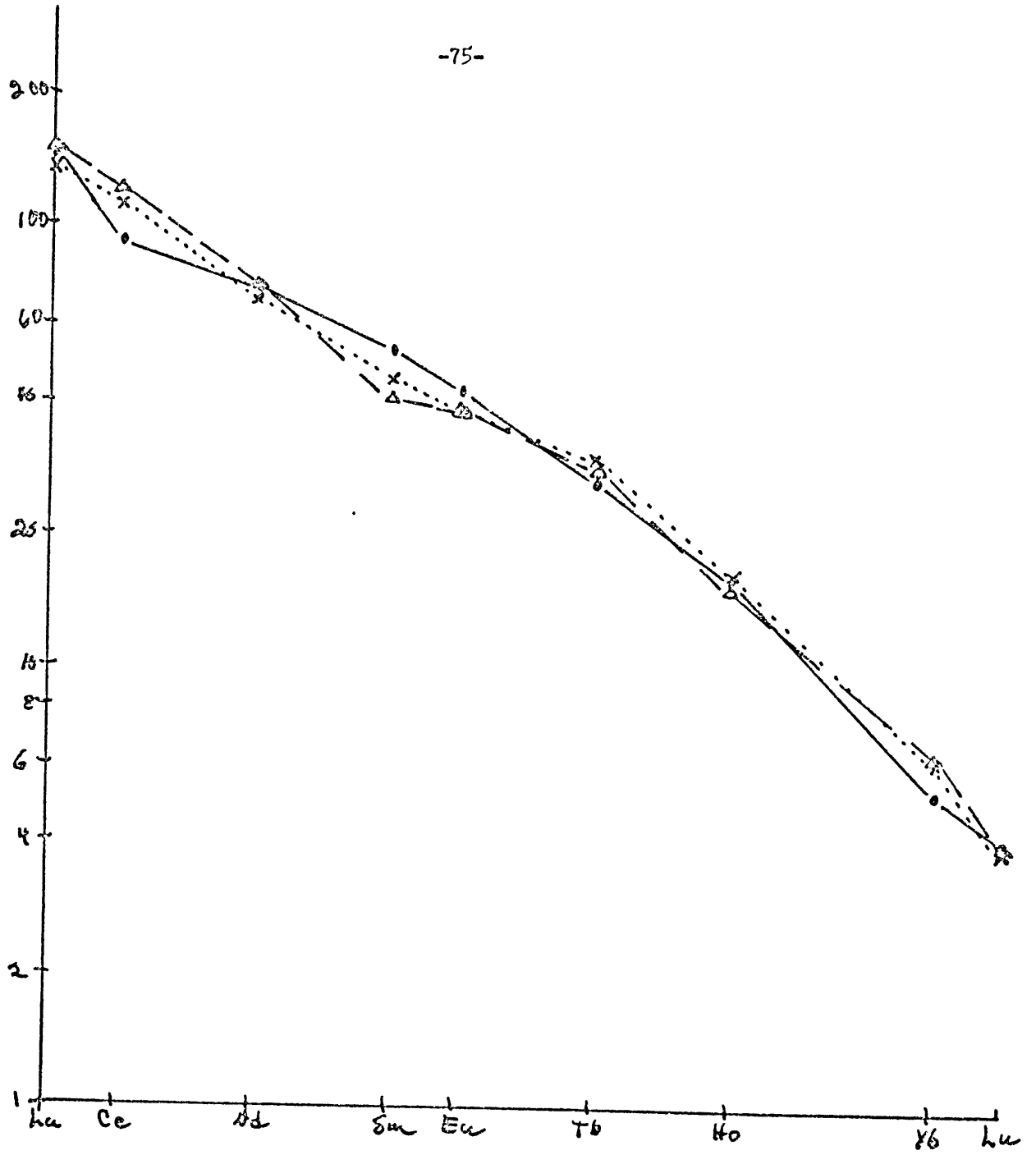
were used. See Table XII. The results are shown in Table XVI, and are not too bad, considering the assumptions involved. Th agrees quite well using the models with the low percent melting; Sc is off by less than a factor of two, Co and Hf by about a factor of two, and Ta by a factor of three.

TABLE XVI

Basanite 2128 models: other trace elements

Model	%	Sc	Co	Hf	Ta	Th	N
2128:Roy		19.6	71.3	7.5	11.3	5.7	
Irving		19.5	72			5.7	
Model A	0.6	13.8	36.8	0.7	3.9	8.3	1.4
	2.8	14.6	37.1	3.3	3.9	1.8	6.3
Model B	0.9	11.1	35.5	1.0	3.7	5.6	1.9
	4.1	11.9	36.0	4.5	3.6	1.2	8.7
Upper Mantle		16	110	0.26N	0.017N	0.05	

% is the percent of melting required by the model.
N is the chondrite factor required by the REE models.

It is worth examining these results and the assumptions that led to them. The question of how well the partition coefficients are known has been dealt with in section IV-C, to some extent, by means of Table XIII. The other important assumption is the abundance of the element in the upper mantle. Each of the five elements will be considered in detail below.

Sc: The initial calculations used Lopez-Escobar's (1974) estimate of 16 ppm for the abundance of Sc in the upper mantle. Alternatively, we can derive a value for pyrolite by combining a value for the abundances in tholeiitic basalt and in peridotite.

Sc in ultramafics:

Turekian et al. 1961:   15 ppm
Vinogradov 1962:   5
Goles 1967:   16
Fisher et al. 1969:   20
Frondel 1969:   4.7-12

Sc in tholeiites:

Turekian et al. 1961:   30 ppm
Hamilton 1961:   24
Vinogradov 1962:   42
Prinz 1967:   29
Norman et al. 1968:   30
Frondel 1969:   35-50
Ewart et al. 1973:   40
Helmke et al. 1973:   25
This paper (appendix III) 31

Pyrolite ≃ 0.75 peridotite + 0.25 tholeiite   (Ringwood 1966)

Therefore, using an average of 12 ppm Sc for the peridotite and an average

of 34 ppm Sc for the tholeiite, 0.75 (12)+0.25 (34)=17.5. Thus Sc in

pyrolite comes to about 17.5 ppm; this raises our results by 9% (Table XVII).

TABLE XVII

Basanite 2128 Sc model: revised

Model	%	Sc
Basanite 2128		19.6
Model A	0.6	15.1
	2.8	16.0
Model B	0.9	12.2
	4.1	13.0

These results are a little closer than the earlier ones. It is worth

noting here the existence of "Sc provinces", found in the abundance of Sc

in crustal rocks, which Frondel (1969) believes reflect inhomogeneities in

the Sc abundance in the upper mantle. Thus this match may be fortuitous; at the same time the existence of Sc inhomogeneitites in the mantle makes the use of averages somewhat dubious.

Co: A brief survey of the literature found the following values for the abundance of Co in ultramafic rocks:

Turekian et al. 1961:   150 ppm
Vinogradov 1962:   200
Goles 1967:   110
Fisher et al. 1969:   110

and the following values for the abundance of Co in tholeiites:

Turekian et al. 1961:   48 ppm
Hamilton 1961:   45
Vinogradov 1962:   45
Prinz 1967:   44
Gunn 1971:   74
Helmke et al. 1973:   35
Ewart et al. 1973:   30
This paper (appendix III) 58

Using values of 110 ppm for the ultramafic componenet and 45 ppm for the tholeiitic component, pyrolite would have about 88 ppm Co. Using Vinogradov's values, pyrolite would have 160 ppm Co. Using both of these values for C_o, the abundance in the source, we get the results shown in Table XVIII. Vinogradov's values are in parentheses.

TABLE XVIII

Basanite 2128 Co model: revised

Model	%	Co	
Basanite 2128		71.3	
Model A	0.6	29.5	(53.6)
	2.8	29.7	(54.0)
Model B	0.9	28.4	(51.6)
	4.1	28.8	(52.4)

Using Vinogradov's numbers brings us closer to the rock value, while using a more average value brings us further away.

Hf: One note on the partition coefficients: the bulk partition coefficient (D_o in Shaw's (1970) equations) for Hf comes to 0.5 for Model A and 1.0 for Model B. Helmke and Haskin (1973), in considering fractional crystallization models for the Steens Mtn basalts, calculate a bulk distribution coefficient of 0.56 for Hf when the average of fifty-two lavas is used; other calculations of theirs have Hf bulk partition coefficients between 0.18 and 0.66. This seems to lend some support to the values of 0.5 and 1.0 used in this thesis.

Hf in ultramafics:

Turekian et al. 1961:	0.6 ppm
Goles 1967:	0.6
Brooks 1970:	1.0

Hf in tholeiites:

Turekian et al. 1961:	2.0 ppm
Brooks 1970:	3.3
Helmke et al. 1973:	4.8
This paper (appendix III)	4.9

Using Brooks' numbers, Hf in pyrolite is 1.55 ppm; using Goles' and Helmke and Haskin's numbers, Hf in pyrolite is 1.85 ppm. Using 1.7 as an average yields the following results (Table XIX). This change in C_o does not really change the results.

One problem arises when the Hf content of the nephelinites is compared with the Hf content of the tholeiites: if the tholeiites are to be derived from a source of identical chemical composition (but different mineralogical composition) to that of the nephelinites, then if Hf is in the garnet phase for the nephelinites and doesn't go into the other phases, then the

TABLE XIX

Basanite 2128 Hf models revised

Model	%	Hf
Basanite 2128		7.5
Model A	0.6	3.4
	2.8	3.4
Model B	0.9	1.7
	4.1	1.7

Hf content of the nephelinites should be less than the Hf content of the tholeiites. A glance at Table III indicates that this is not the case. One possibility is that the two types of basalts come from different types of mantles; this is discussed briefly under Conclusions.

Ta: There is not much data available for Ta.

Ta in ultramafics:

Turekian et al. 1961:   1.0 ppm
Vinogradov 1962:   0.02

Ta in tholeiites:

Turekian et al. 1961:   1.1 ppm
Vinogradov 1962:   0.5
This paper (appendix III) 2.5

Therefore Ta in pyrolite is about 1 ppm (Using Turekian et al.) or about 0.4 ppm (using Vinogradov). We get the following results (Table XX).

This improves the results of the calculation somewhat (compare Table XX with Table XVI) and gives support to the high partition coefficient models. The uncertainty in C_0 more than covers the range allowed by the models.

Th: The following data was collected for Th:

TABLE XX

Basanite 2128 Ta model: revised

Model	%	Ta*	Ta**
Basanite 2128			11.3
Model A	0.6	163	60
	2.8	36	13
Model B	0.9	116	43
	4.1	24	9

* using Turekian et al. 1961
** using Vinogradov 1962

Th in ultramafics:

Turekian et al. 1961:	0.004 ppm
Vinogradov 1962:	0.005
Goles 1967:	0.06
Green et al. 1968: 0.036-	0.1
Rogers et al. 1969:	0.05

Th in tholeiites:

Turekian et al. 1961:	4 ppm
Vinogradov 1962:	3
Rogers et al. 1969:	0.69
"	0.95
This paper (appendix III)	1.4

Using 0.06 for peridotite and 1.0 for tholeiites, we get 0.29 ppm Th in

pyrolite. The results of the calculations are shown in Table XXI.

This value for C_o improves our results if we consider the high per-

cent partial melting (which means the high set of REE partition coeffi-

cients in our model), as did Ta.

As one last calculation, if we consider a chondritic abundance of

Th we can get another estimate of C_o. Using data of Margan (1971) and

estimates of Wakita et al. (1967) and Green et al. (1968) of the chon-

TABLE XXI

Basanite 2128 Th model: Revised I

Model	%	Th
Basanite 2128		5.7
Model A	0.6	48
	2.8	10
Model B	0.9	32
	4.1	7

dritic abundance of Th and multiplying by the factor determined from the REE models, we get the following results (Table XXII).

TABLE XXII

Basanite 2128 Th model: revised II

Model	%	Th	N
Model A	0.6	11.7	1.4
	2.8	11.4	6.3
Model B	0.9	10.9	1.9
	4.1	10.6	8.7

where $C_0 = 0.05N$, where N is the chondrite factor.

This brings us further from the rock value, but not much. Rogers et al. (1969) discuss Th provinces; if Th provinces do indicate Th inhomogeneities in the mantle, then the same comments made about Sc provinces are relevant here.

In general these five trace elements support the partial melting models put forth above, although discrepancies certainly do exist, and further work along these lines is definitely required.

Irving (personal communication) did some trace element analyses of two samples of the Mt. Porndon basanite, which are shown in Table II. We will consider this data briefly to see if it supports the REE models.

V: V in ultramafics:

Turekian et al. 1961:	40 ppm
Vinogradov 1962:	40
Fisher et al. 1969:	100

V in tholeiites:

Turekian et al. 1961:	250 ppm
Hamilton 1961:	300
Vinogradov 1962:	200
Prinz 1967:	339
Ewart et al. 1973:	300

Using 60 ppm for the V content of peridotite and 300 ppm for the tholeiite yields 120 ppm V for pyrolite. The results are shown in Table XXIII.

TABLE XXIII

Basanite 2128 V model

Model	%	V
Basanite 2128		223
Model A	0.6	517
	2.8	494
Model B	0.9	503
	4.1	474

V is off by a factor of two.

Ni: Ni in ultramafics:

Turekian et al. 1961:	2000 ppm
Vinogradov 1962:	2000
Goles 1967:	1500
Fisher et al. 1969:	1600

Ni in basalts:

Turekian et al. 1961:   130 ppm
Hamilton 1961:   70
Vinogradov 1962:   160
Prinz 1967:   164
Gunn 1971:   111-820
Ewart et al. 1973   24

Using 1600 ppm Ni in peridotite and 100 ppm Ni in tholeiites we get about 1200 ppm Ni in pyrolite. Lopez-Escobar (1974) and Shaw (1973) give estimates of 1500 ppm Ni in the upper mantle. Using both these estimates we get the results shown in Table XXIV.

TABLE XXIV

Basanite 2128 Ni model

Model	Ni*	Ni**
Basanite 261-318		
A	147	184
B	154	193

* $C \doteq 1200$ ppm Ni
** $C_o \doteq 1500$ ppm Ni

Percent melt differences insignificant.

The calculation is off by a factor of two; there is less difference between the two models than between the two C_o values.

Cu: Cu in ultramafics:

Turekian et al. 1961:   10 ppm
Vinogradov 1962:   20
Goles 1967:   30

Cu in basalts:

Turekian et al. 1961:   87 ppm
Vinogradov 1962:   100
Hamilton 1961:   143
Prinz 1967:   207

Using 175 ppm Cu in tholeiites and 30 ppm Cu in peridotite yields 66 ppm

Cu in pyrolite. The results are shown in Table XXV.

TABLE XXV

Basanite Cu model

Model	%	Cu
Basanite		53
A	0.6	929
	2.8	881
B	0.9	851
	4.1	793

This calculation is further off than any other, well over an order of mag-

nitude. The partition coefficients indicate that almost all of the Cu will

go into the liquid, while the abundance data indicate that a bulk distribu-

tion coefficient of about 3 would be required. Alternatively, my estimate

of the upper mantle abundance of Cu may be at fault. If we back-calculate

C_o using the basanite value and the given partition coefficients, we get

an upper mantle abundance of 3.7 ppm Cu, much lower than indicated by

any of the ultramafic analyses. Cu is the least understood of the elements

discussed here, and these calculations highlight this fact, a sulfide may
be involved.

Rb: Rb in ultramafics:

Turekian et al. 1961:   0.2 ppm
Vinogradov 1962:   2
Goles 1967:   1
Heier 1970:   0.09-0.16

Rb in basalts:

Turekian et al. 1961:	30 ppm
Vinogradov 1962:	45
Prinz 1967:	0-2
Heier 1970:	8
Gunn 1971:	8

Therefore, using 0.2 ppm for Rb in peridotite and 8 ppm for Rb in tholeiite, we get 2.1 ppm Rb in pyrolite. The results are shown in Table XXVI.

TABLE XXVI

Basanite Rb model

Model	%	Rb
Basanite	43-52	
A	0.6	86
	2.8	46
B	0.9	76
	4.1	36

The calculations fit the data quite well.

Sr: Sr in ultramafics:

Turekian et al. 1961:	1 ppm
Vinogradov 1962:	10
Goles 1967:	20

Sr in basalts:

Turekian et al. 1961:	465 ppm
Hamilton 1961:	560
Vinogradov 1962:	440
Prinz 1967:	652
Gunn 1971:	303

Using 20 ppm Sr for peridotite and 500 ppm Sr for tholeiite yields 140 ppm Sr in pyrolite. Shaw (1973) estimates 25 ppm Sr in the mantle. Using both estimates we get the results shown in Table XXVII.

TABLE XXVII

Basanite Sr model

Model	%	Sr*	Sr**
Basanite	847-897		
A	0.6	3189	569
	2.8	2181	389
B	0.9	2966	529
	4.1	1823	325

* $C_0 = 140$ ppm

** $C_0 = 25$ ppm

The calculations with the model pyrolite are off by a factor of 2 to 4; the calculations using Shaw's estimate fit the data fairly well.

Y: Y in ultramafics:

    Turekian et al. 1961:   0.X ppm
    Goles 1967:   5
    Herrmann 1970:   0.54-5.0

Y in basalts:

    Turekian et al. 1961:   21 ppm
    Hamilton 1961:   46
    Vinogradov 1962:   ?0
    Prinz 1967:   32
    Herrmann 1970:   24

Using 2.5 ppm Y for peridotite and 30 ppm Y for tholeiite we get 9.4 ppm Y for pyrolite. The results of the calculations are shown in Table XXVIII. Model A is a bit low, while model B is low by a factor of 2. Considering the variation in the data on which these calculations are based, this is good agreement.

Zr: Zr in ultramafics:

    Turekian et al. 1961:   45 ppm
    Vinogradov 1962:   30
    Brooks 1970:   26

TABLE XXVIII

Basanite Y model

Model	%	Y
Basanite		30
A	0.6	22
	2.8	24
B	0.9	14
	4.1	15

Zr in basalts:

Turekian et al. 1961:	140 ppm
Hamilton 1961:	146
Vinogradov: 1962:	100
Prinz 1967:	202
Brooks 1970:	190

Using 34 ppm Zr for peridotite and 170 ppm Zr for thoeliite yields 68 ppm

Zr in pyrolite. Using the two different ga/1 partition coefficients, the

results are shown in Table XXIX.

TABLE XXIX

Basanite Zr model

Model	%	Zr*	Zr**
Basanite		323 (XRF)	
		263 (Emis. Spec.)	
A	0.6	553	116
	2.8	488	132
B	0.9	475	63
	4.1	408	70

Zr*: $D^{ga/1}$ 0.33
Zr**: $D^{ga/1}$ 10.0

Agreement is within a factor of two for Zr*, and between two and five for

Zr**.

Ba: Ba in ultramafics:

Turekian et al. 1961:	0.4 ppm
Vinogradov 1962:	6
Goles 1967:	0.4
Puchelt 1972:	25

Ba in basalts:

Hamilton 1961:	420 ppm
Prinz 1967:	175-215
Gunn 1971:	138
Puchelt 1972:	246

Therefore, using 5 ppm Ba in peridotite and 240 ppm Ba in tholeiite we get 64 ppm Ba in pyrolite. The results are shown in Table XXX.

TABLE XXX

Basanite Ba model

Model	%	Ba
Basanite		527
A	0.6	2590
	2.8	1400
B	0.9	2160
	4.1	1060

The calculations are high be a factor of 2 to 5. Shaw (1973) estimates Ba in the mantle to be 0.4 ppm. Using this value for C_0 brings the calculated value down to 10 to 20, even worse than the original assumption.

Thus of Irving's eight analyses (V, Ni, Cu, Rb, Sr, Y, Zr, Ba) all but Cu fit the data within a factor of 2 in one of the models.

2. Olivine nephelinites 2854 and 2896: these two rocks have almost identical REE patterns (see Figure 6), and therefore I am discussing them together. Examination of the RE patterns reveals a change in slope at Eu (Ho was not determined due to counting schedule problems). Following a procedure similar to that outlined above, La/Eu and Eu/Yb ratios were calculated and one starting composition gave acceptable results: 6,

better than with 2128. Starting composition 4 did not yield any patterns which fit the rock data well, and is considered marginal..

The model with the best fit is again model A: using low partition coefficients 0.8% melt is needed, with the upper mantle having a RE content 2.1 x chondrites; using high partition coefficients, 3.5% melt is required, with an upper mantle RE content of 9.0 x chondrites. Model B with low partition coefficients produces 1.3% melt, from an upper mantle 2.9 x chondrites; with high partition coefficients 5.3% melt is called for from a mantle with a RE content 11.9 x chondrites. The two models are compared numerically in Table XXXI, and graphically in Figure 15; olivine nephelinite 2896 is shown in Figure 16 for example only.

Table XXXII shows the Sc, Co, Hf, Ta and Th data, and how they fit the model. Sc and Th and off by less than a fac tor of two, Hf and Co are off by a factor of two and Ta by a factor of three: the same results as for basanite 2128. The figures in parentheses incorporate the changes discussed in the Hf and Sc sections under basanite 2128 above.

TABLE XXXII

Olivine nephelinite 2854 models: other trace elements

Model	%	Sc	Co	Hf	Ta	Th	N
2854		19.2	77.2	8.8	15.7	6.9	
A	0.8	13.8 (16.3)	32.5	1.1 (3.4)	4.5	6.3	2.1
	3.5	14.9 (17.4)	33.1	4.5 (3.3)	4.4	1.4	9.0
B	1.3	11.2 (13.7)	31.7	0.7 (1.7)	3.7	3.8	2.9
	5.3	12.2 (14.7)	32.5	3.0 (1.6)	3.8	0.9	11.9

See text for meaning of parentheses.

TABLE XXXI

Total equilibrium models for olivine nephelinite 2854

Model B	La	Ce	Nd	Sm	Eu
2854	187	133	95.5	66.6	58.2
SC4 1.3% low	60.8	50.2	34.1	23.1	19.5
R1	3.078	2.649	2.798	2.887	2.986
M	173	149	97.4	65.9	55.6
R2	1.091	0.930	0.980	1.011	1.048

Model B	Tb	Ho	Yb	Lu	ave.
2854	34.0	(20.0)	9.3	3.0	
SC4 1.3% low	14.7	6.78	2.3	1.4	
R1	2.310	(2.94)	4.0	2.1	2.855
M	42.0	17.3	6.6	4.0	
R2	0.809	1.156	1.409	0.75	1.0022 ± 0.200

Model B	La	Ce	Nd	Sm	Eu
SC4 5.3% high	15.1	12.7	8.71	5.17	4.74
R1	12.36	10.49	10.96	12.89	12.28
M	180	151	103	61.3	56.2
R2	1.039	0.881	0.927	1.086	1.036

Model B	Tb	Ho	Yb	Lu	ave.
SC4 5.3% high	3.37	1.53	0.55	0.33	
R1	10.09	(13.07)	16.89	8.99	11.87
M	40.0	(18.2)	6.5	4.0	
R2	0.850	(1.099)	1.431	0.75	0.99996 ± 0.207

Ho is an interpolation, since it could not be determined due to scheduling difficulties with the detector. See notes to Table XIV.

TABLE XXXI Continued

Total equilibrium models for olivine nephelinite 2854

Model A	La	Ce	Nd	Sm	Eu
2854	187	133	95.5	66.6	58.2
SC6 0.8% low	87.7	68.0	42.9	29.3	25.2
R1	2.13	1.95	2.24	2.29	2.34
M	186	144	90.8	62.0	53.4
R2	1.007	0.924	1.057	1.081	1.105

Model A	Tb	Ho	Yb	Lu	ave.
2854	34.0	(20.0)	9.3	3.0	
SC6 0.8% low	19.9	11.2	4.35	2.71	
R1	1.71	(1.79)	2.16	(1.10)	2.127
M	42.1	23.5	9.21	5.7	
R2	0.808	0.851	1.010	(0.526)	0.999 ± 0.103

Model A	La	Ce	Nd	Sm	Eu
SC6 3.5% high	20.6	16.3	10.4	6.23	5.91
R1	9.078	8.160	9.183	10.69	9,848
M	185	146	93.3	55.9	53.0
R2	1.011	0.911	1.024	1.191	1.098

Model A	Tb	Ho	Yb	Lu	ave.
SC6 3.5% high	4.44	2.63	1.14	0.73	
R1	7.658	(7.60)	8.158	(4.098)	8.968
M	39.8	23.6	10.2	6.6	
R2	0.854	0.847	0.912	(0.457)	1.00435 ± 0.110

Figure 15: Graphical comparison of the REE pattern of olivine nephelinite
2854 and the pattern produced by Model A,

●——● 2854
X······X Model A low p.c.
+······+ Model A high p.c.
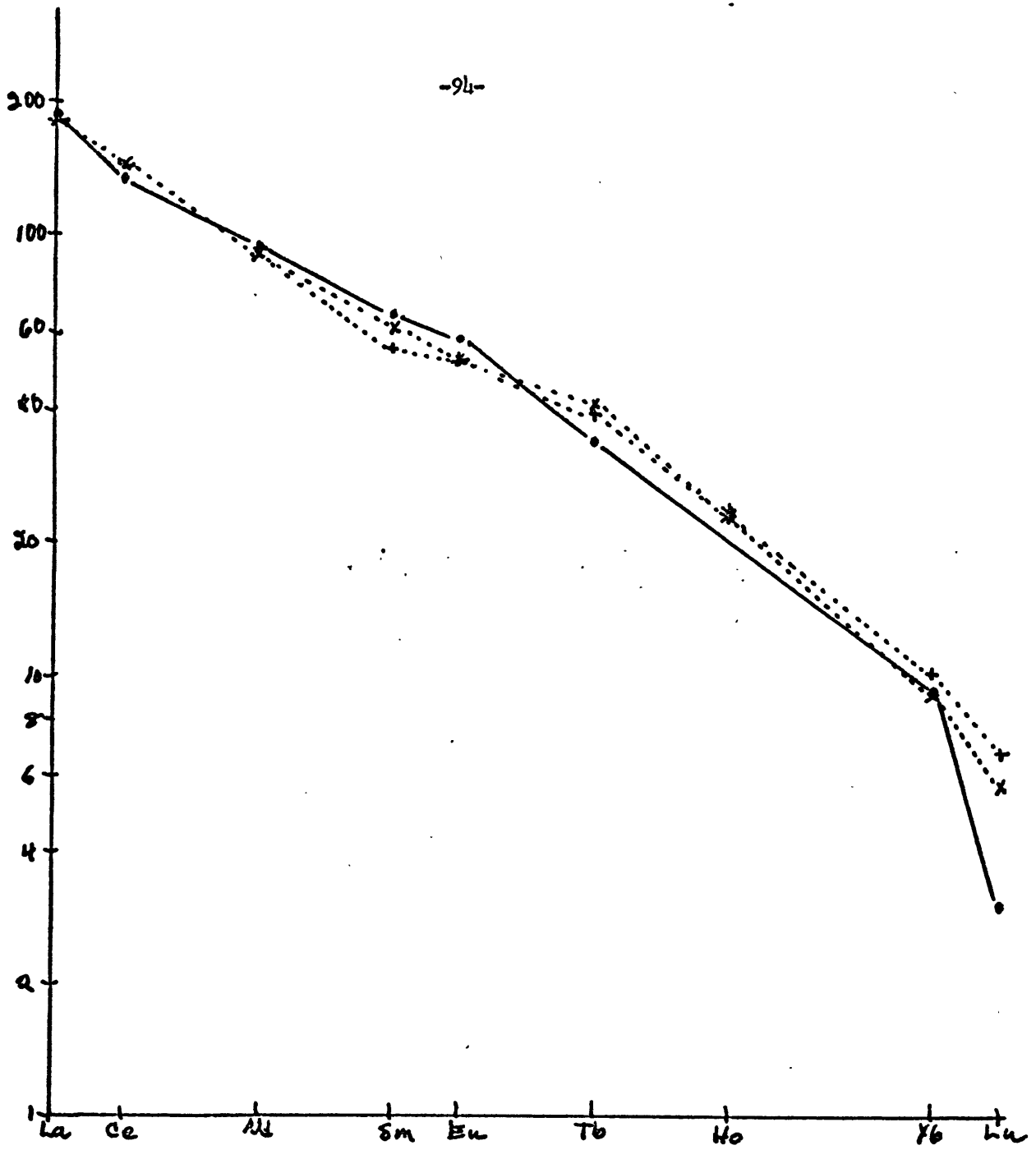
Figure 16: Example of the fit of the Model A pattern to the REE pattern
of olivine nephelinite 2896; R2=1.000±0.122. Ho is an inter-
polation, since Ho could not be determined due to scheduling
difficulties with the detector. Small horizontal lines are
error bars.

●——● 2896

O·····O model (0.8%, Model A low p.c.)
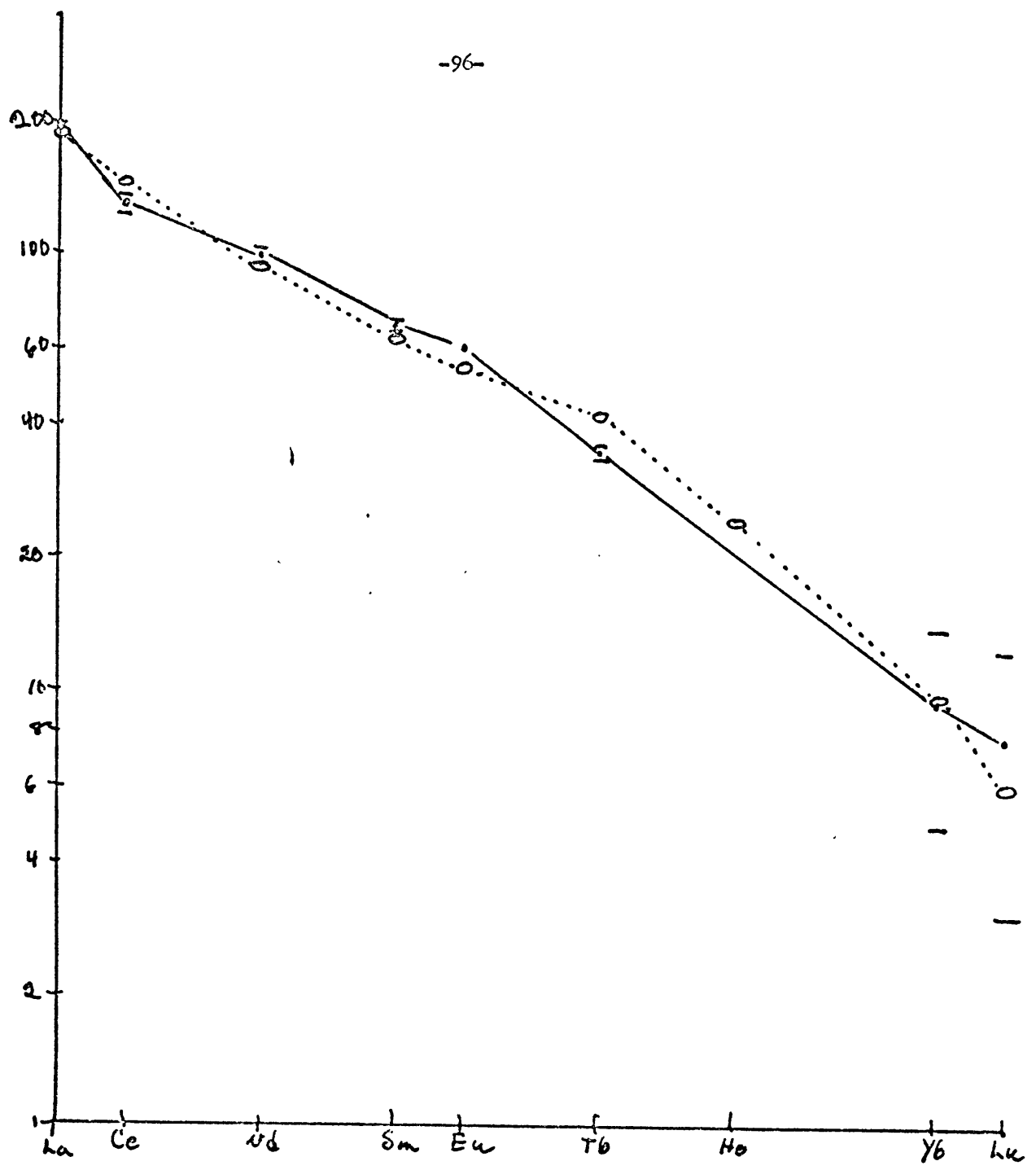
3. Olivine melilite nephelinite 2927: This REE pattern has its change
in slope at Tb; the method described above (La/Tb and Tb/Yb ratios) was used,
with one problem being that the heavy RE trend is not as well defined as
I would have liked. Figure 17 shows two lines for the HREE trend: one
passing through the center of Yb and through the lower section of the Lu
error bar, and the other passing through the upper Yb limit and close to
the center of the Lu analysis. The same two starting compositions (4 and
6) yield satisfactory models of this rock: model A using low partition co-
efficients and 0.5% melt requires an upper mantle RE content 1.9 x chondrites;
using high partition coefficients and 2.7% melt requires an upper mantle
RE content 8.4 x chondrites. Model B with low partition coefficients re-
quires 0.7% melt and an upper mantle RE content of 2.4 x chondrites; with
high partition coefficients it requires 3.7% melt and an upper mantle RE
content 11.0 x chondrites. Starting composition 5 does not yield satis-
factory results. These two models are compared numerically in Table
XXXIII and graphically in Figure 17.

Table XXXIV shows the Sc, Co, Hf, Ta and Th data. In general the
agreement between the models and the data is slightly worse than the two
previous cases.

4. Nephelinite 2860: Green (personal communication) hypothesizes
that nephelinite 2860 might be a low pressure fractionate of olivine
nephelinite 2854, since they are from the same locality and have similar
major element chemistry, with the very notable exception of MgO. Using
the Doherty-Wright (1971) Mineral Distribution program with three dif-
ferent olivines and three different olivine plus clinopyroxene pairs

Figure 17: Graphical comparison of the REE pattern of olivine melilite nephelinite 2927 and the patterns produced by models A and B.

●━━● 2927
X·····X Model A low p.c.
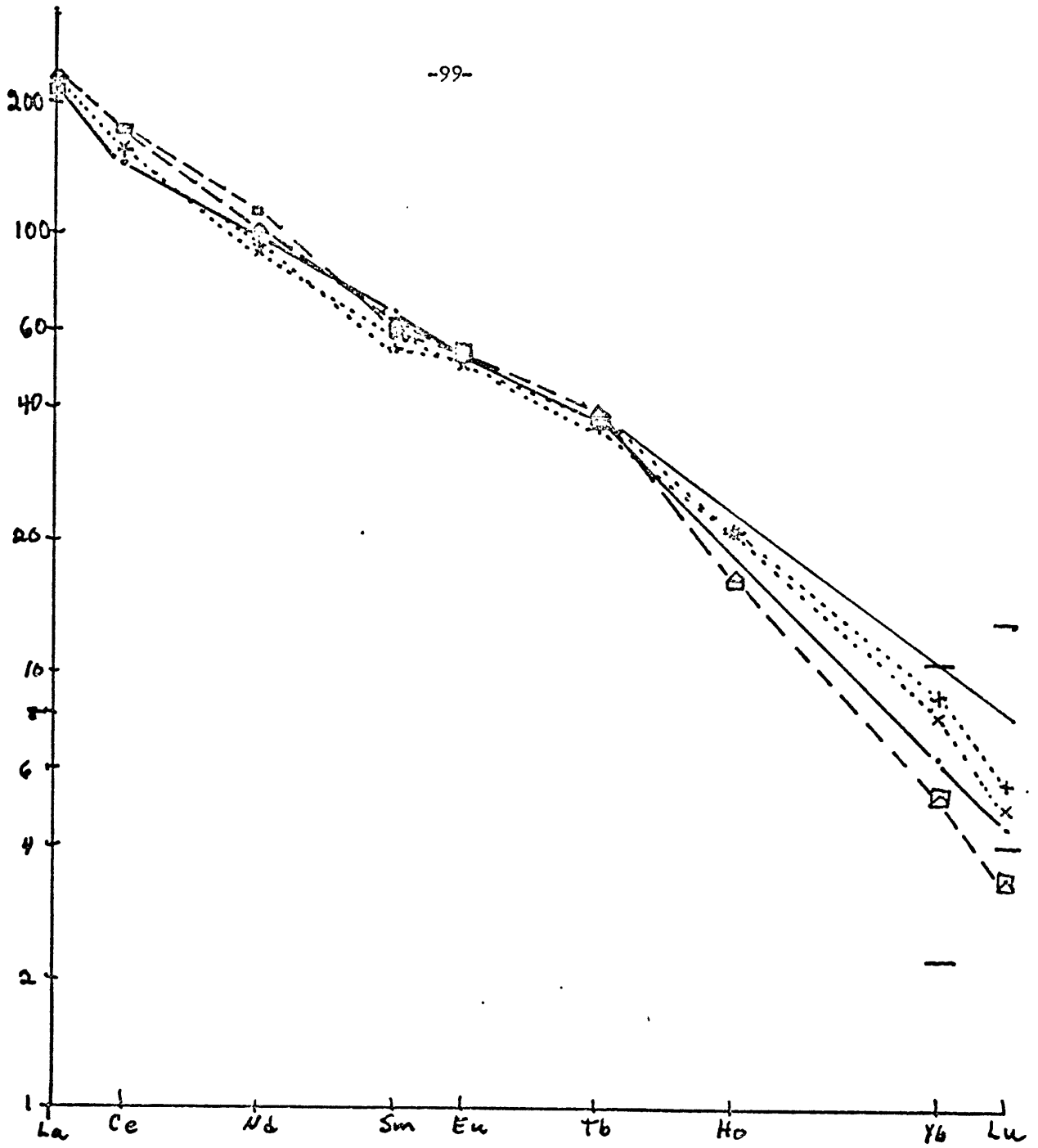+····+ Model A high p.c.
△━━△ Model B low p.c.
▢━━▢ Model B high p.c.

TABLE XXXIII

Total equilibrium models for olivine melilite nephelinite 2927

Model B	La	Ce	Nd	Sm	Eu
2927	219	145	99.2	66.6	53.4
SC4 0.7% low	95.1	71.3	42.5	26.4	21.7
R1	2.303	2.034	2.334	2.523	2.461
M	228	171	102	63.3	52.1
R2	0.961	0.848	0.973	1.052	1.025

Model B	Tb	Ho	Yb	Lu	ave.
2927	37.7	(21)	6.4	(4.4)	
SC4 0.7% low	15.9	6.9	2.3	1.4	
R1	2.371	(3.0)	2.771	(3.14)	2.3995
M	38.2	16.6	5.5	3.3	
R2	0.987	(1.265)	1.155	(1.333)	1.00001±0.094

Model B	La	Ce	Nd	Sm	Eu
SC4 3.7% high	19.7	15.6	9.83	5.40	4.90
R1	11.12	9.29	10.09	12.33	10.90
M	217	172	111	59.6	54.1
R2	1.009	0.843	0.894	1.117	0.987

Model B	Tb	Ho	Yb	Lu	ave.
SC4 3.7% high	3.39	1.47	0.52	0.31	
R1	11.12	(14.3)	12.38	(14.19)	11.033
M	37.4	16.2	5.7	3.4	
R2	1.008	(1.30)	1.122	(1.29)	0.99726±0.104

Ho is an interpolation, since it could not be determined due to scheduling difficulties with the detector. See notes to Table XIV.

TABLE XXXIII Continued

Total equilibrium models for olivine melilite nephelinite 2927

Model A	La	Ce	Nd	Sm	Eu
2927	219	145	99.2	66.6	53.4
SC6 0.5% low	119	85.1	49.0	31.8	27.0
R1	1.84	1.70	2.02	2.11	1.96
M	220	158	90.7	58.9	50.0
R2	0.995	0.918	1.092	1.138	1.060

Model A	Tb	Ho	Yb	Lu	ave.
2927	37.7	(21)	6.4	(4.4)	
SC6 0.5% low	20.9	11.3	4.3	2.7	
R1	1.80	(1.86)	1.49	(1.63)	1.86
M	38.7	21.0	7.9	4.9	
R2	0.974	(1.000)	0.810	(0.897)	0.988±0.107

Model A	La	Ce	Nd	Sm	Eu
SC6 2.7% high	24.6	18.6	11.2	6.41	6.04
R1	8.69	7.79	8.84	10.45	8.77
M	207	157	94.5	55.0	51.0
R2	1.06	0.92	1.05	1.22	1.04

Model A	Tb	Ho	Yb	Lu	ave.
SC6 2.7% high	4.45	2.52	1.05	0.666	
R1	8.47	(8.33)	6.1	(6.606)	8.44
M	36.5	21.1	8.8	5.6	
R2	1.03	(1.00)	0.73	(1.5)	1.01±0.153

TABLE XXXIV

Olivine melilite nephelinite 2927 models: other trace elements

Model	%	Sc	Co	Hf	Ta	Th	N
2927		23.3	83.3	5.8	13.0	13.6	
A	0.5	13.8 (16.3)	32.5	1.0 (3.4)	6.3	10.0	1.9
	2.7	14.6 (17.1)	32.9	4.2 (3.3)	5.3	1.9	8.4
B	0.7	11.1 (13.6)	31.6	0.6 (1.7)	5.8	7.1	2.4
	3.7	11.8 (14.3)	32.2	2.8 (1.7)	5.1	1.4	11.0

See text for meaning of parentheses (under basanite 2128).

(taken from Irving 1971, Green 1973a and b), it was determined that nephelinite 2860 could be roughly matched to olivine nephelinite 2854 by fractional crystallization of approximately 30% olivine. Table XXXV shows one of the computer fits. The match is not especially good; in all the three cases where both olivine and clinopyroxene were used, clinopyroxene was added to 2854 to yield 2860, but not improving the match in general. See Table XXXVI as an example.

The effect of crystallization of 30% olivine on the RE pattern can be calculated using the equation from Gast (1968). The choice of high or low partition coefficients makes negligible difference under these circumstances. Figure 18 shows the 2860 RE pattern and the calculated pattern. The fit is not acceptable.

Looking at the K_2O, P_2O_5 and Th data, it seems a reasonable conclusion that obtaining 2860 from 2854 requires approximately 50% crystallization of certain phases not incorporating these elements. With this assump-

TABLE XXXV

Derivation of 2860 from 2854: olivine

	2854	olivine	2860	Calculation	Difference
SiO_2	41.24	39.75	42.75	41.71	1.04
Al_2O_3	9.92	0.0	14.64	13.07	1.57
FeO	15.87	16.75	13.70	15.60	-1.89
MgO	14.58	43.52	5.74	5.38	0.36
CaO	11.75	0.0	14.99	15.49	-0.50
Na_2O	3.13	0.0	4.33	4.12	0.21
TiO_2	3.54	0.0	3.89	4.66	-0.77

Solution: 131.81   -31.80

Olivine composition from Irving 1971.

This is one of the three olivines used in this attempt; the other two calculations reouired the removal of 29.9 and 28.9% olivine.

The sum of the residuals squared is 7.2832.

TABLE XXXVI

Derivation of 2860 from 2854: olivine-clinopyroxene

	2854	CPX	OL	2860	Calculation	Difference
SiO_2	41.24	51.12	39.75	42.75	42.54	0.21
Al_2O_3	9.92	6.96	0.0	14.64	12.78	1.86
FeO	15.87	5.41	16.75	13.70	14.71	-1.01
MgO	14.58	15.03	43.52	5.74	5.53	0.22
CaO	11.75	19.14	0.0	14.99	16.07	-1.08
Na_2O	3.13	1.49	0.0	4.33	3.97	0.36
TiO_2	3.54	0.89	0.0	3.89	4.43	-0.53
Solution:	122.94	8.50	-31.42			

The olivine and clinopyroxene compositions used in this calculation are taken from Irving 1971; they are a coexisting pair.

This is one of three olivine-clinopyroxene pairs used in this attempt; the other two calculations required i) the removal of 33.99% olivine and the addition of 20.23% clinopyroxene; and ii) the removal of 29.84% olivine and the addition of 11.02% clinopyroxene.

The sum of the residuals squared is 6.1491.

Figure 18: Graphical comparison of the REE pattern of nephelinite 2860 and four attempts to match the pattern by fractional crystallization.

●——● 2860
X·····X 2854 - AMPH
+—·—+ 2854 - 30% OL
△——△ 2854 - OPX - PLAG
□–·-□ 2854 - 1.3% AP - OPX - PLAG
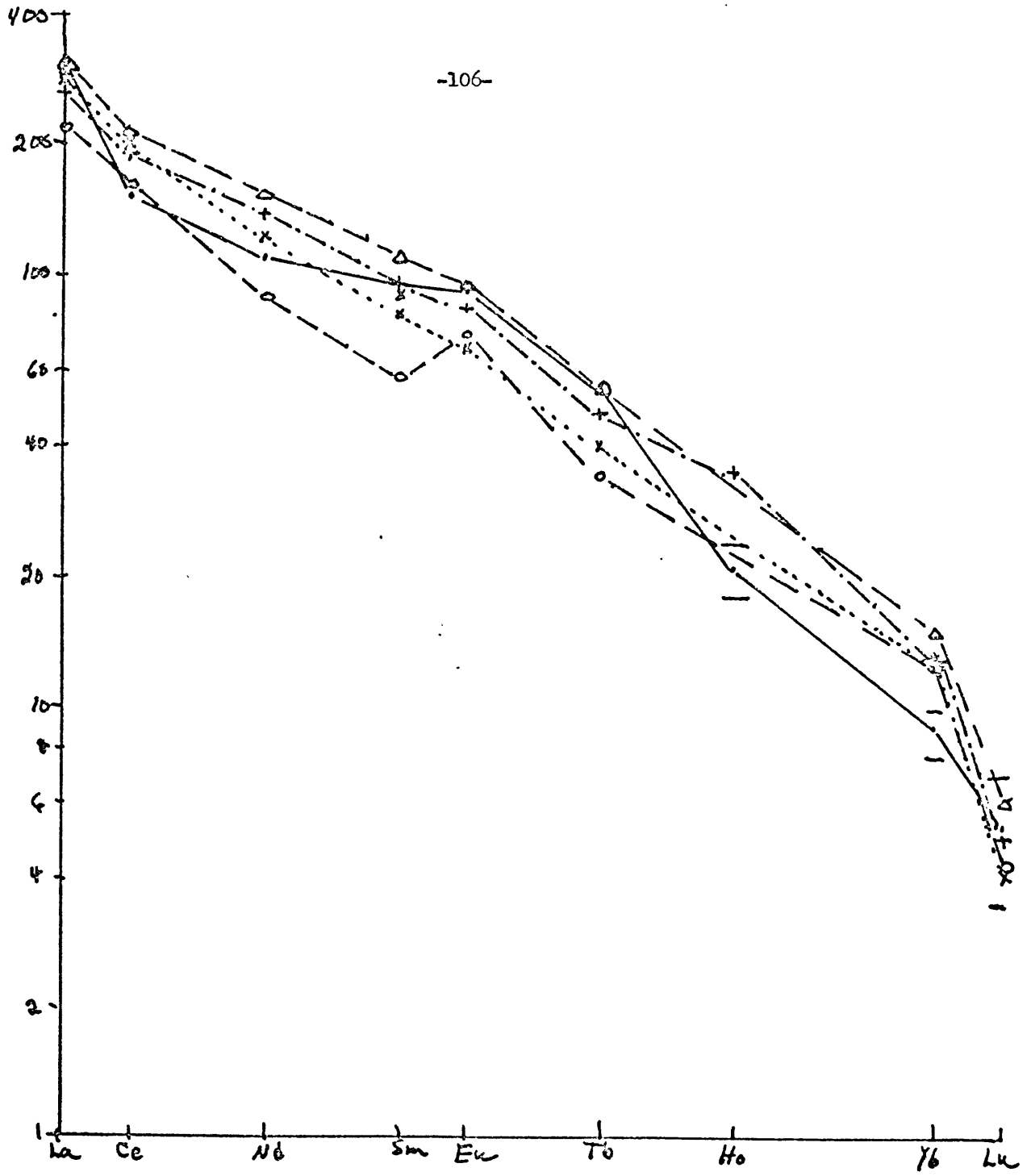
tion, an attempt was made to calculate the bulk composition of the crystallizing phases. See Table XXXVII for the results.

TABLE XXXVII

Derivation of 2860 from 2854: Bulk chemical change

	2854		2860		
SiO_2	39.31	- (0.5)	39.14	19.74	39.7
TiO_2	3.37		3.56	1.59	3.2
Al_2O_3	9.45		13.40	2.75	5.5
Fe_2O_3	2.59		2.16	1.51	3.0
FeO	12.93		10.77	7.54	15.1
MnO	0.20		0.18	0.11	0.2
MgO	13.90		5.25	11.27	22.6
CaO	11.20		13.72	4.34	8.7
Na_2O	2.98		3.96	1.00	2.0
K_2O	1.53		3.10	0.00	0.0
P_2O_5	2.30		4.45	0.00	0.0
				49.85	100.0

Several different procedures were tried in an attempt to figure out a possible mineralogy for this composition. First it was assumed that all of the TiO_2 and Fe_2O_3 with sufficient FeO would form an ilmenite-magnetite solid solution (as implied in Table XXXV). The plagioclase was formed to use the Na_2O, Al_2O_3 and some of the CaO, or alternately, all of the Al_2O_3 and sufficient CaO to form anorthite. Olivine was then formed with the remaining SiO_2 and the MgO (requiring about 25% olivine, very similar

to the Wright-Doherty results). Other attempts were made using diopside

to remove CaO. The end result is that in every attempt a sizable fraction

of the composition could not be taken care of, indicating that the deri-

vation of 2860 from 2854 most probably involves some phases not considered.

Table XXXVIII compares the other trace element data.

TABLE XXXVIII

Comparison of 2854-2860: other trace elements

	Sc	Cr	Co	Hf	Ta	Th
2854	19.2	428	77.2	8.78	15.7	6.91
2860	10.5	11	44.2	10.70	14.9	12.6

The evidence is ambiguous: Co will be enriched in olivine, indicating that

olivine crystallized out; Ni data would be invaluable in confirming this

and in setting limits on the amount of olivine that would have had to

crystalize out. Sc and Cr will both go into clinopyroxene: both go down,

indicating crystallization of clinopyroxene, in conflict with the major

element data. Using Gast's (1968) equation for fractional crystallization,

we can estimate 25% of the residue (the crystallizing phases) to be clino-

pyroxene. Cr indicates only 11%, but Cr may very well be going into a

spinel phase, throwing this calculation off. Hf and Ta are approximately

the same in the two rocks, indicating the bulk solid/liquid distribution

coefficient is approximately one. Since Hf and Ta are not taken into the

olivine or clinopyroxene, perhaps they are being taken into the opaques.

Th (and K_2O, P_2O_5 and La), as mentioned above has increased by a factor

of two, indicating at least 50% crystallization of minerals not containing

these elements.

Several other attempts were made to match the REE pattern, using some less likely minerals: amphibole was considered; apatite, orthopyroxene and plagioclase were tried; the calculated patterns are shown in figure 18, and none of them matches the peculiar LREE pattern shown by 2860.

As one final exercise to find out about the residual phases, the REE were compared, and a bulk distribution coefficient calculated; see Table XXXIX and figure 19.

TABLE XXXIX

Derivation of 2860 from 2854: REE bulk distribution

	2854	2860	c^L/c_o	a
La	187	306	1.636	0.290
Ce	133	151	1.135	0.817
Nd	95.5	110	1.152	0.796
Sm	66.6	93.8	1.408	0.506
Eu	58.2	91.9	1.579	0.341
Tb	34.0	54.3	1.597	0.325
Ho	20.0	21.4	1.070	0.902
Yb	9.3 (7.6)[*]8.7		(1.14)	(0.805)
Lu	3.0	5.3	1.767	0.179

$a = 1 + \ln(c^L/c_o)/\ln F$, where $F = 0.50$

[*] Yb value of 2854 may be lower than 9.3 x chon. see figure 12. About 7.6 x chon would fit a line between Eu and Lu, which would be within the error bars of Tb and Yb. The a value in parentheses uses 7.6 x chon.

Figure 19: Derivation of 2860 from 2854: REE bulk distribution coefficients, calculated in Table XXXIX.
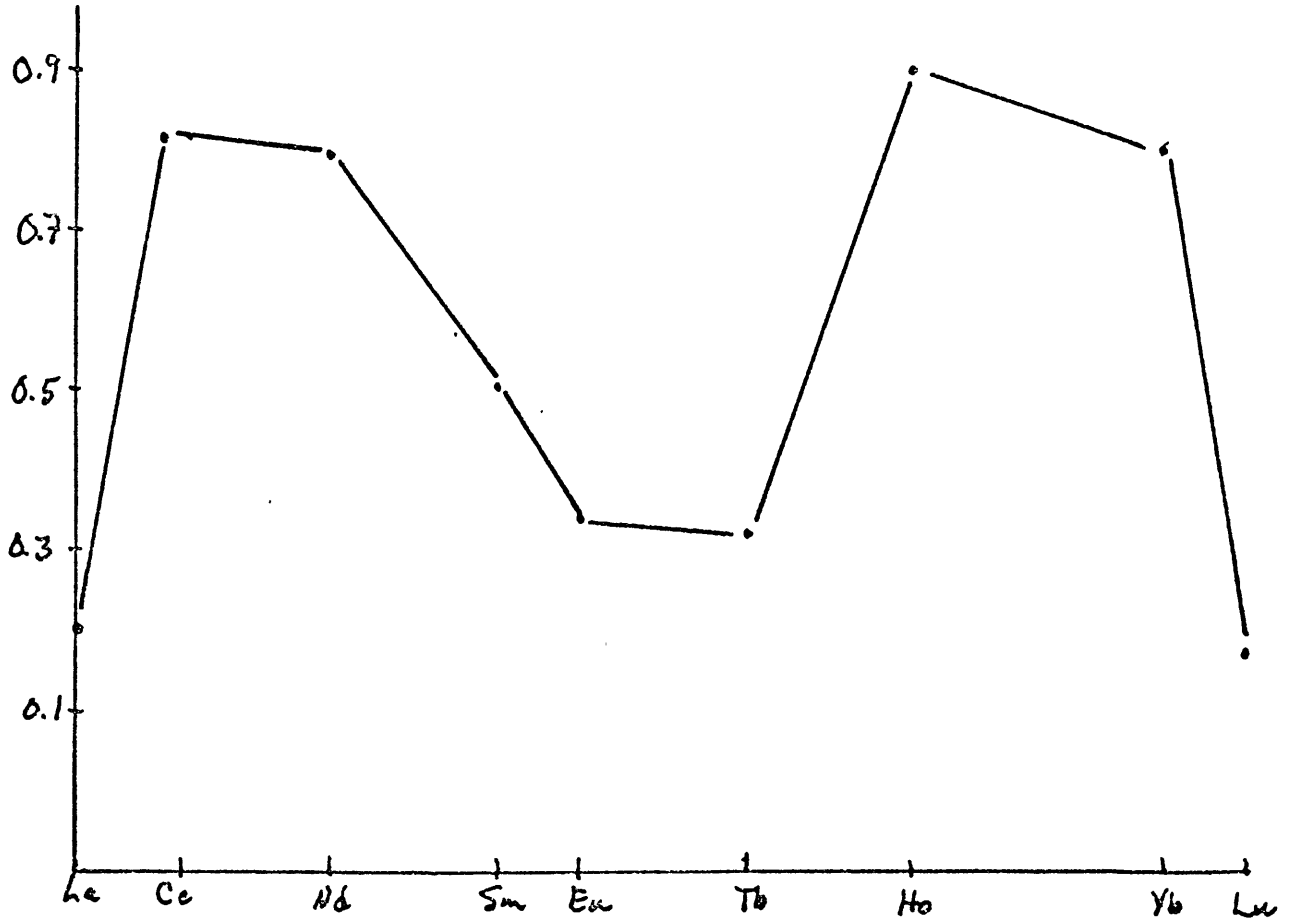
The bulk distribution coefficient for all nine elements is less than one, but has a peculiar shape. No attempt was made to fit this data to a mineralogy, since it is probable that a spinel is one of the crystallizing phases, and spinel partition coefficients are very poorly known (they seem to vary over several orders of magnitude).

In summary, I have not been able to satisfactorily explain the REE pattern in nephelinite 2860.

5. Summary of results for the "nephelinites": If we begin with the assumptions that: 1) partition coefficients are nonvarying and as shown in Table XII; 2) the REE abundances in the source region have chondritic relative abundances; and 3) the melting proceeds under total equilibrium; then the results of this study can be summarized as shown in Table XL, which shows the best fits for the nepheline-normative rocks, for both models using both sets of partition coefficients.

Several trends can be seen in Table XL. In terms of percent melt required, the olivine melilite nephelinite is least, the basanite next, and the olivine nephelinite most. Using Green's models, one would have expected olivine melilite nephelinite < olvine nephelinite < basanite, if the three had come from the same source region. In terms of upper mantle RE content, the basanite requires the lowest concentrations, the olivine melilite nephelinite a medium amount, and the olivine nephelinites the most, though the difference between the olivine melilite nephelinite and the olivine nephelinites is usually less than between the basanite and the olivine melilite nephelinite. In going from low partition coefficients to high partition coefficients, both the percent melt and the RE content of

TABLE XL

Summary for nephelinitic rocks

Model A: (SC6):

58% olivine   22% orthopyroxene   15% clinopyroxene   5% garnet

Rock	% melt	REE Upper Mantle Content (x chon)
Basanite 2128	0.6 - 2.8	1.4 - 6.3
Ol Nephelinite 2854	0.8 - 3.5	2.1 - 9.0
Ol Mel Neph 2927	0.5 - 2.7	1.9 - 8.4

Model B: (SC4):

57% olivine   17.5% orthopyroxene   15.5% clinopyroxene   10% garnet

Rock	% melt	REE Upper Mantle Content (x chon)
Basanite 2128	0.9 - 4.1	1.9 - 8.7
Ol Neph 2854*	1.3 - 5.3	2.9 - 11.9
Ol Mel Neph 2927	0.7 - 3.7	2.4 - 11.0

Assumptions:

1) Partition coefficients are nonvarying and as shown in Table XII;

2) The REE abundances in the source region are relatively chondritic;

3) Melting proceeds under total equilibrium.

* This fit must be considered marginal.

of the upper mantle increase.

In comparing the models we find that for basanite 2128, model A with low partition coefficients fits best, with model B with low partition coefficients very close; olivine nephelinite 2854 fits best with model A with low partition coefficients, and doesn't really fit well with model B, high or low partition coefficients; and olivine melilite nephelinite 2927 fits best with model B with low partition coefficients. The main difference between these models is the clinopyroxene/garnet ratio: in model A it is 3.0, and in model B it is 1.55. Thus the general trend is that the basanite has a higher clinopyroxene/garnet ratio than the olivine melilite nephelinite. This is in agreement with the findings of Kay and Gast (1973) who found the best fits for alkali basalts required a ratio of about 5, the nephelinites a ratio between 1.0 and 1.5, and the potassic basalts a ratio of about 0.3. Looking at the other trace elements, things are ambiguous: we find that usually Co, Hf and Th overlap between model A and model B, with no clear preference for either degree of melting (sometimes high and sometimes low fits better). The Sc and Th models do not overlap (except for 2927); but the difference between the two models is not great. Usually model A is a little bit closer than model B, even for 2927. Considering Irving's data for the Mt. Porndon basanite, the results are still ambiguous: of the seven elements that can be fit by the models, for four of them (V, Rb, Sr and Ba), the models overlap, and three fit better with high percent melting and one with low percent melting. Of the other three elements, Ni calculations are about the same for the two models, for Y, model A is better, and for Zr, model B is better.

Reasons for these discrepancies are not immediately clear: one possibility is that surface equilibrium may be involved to a greater or lesser extent. Surface equilibrium was considered for basanite 2128, generally not changing the results very much: the percent melt was raised (from 0.6% to 1.0% and from 2.8% to 4.0%) and the "x chondrites" factor was also rasied slightly. Thus this does not seem to be too critical a factor for the REE.

It is appropriate at this time to compare the models presented here with those of Kay and Gast (1973).

TABLE XLI

Comparison of Kay and Gast (1973) and this thesis

Nephelinites: % melt: 0.65 - 1.5; x chon: 2.4 - 4.5 ⎫
Alkali basalts: % melt: 0.8 - 2.9; x chon: 1.9   ⎬ Kay and Gast (1973)

Nephelinites: low p.c.: 0.8 - 1.3%; 2.1 - 2.9 x chon ⎫
         high p.c.: 3.5 - 5.3%; 9.0 - 11.9 x chon   ⎪
                                                     ⎬ This thesis
Basanite: low p.c.: 0.6 - 0.9%; 1.4 - 1.9 x chon   ⎪
         high p.c.: 2.8 - 4.1%; 6.3 - 8.7 x chon   ⎭

If the low partition coefficient models of this thesis are considered, the results presented here and those presented by Kay and Gast (1973) are in good agreement. My high partition coefficient models on the other hand differ considerably (as would be expected, considering the partition coefficients used by Kay and Gast). Thus I feel that my work generally agrees with the conclusions of Kay and Gast (1973). This also supports my contention that surface equilibrium vs. total equilibrium modeling does not make very much difference in the conclusions one comes to with respect to undersaturated basalts.

In conclusion, it can be shown that the partial melting of a pyrolite source can generate strongly undersaturated nephelinitic or basanitic magmas when the REE are considered. The other trace elements considered here (Sc, Co, Hf, Ta and Th) on the whole support this hypothesis, but with considerably less consistency. Although the RE patterns may indicate possible source mineralogies, it is not possible at this time to distinguish between several acceptable models on this basis (due to the uncertainty in partition coefficients and melting models). When more is known about both the RE content of the upper mantle, and about the behavior of partition coefficients as a function of composition under upper mantle conditions, perhaps a definitive statement can be made.

B. Rocks with less than 5% normative nepheline (69-1036, 69-1026, 2152, 69-1018 and 2177)

If Figure 3 (page 14) is referred to, it can be seen that the low Al_2O_3 olivine tholeiites can be derived either i) by 25 - 30% melting of pyrolite at 13 - 18 kb, or ii) by 35 - 40% melting of pyrolite at 18 - 27 kb, followed by subsequent crystallization of olivine and aluminous enstatite. Thus to investigate the origin of the tholeiitic rocks it is necessary to have a mineralogy for pyrolite under these conditions. Two sources were used: Green and Ringwood (1963) and Carter (1970); see Table VIII, page 46, starting compositions 7 and 8.

Considering the first derivation mentioned above: Green's olivine tholeiite has 20 - 28% normative olivine and 5 - 15% normative hypersthene. Olivine tholeiite 69-1018 has 14.5% normative hypersthene and 7.5% normative olivine. Therefore if olivine tholeiite 69-1018 has fractionated from Green's olivine tholeiite, it has crystallized and lost 13 - 22% oli-

vine (Irving 1971) (we already determined that olivine tholeiite 69-1018 could not be a primary melt of upper mantle peridotite, see discussion of basalt petrogenesis). This derivation can be checked as follows: the REE pattern for a 22 - 32% partial melt of pyroxene pyrolite can be calculated, and this pattern can be mathematically subjected to crystallization of 13 - 22% olivine.

The first question is: with what mineralogy would this melt be in equilibrium. Green (1970b) states that "Tholeiitic magmas results if the degree of melting is <u>sufficient to eliminate clinopyroxene</u> from the residual phases (p. 230, Green's emphasis)." Thus, the tholeiitic magma will be in equilibrium with olivine and orthopyroxene. This initial mineralogy (pyroxene pyrolite) has an olivine/orthopyroxene ratio approximately equal to three. Therefore, ANATEXIS was run with an initial mineralogy of 67% olivine and 33% orthopyroxene, melting in equal proportions (at 30% melt the olivine/orthopyroxene ratio will be three).

The REE patterns produced by ANATEXIS for the melting interval 15% to 35% are essentially flat: the La/Eu and Eu/Yb ratios vary from 1.01 to 1.00 and 1.05 to 1.01 respectively for low partition coefficients, and from 1.05 to 1.02 and from 1.25 to 1.07 respectively with high partition coefficients. This can be compared with the REE patterns of the rocks, shown in Figure 7 (page 33) and summarized below in Table XLII. Thus we see that none of the tholeiitic rocks can be derived solely from olivine and orthopyroxene. The REE patterns of the rocks just cannot be matched by the equilibrium melting of just these two minerals. This analysis applies also to the second possible derivation mentioned above, since this method

TABLE XLII

Summary of REE patterns of the tholeiitic rocks

Sample	La/Eu	Eu/Yb	La/Tb	Tb/Yb
69-1036	2.43	2.48	4.86	1.24
69-1026	3.14	3.05	4.60	2.04
2152	3.45	2.65	4.55	2.01
69-1018	2.14	2.36	3.17	1.60
2177	2.61	2.24	3.74	1.56

also leads to equilibrium with only olivine and orthopyroxene. Fractional crystallization of olivine or olivine plus clinopyroxene will not change the patterns sufficiently to match the rock patterns.

It remains to be seen if a method can be found that will match the tholeiitic rock patterns.

If we go back to the starting composition used with the nephelinitic rocks, what can we find out? Using starting composition 4 (57% olivine, 17.5% orthopyroxene, 15.5% clinopyroxene and 10% garnet) (model B), the La/Eu and Eu/Yb ratios were calculated for both high and low partition coefficients (see Figure 20 for the RE patterns): none of the calculations fit the rock data. When La/Eu is similar, the Eu/Yb ratio is much higher, indicating that a good match cannot be made. Either the LREE or the HREE will be completely out of line. This also holds true if one considers the La/Tb and Tb/Yb ratios. Using starting composition 6 (58% olivine, 22% orthopyroxene, 15% clinopyroxene and 5% garnet) (model A) the same problem occurs: it is not possible to match both sections of the REE patterns.

Figure 20: REE patterns produced by partial melting of garnet peridotite:
0.5 to 27.0% melt. Solid lines indicate low partition coeffi-
cients. One curve for high partition coefficients is indicated
by the dashed line, equivalent to 0.5% melt. Generally, the
high partition coefficient curves behave similarly to the low
partition coefficient curves, quickly flattening out, so that
results for high degrees of melting are virtually identical for
the two sets of partition coefficients. (The Yb abd Lu values
for the high partition coefficient curve are off scale.)

The other starting composition (no. 5: 68% olivine, 8% orthopyroxene, 11% clinopyroxene and 13% garnet) yields the same results. Thus it has been shown that the tholeiites cannot be produced with garnet in the source region: garnet's affinity for the HREE is too strong, and causes the slope of the HREE trend to be too steep to be able to match the tholeiitic trend. This finding agrees with Helmke and Haskin's (1973) conclusion that a maximum of 1.5% garnet could be present in the source region of the Steens Mtn tholeiites.

As a third attempt, starting compositions with only olivine, orthopyroxene and clinopyroxene were considered. This says, in effect, that the degree of melting required is higher than that required to eliminate all the garnet from the source. This is supported by the Ta data, shown in Figure 21, where those rocks which can be produced by a source with garnet have a trend very different from the tholeiitic rocks. If we begin with starting composition 4, and assume that the garnet and clinopyroxene melt in equal proportions (0.4) and the olivine and orthopyroxene also melt in equal proportions (0.1), then the garnet would be exhausted at 25% partial melting. The composition at this point would be 72.5% olivine, 20.0% orthopyroxene and 7.5% clinopyroxene. If these three remaining minerals melt in the proportions olivine:orthopyroxene:clinopyroxene::1:1:3, we can calculate the resulting REE pattern. The pattern is essentially flat: La/Yb varies from 1.04 to 1.15, with the change in slope at Eu (or Tb) being less than 5%, generally about 1%. Figure 20 shows these patterns. Other three phase starting compositions were tried; principally Green and Ringwood's (1963) pyroxene pyrolite mineralogy (66.6% olivine, 16.1% ortho-

Figure 21: Plot of Ta vs. Yb: note the two trends: the high Ta points
are the nephelinitic rocks, whose REE pattern can be reproduced
by a source with garnet; the low Ta points are the tholei-
itic rocks, whose REE pattern cannot be duplicated by a source
with garnet. It is known that Yb is partitioned into garnet.

● Nephelinites
✗ Tholeiites
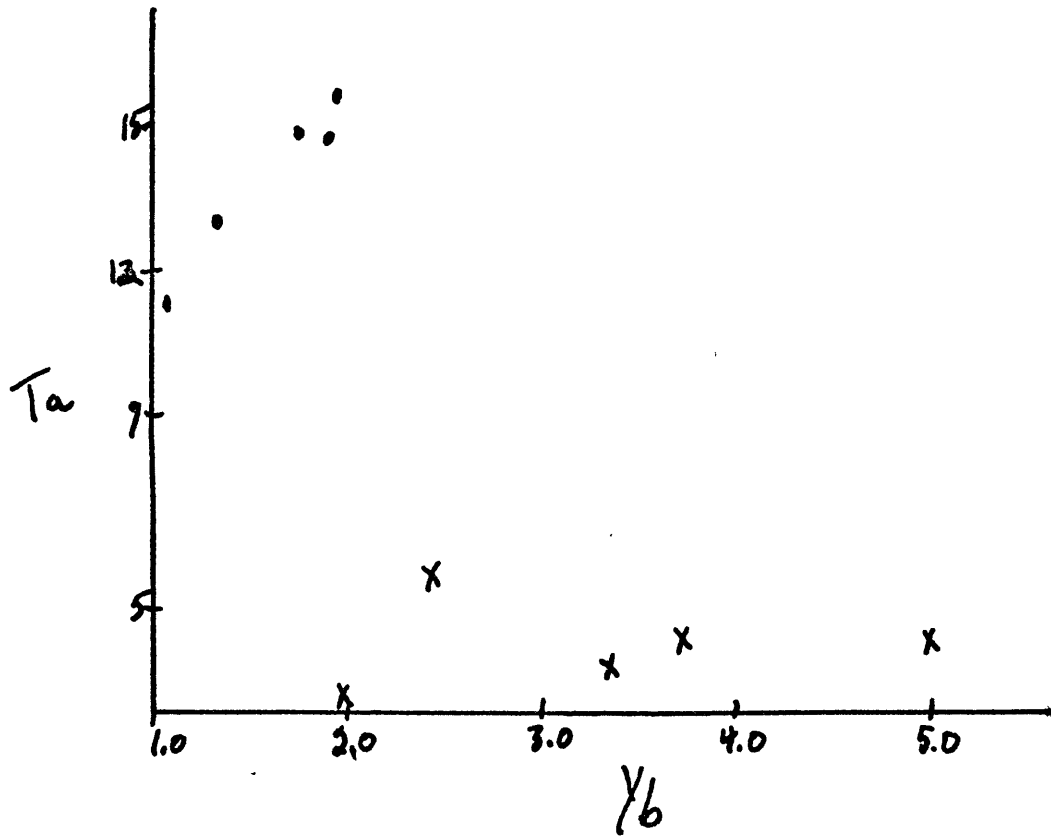
pyroxene and 17.3% clinopyroxene). This did not yield acceptable results:
in every case the REE pattern is much too flat. The tholeiitic rocks have
Eu/Yb ratios varying between 2.2 and 3.1; the calculated patterns vary
between 1.0 and 1.5. Thus an olivine-orthopyroxene-clinopyroxene assem-
blage cannot control the HREE in these rocks. (This was further verified
by considering 10 other starting compositions, varying from 53.9% olivine,
22.5% orthopyroxene and 23.6% clinopyroxene to 87.9% olivine, 7.4% ortho-
pyroxene and 4.7% clinopyroxene).

Another possible source for the tholeiites is olivine, orthopyroxene,
clinopyroxene and spinel. Two spinel-bearing assemblages were considered:
Green and Ringwood (1963) (see Table VIII: SC 7) and Carter (1970) (SC 8).
Using the spinel partition coefficients shown in Table X, we find that
neither of these two compositions can produce the required patterns. One
problem here is that spinel partition coefficients seem to vary over sev-
eral orders of magnitude; however, spinel is not likely to be important
in the production of these basalts.

The specific figures quoted above refer to total equilibrium melting.
The results do not change significantly when surface equilibrium is con-
sidered. In each case the ratios are almost the same, and the difference
decreases with increasing percent of melting.

We seem to have come to a dead end: four different mineralogical assem-
blages have been tried (olivine and orthopyroxene; olivine, orthopyroxene
and clinopyroxene; olivine, orthopyroxene, clinopyroxene and spinel; and
olivine, orthopyroxene, clinopyroxene and garnet) and none of them produce
a REE pattern which comes very close to the patterns exhibited by the rocks.

When high degrees of melting required by Green's hypotheses are considered, the original composition (mineralogically) of the source makes only small differences in the calculated equilibrium REE pattern.

It can also be shown that the tholeiitic patterns cannot be produced by fractional crystallization from one of the nephelinitic magmas. The nephelinitic magmas have REE contents equal to or higher than the tholeiites. Unless one calls into account some mineral like apatite (which produces a Eu anomaly) or a RE mineral like monazite, fractional crystallization would tend to raise the RE content higher.

If we consider fractional crystallization from the tholeiitic magmas (high degrees of partial melting) produced by ANATEXIS, it is clear that olivine alone will not steepen the curve as required, although it will raise it absolutely. If we consider olivine and clinopyroxene, it is possible to calculate that if 90% of the liquid crystallized as 16.5% clinopyroxene and 83.5% olivine, the REE pattern would match the given rock (olivine tholeiite 69-1018) quite well (considering only the La/Yb ratio). This assumes high partition coefficients for both steps of the process (melting of peridotite and crystallizing olivine and clinopyroxene), and that the RE content of the upper mantle is one times chondrites. Raising this to two times chondrites shifts the parameters to 80% crystallization, the crystals being 24.6% clinopyroxene and 75.4% olivine. Raising the RE content of the upper mantle to five times chondrites requires approximately 60% crystallization of 55.9% clinopyroxene and 43.6% olivine. This is still a high percentage of the rock to fractionally crystallize. (No attempt has been made to examine this process on a major element basis.)

The only obvious assumption that might be wrong is that of the chondritic abundance pattern of the source. It might alternatively be fractionated with respect to chondrites, and therefore be able to modify the slope of the REE pattern, necessarily extensively. One point against this

is that neither Kay and Gast (1973) nor this thesis was required to do this for the nephelinitic rocks. If we are to reconsider our conclusions regarding the nephelinitic rocks with this modification, we find that the degree of melting required to match the patterns will be raised, probably significantly. Any estimates of how much the degree of melting would be raised would have to assume a) an assemblage to be in equilibrium with a certain rock, and b) a degree of melting which would produce this particular rock. Then a "fractionation factor" can be calculated for each of the REE. This procedure was followed by Hertogen and Gijbels (1974), using an olivine-orthopyroxene-clinopyroxene-hornblende-apatite source. They assumed their most undersaturated rock to be the product of 5% melting and then calculated C_0 from this assumption. They were able to generate both the tholeiitic rocks and the nephelinitic rocks of their suite by this method. When I attempted this procedure, I was unable to reporduce the nephelinitic rocks.

Summary for the tholeiitic rocks: Considering source mineralogies: olivine and orthopyroxene; olivine, orthopyroxene and clinopyroxene; olivine, orthopyroxene, clinopyroxene and spinel; olivine, orthopyroxene, clinopyroxene and garnet, no pattern like those exhibited by the tholeiitic rocks can be produced within the limits of our assumptions. This indicates that the REE pattern of the source is not chondritic, in agreement with Hertogen and Gijbels (1974). One point worth consideration is the typicalness of these tholeiitic rocks. Comparison of Table XLIII with Table III shows that only 69-1018 can be considered to be a typical tholeiite in terms of REE abundance. This agrees with the data shown in Figure 5, the Coombs plot, where 69-1018 is solidly in the olivine tholeiite part of the diagram. However, while the REE patterns of 2152 and 69-1026 are definitely steeper than typical patterns, the slopes of 2177 and 69-1036 (and 69-1018) are quite similar to the typical pattern. I feel that there is enough similarity between the five basalts that when we can explain the origin of one of them, we will probably be able to explain them all.

TABLE XLIII
Typical tholeiitic REE patterns

	1	2	3	4	5	6
La	64.2	76.3	16.1	27.5	42.5	135
Ce	60.2	61.6	25	35.2	43.6	162
Nd	53.3	50.8	21.3	30.9	37.5	70
Sm	40.3	39.9	20.7	26.7	31.0	45
Eu	31.9	28.6	18.4	24.3	30.4	33
Tb	24.9	24.5	14.0	19.0	25.5	23
Ho	21.4	19.1	8.2	11.1	13.7	21
Yb	16.8	17.4	5.3	8.1	11.5	22
Lu	14.5	15.5	5.6	7.5	10.3	17

1. Helmke and Haskin (1973): average of 52 Steens Mtn tholeiites.

2. Helmke and Haskin (1973): BCR-1.

3, 4, 5. Schilling (1966), Schmitt and Smith (1961) and Wildeman (1971) unpublished: column 3 is the lowest of 9 tholeiites, column 4 the average, and column 5 the highest; all 9 samples were Hawaiian.

6. Frey et al. (1968): Deccan basalt.

In the analyses reported above, La/Yb varied from 2.37 to 6.14, the average being 3.77.

VI. CONCLUSIONS

1) Amphibole is not in equilibrium with the rocks studied in this thesis.

2) The REE patterns of the highly undersaturated, nephelinitic rocks considered in this study can be generated by a partial melting model, beginning with reasonable partition coefficients and a reasonable source composition (both mineralogically and REE-wise). The degree of partial melting required, while generally in agreement with Green's models, is in detail slightly different.

3) The REE patterns of the tholeiitic, less undersaturated basalts considered in this study cannot be produced except by foregoing a chondritic RE abundance pattern in the source region.

Two possibilities to reconcile the last two conclusions exist:

A) The two basalt types come from very different mantles, in terms of REE abundance; this is possible, since consensus attributes the undersaturated basalts to greater depths than the tholeiitic rocks. This leaves un s with the problem of generating these two distinct mantles.

B) Revising the model in such a way as to account for the tholeiitic rocks and then finding out whether such a model could generate the nephelinitic rocks. This may well be the proper alternative: by abandoning the chondritic REE distribtuion one may be able to develop a self-consistent set of models for trace elements and major elements for all basalt types.

FURTHER WORK

Several very basic problems were encountered in interpreting the data

in this thesis. For example, the behavior of partition coefficients for the REE as a function of composition, temperature and pressure is not well understood. Thus one can only handle the situation in a gross way by using a range of partition coefficients. It would be of great use if RE abundances and distributions could be measured in minerals under experimental petrological conditions. This is just as true for the other trace elements considered in this study.

Another basic difficulty was the lack of information on upper mantle abundances of trace elements. This is obviously a very difficult question to which we may never know the complete answer, but this sort of information would be very useful.

As a last suggestion, further work should be done on the origin of continental tholeiites. Petrological studies so far seem to have concentrated on the more undersaturated basalts.

ACKNOWLEDGEMENTS

APPENDIX I

Analytical Details

All irradiations were done at the MIT Nuclear Research Reactor in

Cambridge, Massachusetts between July 17, 1973 and October 29, 1973. The

counting schedule was as follows:

Count	Cooling Time	Counting Time	Detector
1	app. 5 days	2 hrs	LEPS
2	" 8 d	2 h	18cc
3	" 15 d	4 h	LEPS
4	" 30 d	8 h	18cc

The following elements were determined:

TABLE A1-I

Nuclide	Energy (kev)	Count
Sc-46	889.4	4
Cr-51	320.0	4
Co-60	1332.4	4
Ba-131	216.1	4
Ba-131	496.3	4
La-140	486.8	2
La-140	1595.4	2
Ce-141	145.4	3
Nd-147	91.4	3
Sm-153	103.2	1
Eu-152	121.8	4
Eu-152	1407.4	4
Tb-160	298.6	4
Ho-166	80.6	1
Yb-169	63.3	1
Yb-169	63.3	3
Yb-175	282.6	2
Yb-175	396.1	2
Lu-177	208.4	2
Hf-181	482.2	4
Ta-182	1189.0	4
Ta-182	1221.6	4
Th-232	311.8	4

All data from Dams and
Adams (1968).

APPENDIX II

Counting statistics and statistical error
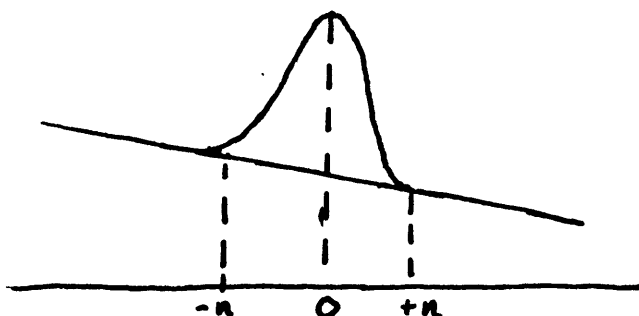
The area under the photopeak is made up of two components: the counts due to the element of interest and the background; therefore, when doing peak integration it is necessary to subtract out the component due to background.

$$A = \sum_{-n}^{n} a_i - B,$$

where A is the area of interest, a_i the counts in channel i, and B the total background. Background is assumed to be linear beneath the peak since there is little evidence to justify fitting a higher-order curve to the raw data. For purposes of calculation, the background is taken as the average of the two points on either side of the peak:

$$B' = \frac{b_n + b_{-n}}{2},$$

where b_n is the count n channels higher than the center of the peak, and b_{-n} the count n channels lower than the center of the peak. B' is then multiplied by the number of channels used in the integration, $2n+1$. Thus the area under the peak, A, is equal to

(1)
$$A = \sum_{-n}^{n} a_i - \left(\frac{b_n + b_{-n}}{2}\right)(2n+1).$$

Statistical error in the number of counts in any channel is equal to the square root of the number of counts in that channel (Friedlander et al. 1964). The error in the first term on the right side of equation 1 is then

$$\sqrt{\sum_{-n}^{n} a_i} \, .$$

The error in a constant times an uncertain number is that constant times the error: $c(B \pm b) = cB \pm cb$. Therefore the error in the background is

$$\sqrt{(2n+1)^2 \, (b_n + b_{-n})/4}$$

The error in the difference between two uncertain number is

$$X \pm x - Y \pm y = X - Y \pm \sqrt{x^2 + y^2}$$

Therefore the error in the peak integration is

$$\sqrt{\sum_{-n}^{n} a_i + (2n+1)^2 \, (b_n + b_{-n})/4}$$

In doing the analysis, the area of the sample peak is compared to the area under the same peak in the standard; the error in this calculation is

$$\frac{X \pm x}{Y \pm y} = \frac{X}{Y} \left(1 \pm \sqrt{\left(\frac{x}{X}\right)^2 + \left(\frac{y}{Y}\right)^2}\right) \, .$$

For a more detailed discussion of statistical error, see Baedecker 1971, Denechaud 1969, or Quittner 1972.

APPENDIX III

TABLE A3-I

Trace element analyses of Hawaiian samples

	A7-43-51	A7-55-29	72 HIG-37-1	A7-44-5	A7-51-20
Sc	36.3	25.8	34.4	33.5	23.4
Cr	319	496	585	52	205
Co	65.2	51.4	82.4	54.7	35.2
La	7.7	12.3	15.8	15.5	21.1
Ce	16.2	29.0	29.6	41.6	49.8
Nd	14	30	19	31	35
Sm	4.2	5.2	5.1	7.9	8.2
Eu	1.69	1.65	2.04	2.25	1.97
Tb	0.82	0.72	1.0	1.1	0.81
Ho	0.83	1.1	1.0	1.5	1.2
Yb	2.5	2.3	2.2	3.3	2.6
Lu	0.25	0.34	0.31	0.51	0.36
Hf	3.1	4.9	3.5	7.1	6.3
Ta	2.6	0.8	5.0	2.4	1.6
Th	0.92	1.5	2.1	1.2	1.5

Chondrite-normalized REE analyses

	A7-43-51	A7-55-29	72 HIG-37-1	A7-44-5	A7-51-20
La	23	37	48	47	64
Ce	18	33	34	47	57
Nd	23	50	32	52	59
Sm	23	29	28	44	45
Eu	24	24	30	33	28
Tb	17	15	21	24	17
Ho	12	15	14	21	18
Yb	12	11	11	17	13
Lu	7	10	9	15	10

Additional information:

Sample	Location		K_2O	TiO_2	Fe_2O_3	CaO
A7-43-51	34°46.7'N	171°49.8'E	0.46	2.09	12.68	10.31
A7-44-5	35°34.9'N	170°57.2'E	0.63	3.45	15.54	9.61
A7-51-20	33°41.6'N	171°33.1'E	0.67	3.63	12.62	16.09
A7-55-29	32°08.2'N	172°15.7'E	0.47	2.54	12.45	9.26
72 HIG-37-1	25°13.3'N	167°47.9'W	0.58	2.44	13.76	10.32

These samples and this data courtesy of David Clague.

Figure A3-1: Chondrite-normalized REE patterns for the five Hawaiian rocks.

△————△ A7-43-51
□······□ A7-55-29
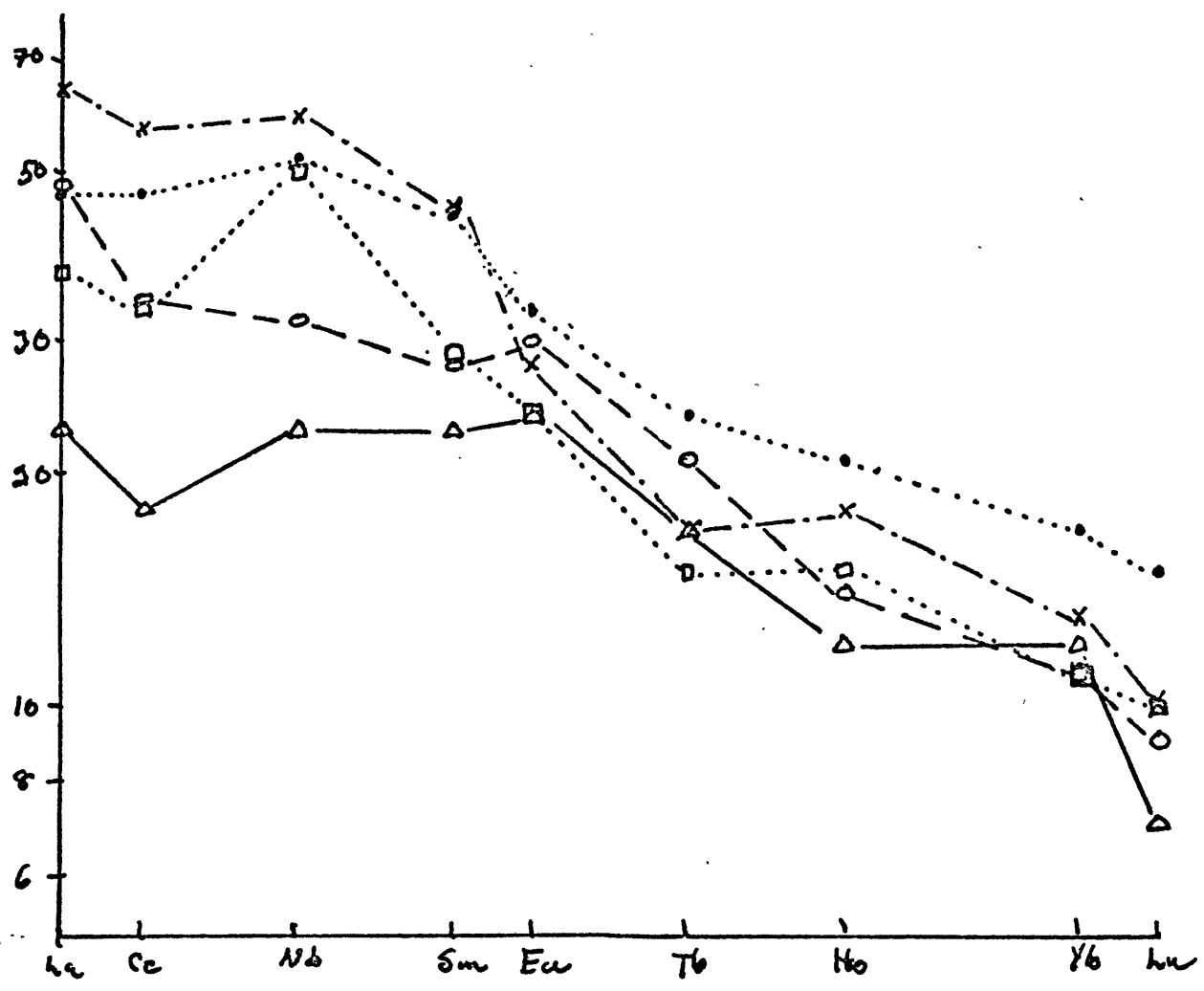○——○ 72 HIG-37-1
●·····● A7-44-5
✗—·—✗ A7-51-20

TABLE A3-II

REE analyses of Hawaiian rocks from the literature

	9948	10396	10398	10403	2201
La	5.30	8.41	6.24	8.78	7.22
Ce	-	-	-	-	25.83
Nd	12.78	19.31	14.59	20.9	20.11
Sm	3.74	5.26	4.09	5.06	4.94
Eu	1.28	2.03	1.31	1.77	1.77
Tb	0.663	1.00	0.728	0.868	0.847
Ho	0.574	0.746	0.666	0.787	0.852
Yb	1.26	1.81	1.45	2.06	1.85
Lu	0.191	0.246	0.199	0.288	0.299

	Pelee's Hair	C-61	KI-22	Kilauea
La	11.42	9.7	10.5	14.04
Ce	33.68	22	35	38.4
Nd	20.12	18.8	17.8	22.5
Sm	5.41	5.2	4.2	5.62
Eu	1.81	2.1	1.27	2.10
Tb	1.20	1.19	0.66	0.872
Ho	0.825	0.96	0.64	0.938
Yb	1.67	2.3	1.05	1.53
Lu	0.238	0.35	0.20	0.275

Sources:

9948	Tholeiite, Koolau series, Schilling 1966
10396	" " " "
10398	" " " "
10403	" " " "
2201	" Mauna Loa "
Pelee's Hair	" Halemaumau "
C-61	Kohala "
KI-22	Kilauea Iki, Schmitt and Smith 1961
Kilauea	Wildeman 1971, unpublished

REFERENCES

Ahrens, L.H., ed., 1968, Origin and Distribution of the Elements, Intern. Ser. Monographs Earth Sci. 30, Pergamon, New York.

Arth, J.G., Jr., 1973, Geochemistry of Early Precambrian Rocks, Minnesota-Ontario, Ph.D. thesis, State Univ. of N.Y. at Stony Brook.

Baedecker, P.A., 1971, "Digital Methods of Photopeak Integration in Activation Analysis" in A.O. Brunfelt and E. Steinnes, eds., Activation Analysis in Geochemistry and Cosmochemistry, p. 175-182.

Brooks, C.K., 1970, "The Concentrations of Zr and Hf in some igneous and metamorphic rocks and minerals", Geochim. Cosmochim. Acta 34: 411-416.

Brunfelt, A.O. and E. Steinnes, eds., 1971, Activation Analysis in Geochemistry and Cosmochemistry, Universitetsforlaget, Oslo, 468 pp.

Bultitude, R.J. and D.H. Green, 1968, "Experimental studies at high pressures on the origin of olivine nephelinite and olivine melilite nephelinite magmas", Earth Planet. Sci. Letters 3: 325-337.

Carter, J.L., 1970, "Mineralogy and chemistry of the earth's upper mantle based on the partial fusion-partial crystallization model", Geol. Soc. Am. Bull. 81: 2021-2034.

Chen, J.C., 1971, "Petrology and chemistry of garnet lherzolite nodules in kimberlite from South Africa", Am. Minerlogist 56: 2098-2110.

Coleman, R.G., D.E. Lee, L.B. Beatty and W.W. Brannock, 1965, "Eclogites and eclogites: their differences and similarities", Geol. Soc. Am. Bull. 76: 483-508.

Coombs, D.S., 1963, "Trends and affinities of basaltic magmas and pyroxenes as illustrated on the diopside-olivine-silica diagram", Min. Soc. Am. Spec. Paper 1: 227-250.

Corliss, J.B., 1970, Mid-Ocean ridge basalts, Ph.D. thesis, U. of Calif., San Diego.

Dale, I.M. and P. Henderson, 1972, "The partition of transition elements in phenocryst-bearing basalts and implications about melt structure", in Twenty-fourth International Geological Congress Proceedings, Section 10, p. 105-111.

Dams, R. and F. Adams, 1968, "Gamma-ray energies of radionuclides formed by neutron capture determined by Ge(Li) spectrometry", Radiochemica Acta 10: 1 - 11.

Deer, W.A., R.A. Howie, and J. Zussman, 1962, Rock-Forming Minerals, 5 vols., Longman, Green and Co., Ltd, London.

DeLong, S.E., 1974, "Distribution of Rb, Sr and Ni in igneous rocks, central and western Aleutian Islands, Alaska", Geochim. Cosmochim. Acta 38: 245-266.

Denechaud, E.B., 1969, Rare-Earth Activation Analysis: Improvement and Application to Stretishorn Dike and Duluth Complex, Ph. D. Thesis, U. of Wisconsin.

Doherty, P.C. and T.L. Wright, 1971, Mineral Distribution Program- Mod II, Geological Survey Computer Contribution 7, 93 pp.

Early, T.O., 1973, "Rare earths in eclogites from the Roberts Victor kimberlite, South Africa", in preparation.

Ehmann, W.D., 1971, "Tantalum" in Mason, ed., Handbook of Elemental Abundances in Meteorites, pp. 425-428.

--------, and T.V. Rebagay, 1971, "Zirconium and Hafnium" in Mason, ed., Handbook of Elemental Abundances in Meteorites, pp. 307-318.

Ewart, A., W.B. Bryan and J.B. Gill, 1973, "Mineralogy and geochemistry of the Younger Volcanic Islands of Tonga, S.W. Pacific", J. Petrol. 14: 429-465.

Fisher, D.E., O. Joensuu and K. Boström, 1969, "Elemental Abundances in Ultramafic Rock and their Relation to the Upper Mantle", J. Geophys. Res. 74: 3865-3873.

Flanagan, F.J., 1973, "1972 values for international geochemical reference samples", Geochim. Cosmochim. Acta 37: 1189-1200.

Frey, F.A., 1969, "Rare earth abundances in a high temperature peridotite intrusion", Geochim. Cosmochim. Acta 33: 1429-1447.

--------, M.A. Haskin, J.A. Poetz and L.A. Haskin, 1968, "Rare earth abundances in some basic rocks", J. Geophys. Res. 73: 6085-6098.

Friedlander, G., J.W. Kennedy and J.M. Miller, 1964, Nuclear and Radiochemistry, 2nd edition, John Wiley and Sons, New York, 585p.

Frondel, C., 1970, "Scandium", in K.H. Wedepohl, ed., Handbook of Geochemistry, vol. II, ch. 21.

Gast, P.W., 1968, "Trace element fractionation and the origin of tholeiitic and alkaline magma types", Geochim. Cosmochim Acta 32: 1057-1086.

Gast, P.W., N.J. Hubbard and H. Wiesman, 1970, "chemical composition and petrogenesis of basalts from Tranquility Base", Proc. Apollo 11 Lunar Science Conf., v. 2, pp. 1143-1163.

Gill, J.B., 1974, "Role of underthrust oceanic crust in the genesis of a Fijian calc-alkaline suite", Contr. Mineral. Petrol. 43: 29-45.

Goles, G.G., 1967, "Trace elements in ultramafic rocks", in P.J. Wyllie, ed., Ultramafic and Related Rocks

Gordon, G.E., K. Randle, G.G. Goles, J.B. Corless, M.N. Beeson and S.S. Oxley, 1968, "Instrumental activation analysis of standard rocks with high-resolution gamma-ray detectors", Geochim. Cosmochim. Acta 32: 369-396.

Green, D.H., 1970a, "The origin of basaltic and nephelinitic magmas", Trans. Leicester Literary and Philosophical Soc. 64: 28-54.

————————, 1970b, "A review of experimental evidence on the origin of basaltic and nephelinitic magmas", Phys. Earth Planet. Interiors 3: 221-235.

————————, 1971, "Compositions of basaltic magmas as indicators of conditions of origin: application to oceanic vulcanism", Phil. Trans. Roy. Soc. A268: 707-725.

————————, 1973a, "Conditions of melting of basanite magma from garnet peridotite", Earth Planet. Sci. Letters 17: 456-465.

————————, 1973b, "Experimental melting studies on a model upper mantle composition at high pressure under water-saturated and water-undersaturated conditions", Earth Planet. Sci. Letters 19: 37-53.

————————, J.W. Morgan and K.S. Heier, 1968, "Thorium uranium and potassium abundances in peridotite inclusions and their host basalts", Earth Planet. Sci. Letters 4: 155-166.

————————, and A.E. Ringwood, 1963, "Mineral assemblages in a model mantle composition", J. Geophys. Res. 68: 937-945.

———————— and ————————, 1967, "The genesis of basaltic magma", Contr. Mineral. Petrol. 15: 103-190.

———————— and ————————, 1970, "Mineralogy of peridotitic compositions under upper mantle conditions", Phys. Earth Planet. Interiors 3: 359-371.

Grutzek, N.W., S.J. Kridelbaugh and D.F. Weill, 1973, "REE partitioning between diopside and silicate liquid", Trans. Am. Geophys. Un. 54: 1222.

Gunn, B.M., 1971, "Trace element partition during olivine fractionation of Hawaiian basalts", Chem. Geol. 8: 1-13.

Hamilton, W., 1961, "Columbia River basalt in the Riggins quadrangle, western Idaho", USGS Bull. 1141-L.

Harris, P.G., R. Hutchison and D.K. Paul, 1972, "Plutonic xenoliths and their relation to the upper mantle", Phil. Trans Roy. Soc. Lond. A271: 313-323.

Haskin, L.A., F.A. Frey, R.A. Schmitt and R.H. Smith, 1966, "Meteoritic, solar and terrestrial rare-earth distributions", Phys. Chem. Earth 7: 167-321.

—————————, M.A. Haskin, F.A. Frey and T.R. Wildeman, 1968, "Relative and absolute terrestrial abundances of the rare earths" in L.A. Ahrens, ed., Origin and Distribution of the Elements, pp. 889-912.

—————————, R.O. Allen, P.A. Helmke, T.P. Paster, M.R. Anderson, R.L. Korotev and K.A. Zwiefel, 1970, "Rare earths and other trace elements in Apollo 11 lunar samples", Proc. Apollo 11 Lunar Sci. Conf. v. 2, pp. 1213-1231.

Heier, K.S., 1970, "Rubidium", in Wedepohl, ed., Handbook of Geochemistry, ch 37B-E.

Helmke, P.A. and L.A. Haskin, 1973, "Rare-earth elements, Co, Sc and Hf in the Steens Mountain basalts", Geochim. Cosmochim. Acta 37: 1513-1530.

Henderson, P. and I.M. Dale, 1970, "The partitioning of selected transition element ions between olivine and groundmass of oceanic basalts", Chem. Geol. 5: 267-274.

Herrmann, A.G., 1970, "Yttrium and Lanthanides", in Wedepohl, ed., Handbook of Geochemistry, ch 39, 57-71 B-O.

Hertogen, J. and R. Gijbels, 1974, "Trace element fractionation during partial melting", submitted for publication.

Hess, H.H. and A. Poldervaart, eds., 1967, Basalts: The Poldervaart Treatise on Rocks of Basaltic Composition, 2 vols., Interscience, New York.

Higuchi, H. and H. Nagasawa, 1969, "Partition of trace element between rock-forming minerals and the host volcanic rocks", Earth Planet. Sci. Letters 7: 281-287.

Hurley, P.M., ed., 1966, Advances in Earth Science, MIT Press, Cambridge.

Irving, A.J., 1971, Geochemical and high pressure experimental studies of xenoliths, megacrysts and basalts from southeastern Australia, Ph.D. thesis, Australian Nat. Univ.

Irving, A.J. and D.H. Green, 1974, "Geochemistry and petrogenesis of the Newer Basalts of Victoria and South Australia", in preparation.

Ito, K., and G.C. Kennedy, 1967, "Melting and phase relations in a natural peridotite to 40 kilobars", Am. J. Sci. 265: 519-538.

Jensen, B.B., 1973, "Patterns of trace element partitioning", Geochim. Cosmochim. Acta 37: 2227-2242.

Kay, R.W. and P.W. Gast, 1973, "The rare earth content and origin of al-kali-rich basalts", J. Geol. 81: 653-682.

Kesson, S.E., 1973, "The primary geochemistry of the Monaro alakaline vol-canics, southeastern Australia; evidence for Upper Mantle heterogen-eity", Contr. Mineral. Petrol. 42: 93-108.

Kushiro, I., N. Shimizu, Y. Nakamura and S. Akimoto, 1972, "Compositions of coexisting liquid and solid phases formed upon melting of natural garnet and spinel lherzolites at high pressure: a preliminary report", Earth Planet. Sci. Letters 14: 19-25.

————————, Y. Syono and S. Akimoto, 1968, "Melting of a peridotite nodule at high pressures and high water pressures", J. Geophys. Res. 73: 6023.

Laul, J.E., H. Wakita, D.L. Showalter, W.V. Boynton and R.A. Schmitt, 1972, "Bulk,rare earth,and other trace elements in Apollo 14 and 15 and Luna 16 samples", Proc. Third Lunar Sci. Conf., v.2, pp. 1181-1200.

Lopez-Escobar, L. F.A. Frey and M. Vergara, 1974, "Andesites from central-south Chile: trace element abundances and petrogenesis", pre-print from Symposium Internacional de Volcanologia: Problemas volcanoligicos, Andinos y Antarticos, held in Santiage, Chile, Septermber 9-14, 1974.

Mason, B., ed., 1971, Handbook of Elemental Abundances in Meteorites, Gordon and Breach, New York.

Masuda, A. and I. Kushiro, 1970, "Experimental determinations of partition coefficients of ten rare earth elements and barium between clinopyrox-ene and liquid in the synthetic silicate system at 20 kilobar pressure", Contr. Mineral. Petrol. 26: 42-49.

Morgan, J.W., 1971, "Thorium", in Mason, ed., Handbook of Elemental Abun-dances in Meteorites, pp. 517-528.

Nagasawa, H., 1970, "Rare earth elements in zircon and apatite in acidic volcanic and igneous rocks", Earth.Planet. Sci. Letters 9: 359-364.

————————, H. Wakita, H. Higuchi and N. Onuma, 1969, "Rare earths in peridotite nodules: an explanation of the genetic relationship be-tween basalt and peridotite nodules", Earth Planet. Sci. Letters 5: 377-381.

Nakamura, N., A. Masuda, T. Tanoka, and H. Kurasawa, 1973, "Chemical compositions and rare earth features of 4 Apollo 16 samples", Proc. Fourth Lunar Sci. Conf., v.2, pp. 1407-1414.

Nicholls, G.D., 1967, "Geochemical studies in the ocean as evidence for the composition of the mantle" in S.K. Runcorn, ed., Mantles of the earth and terrestrial planets, pp. 285-304.

Norman, J.C. and L.A. Haskin, 1968, "The geochemistry of Sc: a comparison to the rare earths and Fe", Geochim. Cosmochim. Acta 32: 93-108.

O'Hara, M.J. and H.S. Yoder, 1967, "Formation and fractionation of basic magmas at high pressures", Scot. J. Geol. 3: 67-117.

Onuma, N., II. Higuchi, H. Wakita and H. Nagasawa, 1968, "Trace element partition between two pyroxene and the host lava", Earth Planet. Sci. Letters 5: 47-51.

Paster, T.P., D.S. Schauwecker and L.A. Haskin, 1974, "The behavior of some trace elements during solidification of the Skaergaard lyered series", Geochim. Cosmochim. Acta 38: 1549-1578.

Philpotts, J.A. and C.C. Schnetzlar, 1968a, "Europium anomalies and the genesis of basalt", Chem Geol. 3: 5-13.

----------, and ----------, 1968b, "Genesis of continental diabases and oceanic tholeiities considered in light of rare earth and Ba abundances and partition coefficients", in L.A. Ahrens, ed., Origin and Distribution of the Elements.

----------, and ----------, 1970a, "Phenocryst-matrix partition coefficients for K, Rb, Sr and Ba, with applications of anorthosite and basalt genesis", Geochim. Cosmochim. Acta 34: 307-322.

----------, and ----------, 1970b, "Apollo 11 lunar samples: K, Rb, Sr, Ba and rare-earth concentrations in some rocks and separated phases", Proc. Apollo 11 Lunar Sci. Conf., v.2, pp. 1471-1486.

----------, ----------, and H.H. Thomas, 1972, "Petrogenetic implications of some new geochemical data on eclogitic and ultrabasic inclusions", Geochim. Cosmochim. Acta 36: 1131-1166.

Prinz, M., 1967, "Geochemistry of basaltic rocks: trace elements" in H.H. Hess and A. Poldervaart, eds., Basalts, v. 1, pp. 271-324.

Puchelt, H., 1972, "Barium" in Wedepohl, ed., Handbook of Geochemistry, ch 56B-O.

Quittner, P., 1972, Gamma-Ray Spectroscopy, Halsted Press, New York, 111 p.

Reid, J.B., Jr., and F.A. Frey, 1971, "Rare earth distributions in lherzolite and garnet pyroxenite xenoliths and the constitution of the upper mantle", J. Geophys. Res. 76: 1184-1196.

Ringwood, A.E., 1966, "The Chemical composition and origin of the earth", in P.M. Hurley, ed., Advances in Earth Science, pp. 287-356.

Roeder, P.L. and R.F. Emslie, 1970, "Olivine-liquid equilibrium", Contr. Mineral. Petrol. 29: 275-289.

Rogers, J.J. and J.A.S. Adams, 1969, "Thorium", in Wedepohl, ed., Handbook of Geochemistry, ch 90B-0.

Runcorn, S.K., ed., 1967, Mantles of the Earth and Terrestrial Planets, Interscience, New York.

Schilling, Jean-Guy, 1966, Rare-Earth Fractionation in Hawaiian Volcanic Rocks, Ph.D. thesis, M.I.T.

——————, and J.W. Winchester, 1969, "Rare earth contribution to the origin of Hawaiian lavas", Contr. Mineral. Petrol. 23: 27-37.

Schmitt, R.A. and R.H. Smith, 1961, "A program of research for the determination of rare-earth abundances in meteorites", General Atomic Report GA-2782.

Schnetzlar, C.C. and J.A. Philpotts, 1968, "Partition coefficients of rare-earth elements and barium between igneous matrix material and rock-forming mineral phenocrysts - I" in L.A. Ahrens, ed., Origin and Distribution of the elements, pp. 929-938.

——————, and ——————, 1970, "Partition coefficients of rare-earth elements between igneous matrix material and rock-forming mineral phenocrysts - II", Geochim. Cosmochim. Acta 34: 331-340.

Shaw, D.M., 1970, "Trace element fractionation during anatexis", Geochim. Cosmochim. Acta 34: 237-243.

——————, 1973, "Development of the early continental crust. Part 1. Use of trace element distribution coefficient models for the Proto-archean crust", Can. J. Earth Sci., 9: 1577-1595.

Shimizu, N., 1974, "Rare earth elements in garnets and clinopyroxenes from garnet lherzolite nodules in kimberlites", Earth Planet. Sci. Letters in press.

Singleton, O.P. and E.B. Joyce, 1969, "Cainozoic volcanicity in Victoria" Spec. Publs. Geol. Soc. Aust. 2: 145-154.

Sutherland, F.L., 1969, "A review of the Tasmanian Cainozoic volcanic province", Spec. Publs. Geol. Soc. Aust. 2: 133-144.

Taylor, S.R., M. Kaye, A.J.R. White, A.R. Duncan and A.Ewart, 1969, "Genetic significance of Co, Cr, Ni, Sc and V content of andesites", Geochim. Cosmochim. Acta 33: 275-286.

Turekian, K.K. and M.H. Carr, 1960, "The geochemistries of Cr, Co and Ni", Int. Geol. Cong. 21st session, Part 1, pp. 14-29.

——————, and K.H. Wedepohl, 1961, "Distribution of the elements in some major units of the earth's crust", Bull. Geol. Soc. Am. 72: 175-192.

Vinogradov, A.P., 1962, "Average contents of chemical elements in the principal types of igneous rocks of the earth's crust", Geochemistry 1962: 641-664.

Vlasov, K.A., ed., "Geochemistry and mineralogy of rare elements and genetic types of their deposits", vol. 1, trans. from Russian by Israel program for scientific translations, Jerusalem 1966.

Wager, L.R. and R.L. Mitchell, 1951, "The distribution of trace elements during strong fractionation of basic magam - a further study of the Skaergaard intrusion, East Greenland", Geochim. Cosmochim. Acta 1: 129-208.

Wakita, H., H. Nagasawa, S. Uyeda and H. Kuno, 1967, "Uranium and thorium contents in ultrabasic rocks", Earth Planet. Sci. Letters 2: 377-381.

Wedepohl, K.H., ed., 1970, Handbook of Geochemistry, 2 vols., Springer-Verlag, Berlin.

Whittaker, E.J.W. and R. Muntus, 1970, "Ionic radii for use in geochemistry", Geochim. Cosmochim. Acta 34: 945-956.

Wyllite, P.J., ed., 1967, Ultramafic and Related Rocks, Wiley and Sons, New York, 464 pp.

Zielinski, R.A. and F.A. Frey, 1970, "Gough Island: evaluation of a fractional crystallization model", Contr. Mineral. Petrol. 29: 242-254.